NOVEL PHENANTHROCARBAZOLE CONTAINING CONJUGATED
POLYMERS AS HIGH PERFORMANCE ELECTROCHROMIC MATERIALS

A THESIS SUBMITTED TO
THE GRADUATE SCHOOL OF NATURAL AND APPLIED SCIENCES
OF
MIDDLE EAST TECHNICAL UNIVERSITY

BY

GİZEM ATAKAN

IN PARTIAL FULFILLMENT OF THE REQUIREMENTS
FOR
THE DEGREE OF MASTER OF SCIENCE
IN
CHEMISTRY

AUGUST 2016

Approval of the thesis:

NOVEL PHENANTHROCARBAZOLE CONTAINING CONJUGATED POLYMERS AS HIGH PERFORMANCE ELECTROCHROMIC MATERIALS

submitted by **GİZEM ATAKAN** in partial fulfillment of the requirements for the degree of **Master of Sciences in Chemistry Department, Middle East Technical University** by,

Prof. Dr. Gülbin Dural Enver   _____
Dean, Graduate School of **Natural and Applied Sciences**

Prof. Dr. Cihangir Tanyeli   _____
Head of Department, **Chemistry**

Assist. Prof. Dr. Görkem Günbaş   _____
Supervisor, **Department of Chemistry, METU**

Examining Committee Members:

Prof. Dr. Levent Toppare   _____
Department of Chemistry, METU

Assist. Prof. Dr. Görkem Günbaş   _____
Department of Chemistry, METU

Assoc. Prof. Dr. Ali Çırpan   _____
Department of Chemistry, METU

Assoc. Prof Dr. Yasemin Arslan Udum   _____
Department of Advanced Technologies, Gazi University

Assist. Prof. Dr. Salih Özçubukçu   _____
Department of Chemistry, METU

Date: 22.08.2016

I hereby declare that all information in this document has been obtained and presented in accordance with academic rules and ethical conduct. I also declare that, as required by these rules and conduct, I have fully cited and referenced all material and results that are not original to this work.

Name, Last name: Gizem ATAKAN

Signature:

ABSTRACT

NOVEL PHENANTHROCARBAZOLE CONTAINING CONJUGATED POLYMERS AS HIGH PERFORMANCE ELECTROCHROMIC MATERIALS

Atakan, Gizem

Ms., Department of Chemistry

Supervisor: Assist. Prof. Dr. Görkem Günbaş

August 2016, 79 Pages

For potential application of electrochromic materials in display technologies, materials having additive or subtractive primary colors in their neutral states that switch to a highly tranmissive states are desired since the entire color spectrum can be created using these materials. The RGB color model requires three complementary colors; red, green and blue. Even though the RGB colored polymers in the electrochromic research area were fulfilled over the past decade, towards high quality display applications, electrochromic materials with better optical contrasts and faster switching times are needed. As a result, realization of novel electrochromic materials is still a major aim in the field. Additionally, a well-defined neutral state red polymeric materials appear to be absent in the literature. Donor-acceptor type polymers generally result in two absorption bands. But for the red to transmissive polymeric materials, single absorption band is needed. Therefore, based on the previous observations in the field, the key approach for the synthesis of well-defined novel red to transmissive polymeric materials was appeared to be the coupling of units that are known to polymerize to give superior electrochromic properties, with highly conjugated donor materials. Under the light of this approach, a monomer which consists of EDOT and phenanthrocarbazole units was designed and polymerized electrochemically. Its electrochromic properties were investigated in detail. The polymer showed the well

promised red to transmissive color change with a high optical contrast value of 51% and fast switching times of 0.65 s for oxidation and 0.52 s for reduction. Additionally, towards realization of a solution processable derivative, a novel monomer with ProDOT unit that contains alkyl chains and phenanthrocarbazole was successfully synthesized. The corresponding polymer was synthesized both by electrochemical and chemical methods. Unlike its EDOT containing analogue, the polymer switches between orange and transmissive grey color with a green intermediate with high optical contrast values of 58% for the electrochemically synthesized and 60% for chemically synthesized polymer. The materials showed fast switching times of 1.3 s and 0.9 s respectively. Additionally, the polymer showed strong orange luminescence in its neutral state which completely diminishes upon oxidation. Hence polymer is one of the rare examples of a semiconducting polymer that shows both color and luminescence change upon applied potential.

Keywords: Electrochromism, Red to Transmissive Polymers, High Optical Contrast.

ÖZ

YENİ FENANTROKARBAZOL İÇEREN KONJÜGE POLİMERLERİN YÜKSEK PERFORMANS ELEKTROKROMİK MATERYALLER OLARAK KULLANIMI

Atakan, Gizem

Yüksek Lisans, Kimya Bölümü

Tez Yöneticisi: Yrd. Doç. Görkem Günbaş

Ağustos 2016, 79 Sayfa

Elektrokromik malzemelerin görüntü teknolojilerindeki potansiyel uygulamaları için, nötr hallerinde toplamsal ya da çıkarımsal ana renklere sahip, yükseltgendiğinde ise şeffaf duruma geçen materyaller tercih edilmektedir. Böylelikle, tüm renk spektrumu oluşturulabilmektedir. KYM renk uzayı üç toplamsal ana renkten oluşmaktadır; kırmızı, yeşil ve mavi. Elektrokromik araştırma alanında yüksek kalitedeki görüntü teknolojilerinin uygulaması için KYM renk uzayını tamamlayan polimerler tanımlanmış olsa da, bu tür uygulamalar için yüksek optik kontrastlı ve daha hızlı dönüş sürelerine sahip polimerlere ihtiyaç duyulmaktadır. Bunun sonucu olarak alanda yeni elektrokromik materyaller tanımlama ihtiyacı doğmuştur. Buna ek olarak, literatürde iyi tanımlanmış kırmızıdan şeffafa geçen materyaller bulunmamaktadır. Donör-akseptör polimerler genellikle iki soğurma bandı oluşturmaktadırlar. Kırmızıdan şeffafa dönen elektrokromik polimerler oluşturmak için ise tek soğurma bandına ihtiyaç vardır. Alandaki önceki çalışmalara dayanarak, iyi tanımlanmış yeni kırmızıdan şeffafa dönen polimerler üretmek için gerekli olan yaklaşımın polimerler halleri iyi elektrokromik özellikler gösteren materyaller ile yüksek konjugasyona sahip donör materyallerin bağlantılanması olduğu öngörülmüştür. Bu yaklaşımın ışığında EDOT ve fenantrokarbazol ünitelerini içeren monomer sentezlenmiş ve elektrokimyasal olarak polimerleştirilmiş, polimerin elektrokromik özellikleri incelenmiştir. Polimer tasarlandığı üzere kırmızıdan transpara yüksek optik kontrast (% 51) ve hızlı dönme zamanları (oksidasyon için 0.65 s, indirgeme için 0.52 s) ile dönmüştür. Ek olarak, polimere çözünürlük kazandırmak adına monomerin alkil

zincirleri içeren ProDOT ve fenantrokarbazol içeren türevi de elde edilmiştir. Bu polimer hem elektrokimyasal hem de kimyasal yöntemler ile polimerleştirilmiştir. EDOT içeren türevinden farklı olarak, bu polimer yeşil ara renk ile turuncudan transparan griye dönmüştür. Elektrokimyasal yöntemlerle sentezlenen polimer % 58, kimyasal olarak sentezlenen ise 60 % optik kontrast değeri göstermiştir. Dönme zamanları ise sırası ile 1.3 s ve 0.9 s olarak hesaplanmıştır. Bu özelliklere ek olarak bu polimer nötr halinde güçlü turuncu bir lüminesans gösterirken okside olmuş halinde bu özelliğini tamamen kaybetmiştir. Bundan dolayı, bu polimer elekrokromizm ve elektrokimyasal lüminesans gösteren yarıiletken polimerlerin nadir örneklerinden biridir.

Anahtar Sözcükler: Elektrokromizm, Kırmızı-Şeffaf Polimerler, Yüksek Optik Kontrast.

ACKNOWLEDGMENTS

To what makes me stronger,

TABLE OF CONTENTS

xiv

LIST OF SCHEMES

SCHEMES

LIST OF ABBREVATIONS

ACN	Acetonitrile
Ag	Silver
AFM	Atomic Force Microscopy
ATR	Attenuated Total Reflectance
CE	Counter Electrode
CMYK	Cyan Magenta Yellow Key
D-A-D	Donor-Acceptor-Donor
DCM	Dichloromethane
D-D-D	Donor-Donor-Donor
DEP	3,10-Bis(2,3-dihydrothieno[3,4-b][1,4]dioxin-5-yl)-1-dodecyl-1*H*-phenanthro[1,10,9,8-c,d,e,f,g]carbazole
DMSO	Dimethyl sulfoxide
DPP	3,10-Bis(3,3-bis(((2-ethylhexyl)oxy)methyl)-3,4-dihydro-2*H*-thieno[3,4-*b*][1,4]dioxepin-6-yl)-1-dodecyl-1*H*-phenanthro[1,10,9,8-*cdefg*] carbazole
ECD	Electrochromic Device
EDOT	3,4-Ethylenedioxythiophene
E$_g$	Band gap
FTIR	Fourier Transform Infrared Spectroscopy
HOMO	Highest Occupied Molecular Orbital
HRMS	High Resolution Mass Spectrometry
IR	Infrared
ITO	Indium Tin Oxide
L, a, b	Luminance, hue, saturation
LUMO	Lowest Occupied Molecular Orbital

NBS	N-Bromosuccinimide
NIR	Near Infrared
NMR	Nuclear Magnetic Resonance Spectrometry
OFET	Organic Field Effect Transistor
PEDOT	Poly(3,4-ethylenedioxythiophene)
PC	Propylene Carbonate
PDEP	Poly-3,10-bis(2,3-dihydrothieno[3,4-b][1,4]dioxin-5-yl)-1-dodecyl-1*H*-phenanthro[1,10,9,8-c,d,e,f,g]carbazole
PDPP	Poly-3,10-bis(3,3-bis(((2-ethylhexyl)oxy)methyl)-3,4-dihydro-2*H*-thieno[3,4-*b*][1,4]dioxepin-6-yl)-1-dodecyl-1*H*-phenanthro[1,10,9,8-*cdefg*] carbazole
ProDOT	3,4-Propylenedioxythiophene
Pt	Platinum
PTh	Polythiophene
RE	Reference Electrode
R_f	Retardation factor
RGB	Red Green Blue
RT	Room Temparature
SEM	Scanning Electron Microscope
$TBAPF_6$	Tetrabutylammonium hexafluorophosphate
THF	Tetrahydrofuran
TLC	Thin Layer Chromatography
UV	Ultraviolet
WE	Working Electrode
VIS	Visible

CHAPTER 1

INTRODUCTION

1.1.   Electrochromism

Theoretical definition of electrochromism suggests that if a strong electric field is applied to a certain dye, their absorption and emission spectra may be shifted by hundreds of angstroms. This change was named as electrochromism. However, as the research in the field advanced, this definition does not fit within the modern understanding of electrochromism [1]. In electrochromic materials, a persistent but reversible change of color is observed upon application of external potential and this effect is called electrochromism [1,2]. In order words, electrochromism is the reversible and visible change in transmittance and/or reflectance which results from electrochemical redox reactions [3]. Materials utilizing electroactive properties can gain electrons upon reduction and lose electrons upon oxidation. As a result of these electron transfers, different redox states are generated. Different energy states are occupied by these redox states; thus new bands are generated in the spectrum which are generally formed in near IR region other than the VIS region. The different electronic absorption bands, occurred by different redox states, generates the color change. The color change is generally between a transmissive state and a color state, or it can be between two colored states [1]. Being one of the most commercially utilized type of chromism, electrochromic materials has many applications such as E-paper, smart windows, camouflage materials and simple electronic displays [1,4]. Over the past few decades, various electrochromic materials have been synthesized and characterized [3, 5-10]. It is a lively research area, where over 30000 publications are present in the literature and the number of articles published increases every year. The major parameters of the electrochromic materials that are important for their

applications are the switching times, the contrast ratio, coloration efficiency, electrochromic memory and long term stability. The contrast ratio is the difference between the transmittance values of the different colored states. The electrochromic memory is the time that the material remembers its color after the applied current is removed. The long term stability is simply the lifetime of the electrochromic material where the desired case is to retain its electrochromic properties after substantial amount of switching cycles.

Up to date, three classes of electrochromic materials are known; metal oxide films, molecular dyes and organic semiconductors. Among the class of metal oxides, the most studied example is the tungsten trioxide (WO_3) system. Tungsten trioxide is a transparent film and a blue coloration in the film occurs upon electrochemical reduction. The reason for the electrochromism is the generation of W_V sites upon reduction. Despite the controversies about the coloration mechanism, it is assumed that the injection and extraction of electrons and metal cations (Li^+, H^+, etc) are responsible for the color change [11]. The blue coloration in the film can be reversed simply by electrochemical oxidation. The equation is as follows:

$$WO_3 \quad + \quad xM^+ \quad + \quad xe^- \quad \rightarrow \quad M_xO_3$$

(transparent) (blue)

One of the oldest classes in electrochromic materials is Prussian blue systems. Prussian blue is a synthetic pigment used in carbon paper, paint formulation and printing for over hundred years. The Prussian blue pigment has intense blue color stems from iron(III) hexacyanoferrate(II) and its corresponding thin film shows yellow, green, blue and transparent forms at different potentials [12].

Another important class in electrochromic materials is the viologens (1,1'-disubstituted-4,4'- bipyridilium salts). Viologens have three redox states (Figure 1.1). The dication form is the most stable and it is colorless. Viologen dications yield radical cations upon reductive electron transfer. The viologen radical cations are generally intensely colored and the choice of nitrogen substituents are responsible from the resulting color.

2

Figure 1.1. The three common viologen redox states, dication, radical cation, neutral species.

For the organic semiconductors, the frontier research is now evolved into three major areas; synthesis of novel polymeric materials [13,14], synthesis of novel small molecules [15, 16] and fabrication of ECDs using organic semiconductors via novel device structures [17].

Among these three main areas, research in the field mainly focuses on the synthesis of novel polymeric materials because polymeric materials carry several advantages such as: low cost, processability, enhanced mechanical properties, high optical contrast ratio, fast switching times and high stability [18].

1.2. Electrochromism in Conducting Polymers and Importance of Novel Polymeric Materials

In their polymeric forms, whether synthesized by electrochemical or chemical means, thiophene, aniline, pyrrole and carbazole show electrochromic properties [19]. As mentioned in the previous section; in the field of electrochromism, the growing interest on conducting polymers resides based on the fact that they carry several additional advantages over their small molecule and inorganic counterparts. However, without a doubt, the ease of structural modifications is what reinforces conducting polymers among other molecules. Structural modifications simply offer alternation of electrochemical properties, which can lead to low oxidation potential values for the monomers and fast switching times, low band gaps, solubility and high optical contrast ratios for the polymers [20]. Several monomer design methods are now present in order to fulfill these parameters for excellent electrochemical properties. The methods for low band gap polymers includes; controlling bond-length alternation, creating highly planar systems, inducing order by interchain effects, resonance effects along the polymer backbone, and using donor-acceptor theory. The most popular one among these methods is the donor-acceptor theory, and it will be further discussed in the following sections.

With the proper modifications of the electronic character of the π system on the neutral polymer backbone, variation of the π-π^* transition across the electromagnetic spectrum can be achieved [21]. These changes in electronic transitions are accompanied with the corresponding color change in the polymers. Towards realization of conducting polymers with enhanced electrochromic properties, the importance of discovering novel units with different electronic characteristics is significantly important. The increasing industrial demand of electrochromic materials bring along the fact that, towards high quality display applications, electrochromic materials with better optical contrasts and faster switching times are needed.

1.3. Color Models for the Application of Simple Display Devices

For the creation of multicolor displayed E-papers and similar simple display devices, RGB and/or CMYK colored polymers that switch to a highly transmissive state are desired. By modification of the intensity of the primary components of these models, any color in the spectrum can be expressed. Generation of simple display devices utilizing electrochromic polymers are today an important area in materials research, mainly due to their ability to be viewed in a wide variety of lightning conditions and their easy fabrication [22].

1.3.1. RGB Color Space

RGB color model is the trichromatic model of representation which is fundamental to the human perception of color. The trichromatic input is based on the additive primary colors red (R), green (G) and blue (B) [23, 24]. Thus RGB color space is also known as the additive color model. This model corresponds most closely to the sensors of colored light, for example human eye, and for this reason it is mainly used in display of images in electronic systems.

In order to form a color with RGB model; the three components, red, green and blue light, must be superimposed by emission from a black screen or by reflection from a white screen. The complete color scheme can be achieved by mixing combination of

4

different components with different intensities. Zero intensity results in darkest color black and full intensity of each component gives white.

The RGB color model is said to be the additive color model because the three components are added together meaning their light spectra add wavelength to wavelength, forming the final color [25, 26]. By using this property; red, green and blue colored electrochromic polymers can be used in simple display device applications.

1.3.1.1. Blue to Transmissive Electrochromic Polymers

One of the biggest candidates of the blue to transmissive polymer is the PEDOT due to its good electrochromic properites and chemical stability. It is a well-researched electrochromic polymer that is light blue-transparent, in the oxidized state, and dark blue in the reduced state [27]. Research in the field over the past decade though resulted, in several examples of the blue to transmissive type electrochromic polymers with improved electrochromic properties with respect to PEDOT [28-31].
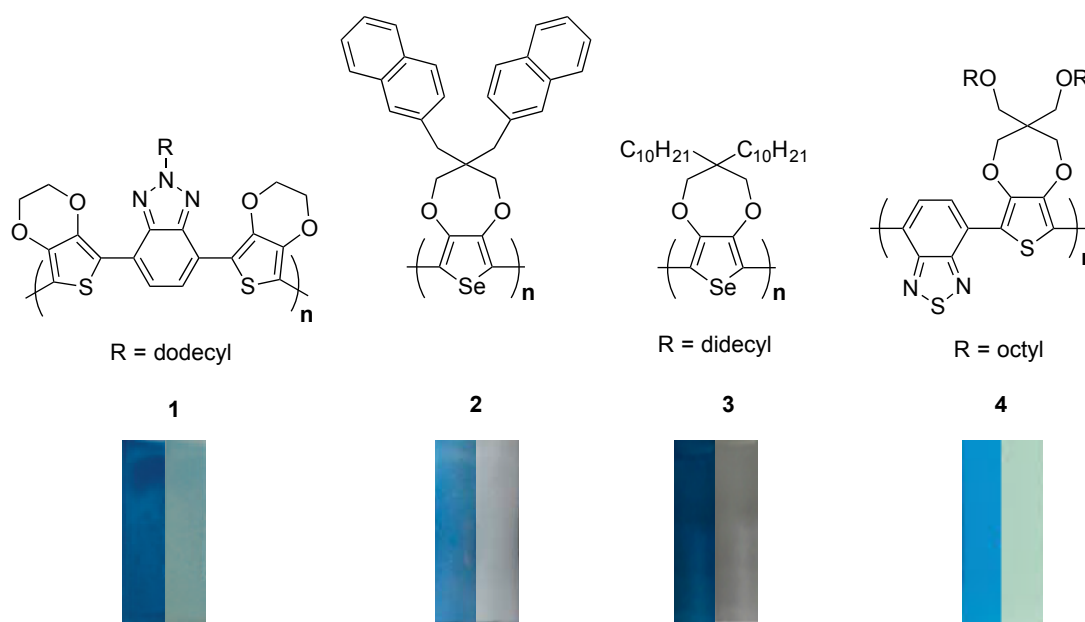
Figure 1.2. Examples of blue to transmissive polymers from the literature [28-31].

1.3.1.2. Green to Transmissive Electrochromic Polymers

For the RGB color space, green color was the missing link for many years. The first donor-acceptor type green electrochromic polymer was synthesized in 2004, however

5

it was switching between a green and brown state [32]. The first green to transmissive electrochromic polymer was synthesized successfully by the Toppare group in 2007 [33]. It was a donor- acceptor type polymer having two simultaneous absorption bands in the red and blue regions of the visible spectrum. The polymer is green in its neutral state and upon application of positive potential, both of the absorption bands depletes simultaneously, resulting in a highly transmissive state. Following this work, a number of other examples to green to transmissive electrochromic polymers were produced over the last decade [34-36].
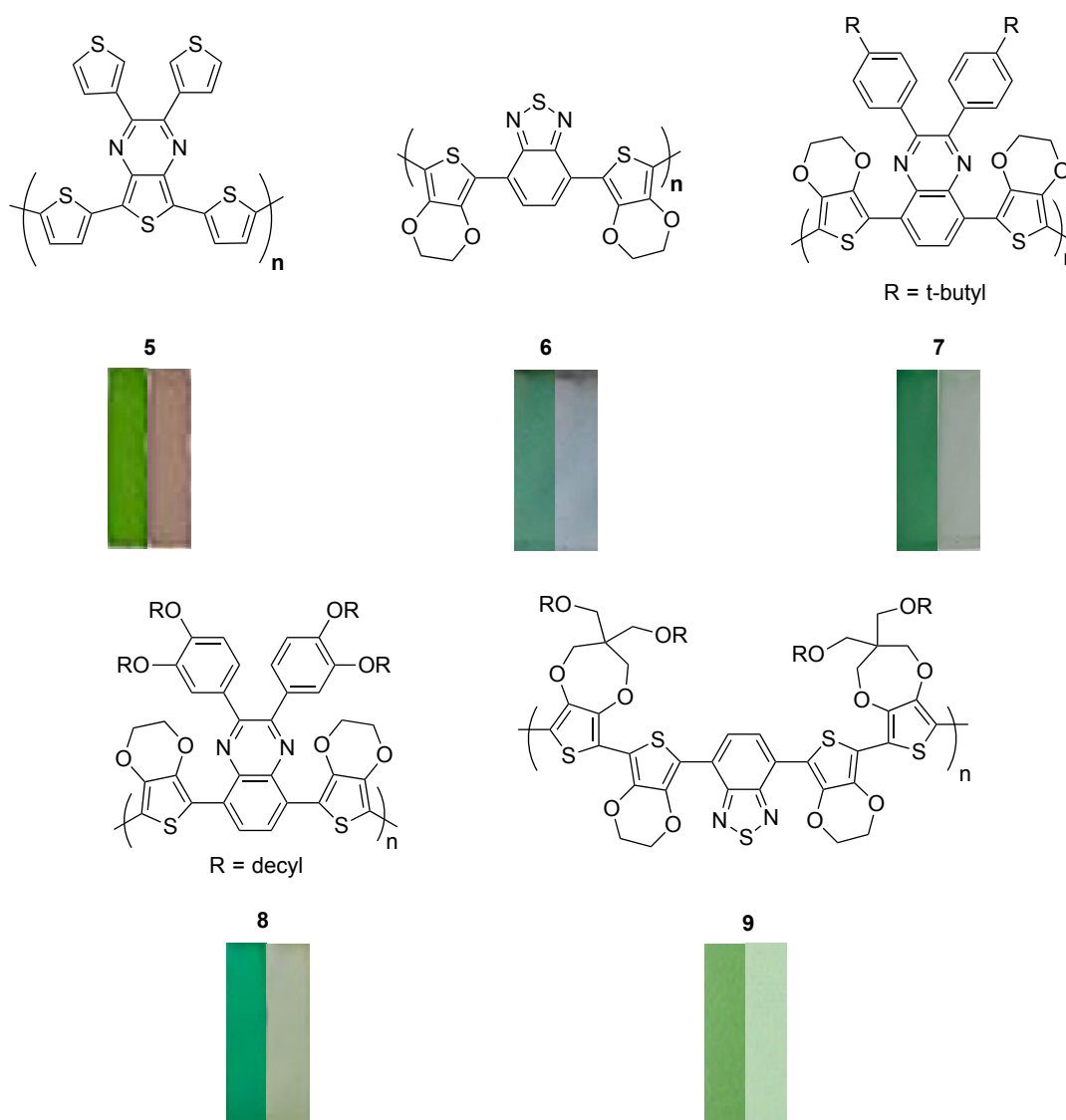
Figure 1.3. Examples of green electrochromic polymers from the literature [32-36].

6

1.3.1.3. Red to Transmissive Electrochromic Polymers

There are a few examples present in the literature for the red to transmissive polymers that were recently published [37-39]. They are random copolymers and high optical contrast and good stability values were reported for these materials. The drawback of these polymers is that they are formed by oxidative polymerization utilizing two or three monomer units, which might cause a reproducibility issue. Additionally, the switching times of these polymers are in order of couple seconds, which might hinder their use in certain applications.
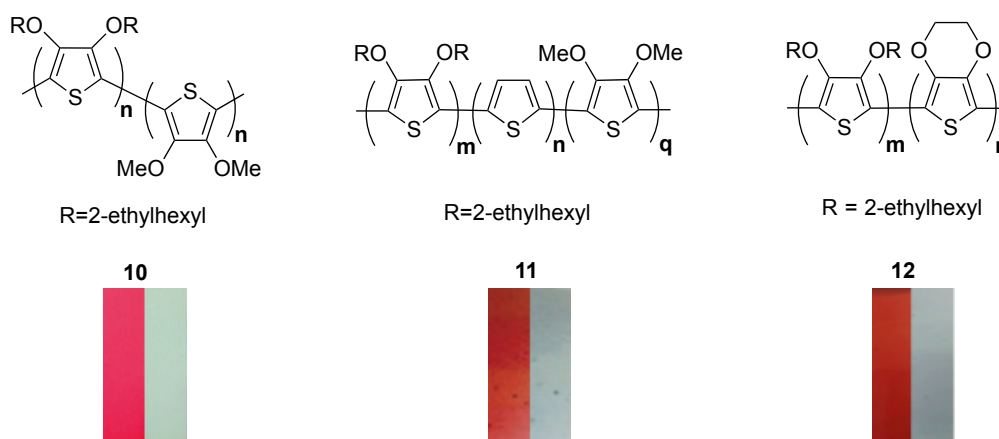
Figure 1.4. Examples of red to transmissive electrochromic copolymers from the literature [37-39].

1.3.2. CMYK Color Space

The CMYK color space is used in print production and it is composed of four color inks used in printing; cyan (C), magenta (M), yellow (Y) and key (K, black). CMYK color model is the subtractive color model meaning that it works by partially or entirely masking colors on a lighter background which is usually white. Some of the light is absorbed by the ink and we see the transmitted light, in other words the inks subtract brightness from white.

As discussed before, in the RGB color model, white is achieved via additive combination of the three primary components and black is achieved in the presence of no light. On the contrary, the CMYK color model is the complete opposite where white is the natural color of the background and achieved in the absence of inks while black

is achieved from the full combination of inks. The combination of cyan, magenta and yellow results in a murky dark brown color. In order to obtain darker black tones and to save ink cost, black ink is used instead of the combination. By using the working principle of CMYK color model, simple display devices can be fabricated using cyan, magenta and yellow colored electrochromic polymers [40].

In the literature, for the CMYK color space, there are high performance materials for the cyan and magenta colored electrochromic polymers, that switch to transmissive state [41, 42]. However, the yellow color was the important missing link. Recently realization of the yellow to transmissive electrochromic polymer was achieved [22], and the CMYK color model is now completed.
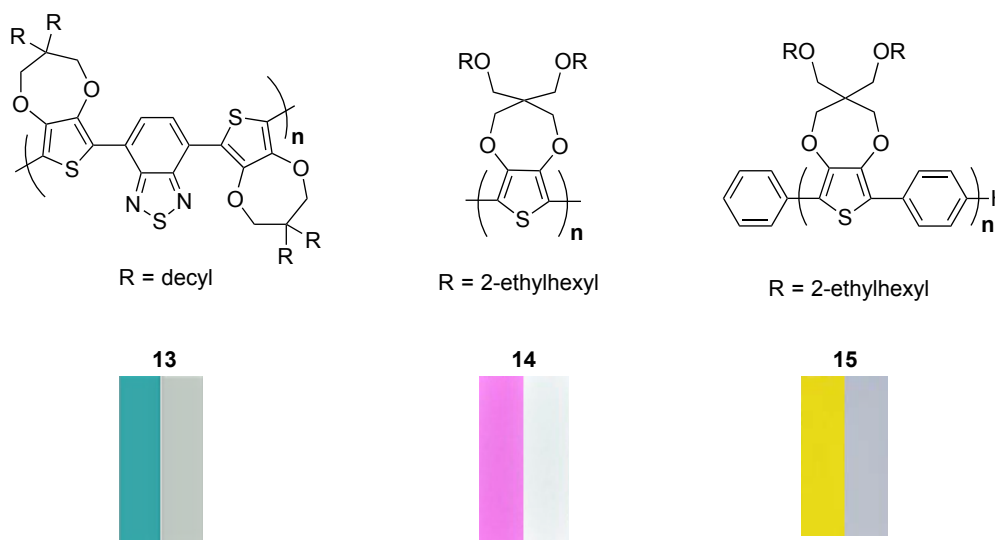
Figure 1.5. Examples of the CMYK color space based electrochromic polymers from the literature [41, 42, 22].

1.4. Bifunctional Materials for Electrochromic Device Applications

As discussed previously, development of polymeric materials towards realization of high quality electrochromic applications is a lively research area. Up to date, various materials that switch between most of the colors in the visible spectrum were realized however materials with better electrochromic properties are always desired for the industrial applications. As the research in the field and its applications develop and expand, in the near feature, it is envisioned that the field will evolve towards realization

of bifunctional materials. It is known from the literature that there are electrochromic polymers which shows fluorescent properties when in solution form [43, 44]. However, to best of our knowledge, only one literature example is present for a polymer which is capable of both fluorescence and electrochromic switching in the solid state [45], meaning that both the polymer film's color and fluorescence state can be synchronously switched upon applied potential (Figure 1.6).
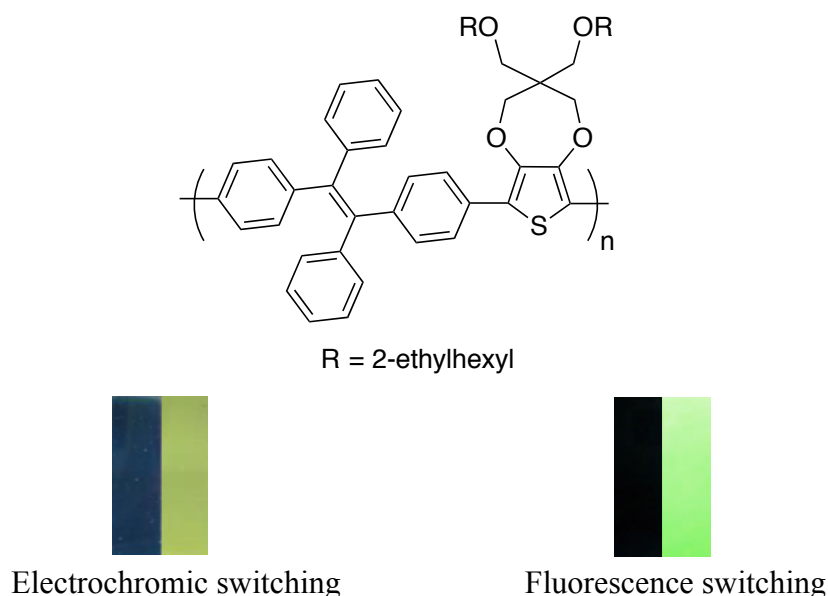
Figure 1.6. A novel alternating polymer from the literature which is capable of both electrochromic and fluorescence switching [45].

1.5. Monomer Design

1.5.1. Donor Acceptor Theory

In order to maximize the neutral conductivity of conducting polymers, minimization of the band gap is extremely important [46]. The importance of band gap originates from the fact that it determines the conductivity and the neutral state color of the polymer. Additionally, the band edges are important parameters for deciding the ease of doping and the stability in the doped stated with respect to the neutral state. The recent research interest in the polymer chemistry world resides in the low band gap polymers and many applications of these type polymers are found in the literature [47]. Research in the field clearly showed that band gap lowering is possible by synthesizing

polymers with alternating donor and acceptor moieties. To explain in its most basic form, donor acceptor theory is the connection of one donor unit with an acceptor unit. From the alternation of this electron rich and electron poor units, valence and conduction bands are broadened. As a result of this broadening, lowering of the band gap is achieved [48]. To explain in further detail, HOMO of the donor unit contributes to HOMO level of the polymer while the LUMO of the acceptor group contributes to the LUMO level of the polymer [49]. The most important advantage of utilizing this theory is the fact that the donor and acceptor moieties can be easily modified and as a result, the magnitude of the band gap can be controlled via controlling the electron donating and withdrawing abilities of the corresponding groups.

1.5.2. Thiophene Based Donor Units

The electron rich nature of thiophene based molecules makes them important candidates for donor units in D-A-D type monomers. When donor units are substituted into the β- positions of thiophene unit, low monomer oxidation potential is achieved and overoxidation of polythiophene ring is prevented. In 1992, the research carried out by Heywang and Jonas showed that by introducing an ethylenedioxy group into thiophene ring (EDOT), the resulting polymer (PEDOT) showed higher stability than polythiophene (PTh) [50]. Besides stability, it was also verified that this new polymer is a paramount choice for RGB color based electrochromic device applications due to its blue to transmissive transition, high optical contrast in the visible region and fast switching time [51].

The main differences between PEDOT and PTh are as follows:

Firstly, PEDOT has higher electron density due to the oxygen atoms present in its structure which leads to a higher HOMO level than PTh. Secondly, EDOT containing molecules have lower oxidation potentials than their thiophene analogs. And lastly, studies in 2004 revealed that increasing the number of EDOT units in the polymer backbone results in decrease in the band gap value [52].
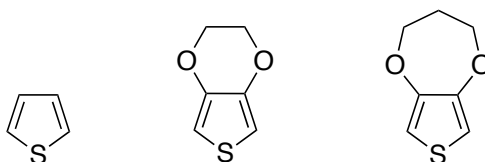
Figure 1.7. Thiophene, EDOT and ProDOT moieties.

Another advance in the field was the realization of 3,4-propylenedioxythiophene (ProDOT) containing electrochromic polymers which show higher contrast values with respect to EDOT containing analogues [53]. The significant difference between ProDOT and EDOT is the extra methylene group present in ProDOT located at the cyclic dioxane structure. Under the light of this data, research in the field demonstrated that variation of the substituent positioned on the cyclic dioxane rings of EDOT and ProDOT, resulted in higher contrast values at their maximum wavelengths for the corresponding polymers of these monomers. Another improvement that ProDOT unit brings to its corresponding polymers is solution processability due to the alkyl chains that can be attached to the cyclic dioxane ring [54].

1.5.3. Importance of Novel Well-defined Neutral State Red Polymeric Materials

The electrochromic polymers that absorb or reflect red and blue colors, a single dominant wavelength is required whereas at least two simultaneous absorption bands in the red and blue regions of the visible spectrum is needed for the green electrochromic polymers. These materials are well studied in the polymeric electrochromic materials research area and the three components of the additive primary color space is well covered. However, novel electrochromic materials with better optical contrasts and faster switching times are required on the way of realization of high quality display applications. The reported blue and green colored electrochromic polymers are generally homopolymers. On the contrary, the red colored electrochromic polymers were reported as copolymers in the recent literature. Homopolymers are preferable over copolymers in industrial production in order to overcome reproducibility issues.

11

For the industrial applications, another important parameter is the switching time. The current state of the art solution processable red to transmissive polymers have switching time in the order of seconds. Electrochromic polymers with faster switching times are preferable for the applications of simple high quality displays. In other words, switching time is an everlasting criterion for electrochromic materials that needs to be constantly improved.

1.5.4. Monomer Design Principle

For the synthesis of the red electrochromic polymer with enhanced electrochromic properties, our monomer design principle was built on two significant observations based on the previous reports in the literature.

Firstly, most of the EDOT and ProDOT containing conjugated polymers utilizes remarkable electrochromic properties as implied from the literature distinctly.

Secondly, donor-acceptor type polymers tend to yield two absorption bands whereas a single absorption band is required for the red to transmissive materials.

Hence, it was envisioned that if EDOT was combined with a highly conjugated donor material, the corresponding polymer should yield a single absorption band in the visible region that is red-shifted with respect to PEDOT.

1.5.5. The Central Unit: Phenanthrocarbazole Moiety
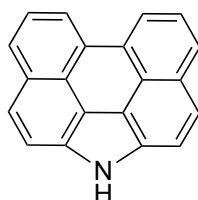
Figure 1.8. Phenanthrocarbazole moiety.

Carbazole containing conjugated polymers shows good electrochromic characteristics [43]. In the light of this information and following our quest on discovering a novel

unit to be utilized in electrochromic polymers, phenanthrocarbazole was chosen as the central unit. Phenanthrocarbazole is a highly conjugated donor structure and it also carries several advantages such as ease of modification and relatively straightforward synthesis which are favorable for the industrial applications. Phenanthrocarbazole containing materials were used in solar cell [55] and OFET [56] applications successfully, however this unit was never utilized in electrochromic polymeric materials.

1.6. Palladium Mediated Cross Coupling Reactions

For the construction of the monomer units, efficient formation of carbon-carbon single bond between two unsaturated carbons in the aromatic units is required. In general, the reaction includes the following steps: a transition-metal-catalyzed oxidative addition reaction across the C-X bond of an electrophile, transmetalation with a main group organometallic nucleophile, and a reductive elimination step leading to the formation of carbon-carbon bond respectively [57, 58].
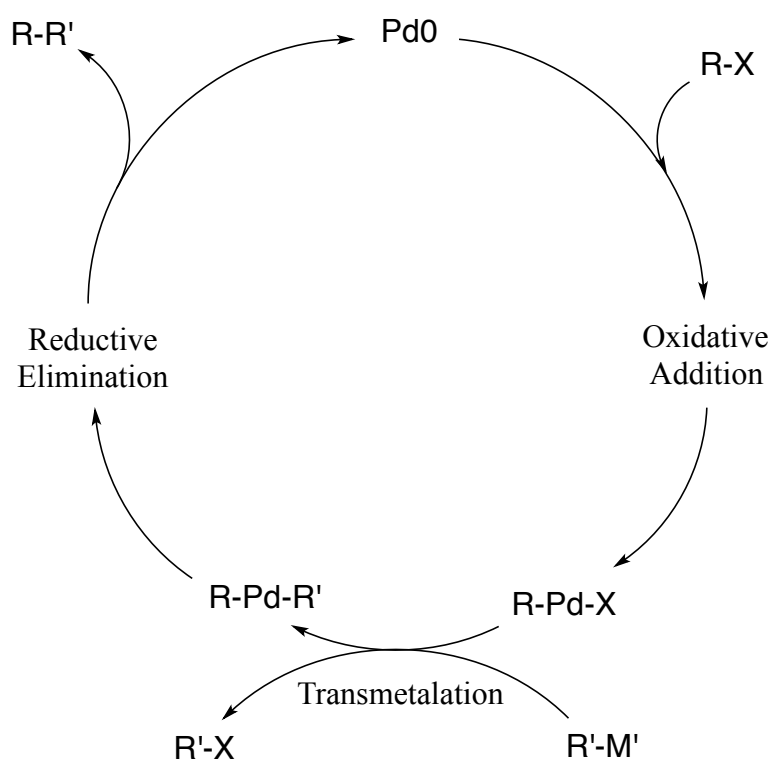
Scheme 1.1. General reaction mechanism of a cross coupling reaction.

13

The most commonly used transition-metal catalysts are palladium and nickel based complexes. And the choice for organometallic nucleophiles are Grignard reagents for Kumada-Corriu, stannyl derivatives for Stille and boron containing species for Suzuki-Miyaura reactions.
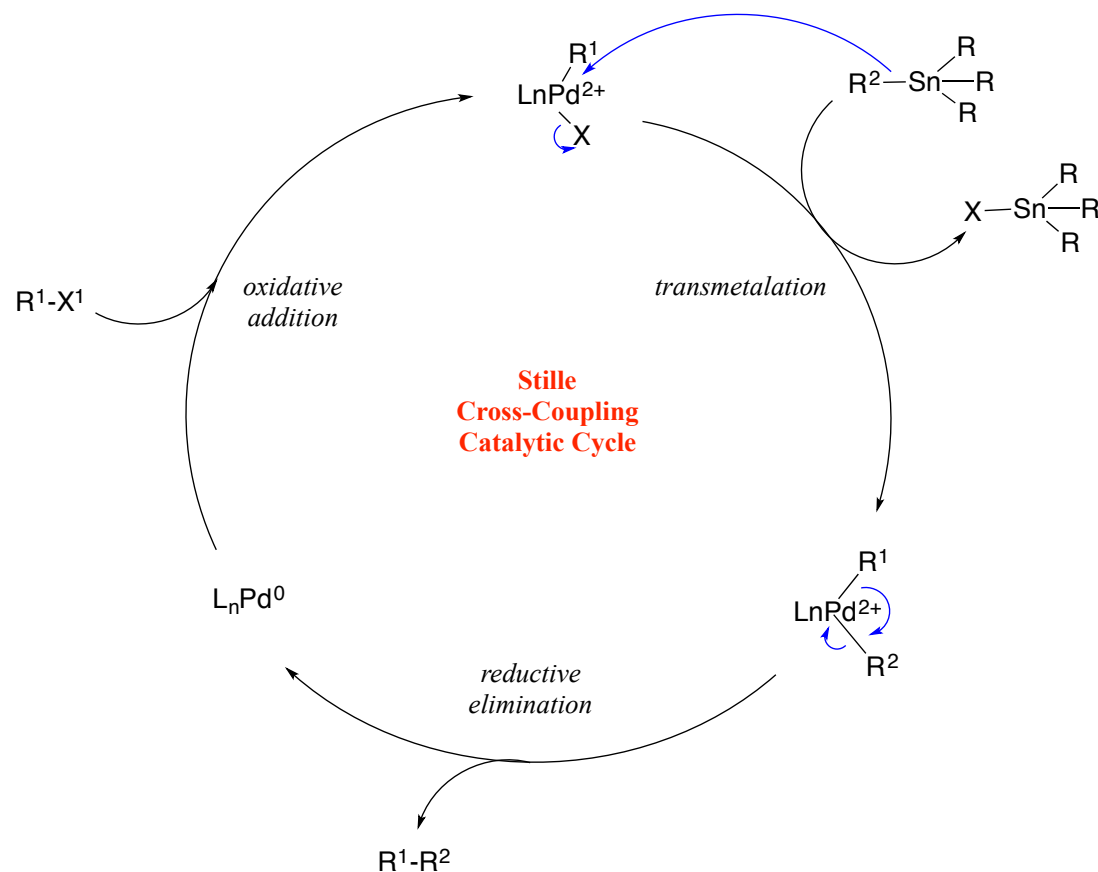
Scheme 1.2. Stille coupling mechanism.

Formation of carbon-carbon bonds are extremely essential for organic chemistry. Richard F. Heck, Ei-ichi Negishi and Akira Suzuki was jointly awarded for Nobel Price in Chemistry in 2010 for palladium-catalyzed cross couplings in organic synthesis [59]. The main advantage of these kind of coupling reactions is that the conditions are generally mild and many functional groups can be tolerated which is important for the synthesis of advanced functional monomers. The most profitable and widely used ones among these reactions are Stille and Suzuki coupling reactions. The main difference between them is that stannyl substituted benzene rings give poor reactivity under Stille coupling conditions. Applications of these reactions with

14

various aromatic units showed that Suzuki coupling is more conventional for the synthesis of benzene containing monomers with boronic groups on the benzene ring, whereas Stille coupling is more applicable for thiophene-containing monomer synthesis with stannyl groups on the thiophene ring [57, 58].

1.7. Polymerization Methods

1.7.1. Electrochemical Polymerization

Electrochemical polymerization is an important method for synthesis and rapid characterization of conjugated polymers. This method has the advantage of synthesizing the polymer film directly on the electrode and its better suited for studying electrochemical and optical properties of the polymer. Additionally, no further purification is required in this method. Electrochemical polymerization is basically the self-coupling reaction of a monomer in an inert organic solvent – supporting electrolyte system, yielding a homopolymer [60]. It can be carried out potentiostatically or galvanostatically. Regardless of the method being used, the mechanism is the same. In a typical electrochemical polymerization experiment firstly, the monomer is dissolved in an appropriate solvent that contains the supporting electrolyte. Choice of solvent and supporting electrolyte is extremely crucial and they should fulfill the following requirements:

1) Both the solvent and the supporting electrolyte should be stable at the potential range required for the electrochemical polymerization.
2) The solvent should dissolve both the monomer and the supporting electrolyte effectively.

Acetonitrile is an excellent choice as the solvent due to its high permittivity and large potential range. Secondly, in order to oxidize the monomer on the electrode surface, anodic potential is applied. In anodic polymerization irreversible oxidation takes place and for cathodic polymerization, irreversible reduction takes place. Generally anodic polymerization is preferred for the synthesis of homopolymers of electron rich monomers due to their tendencies for oxidation [61].

15
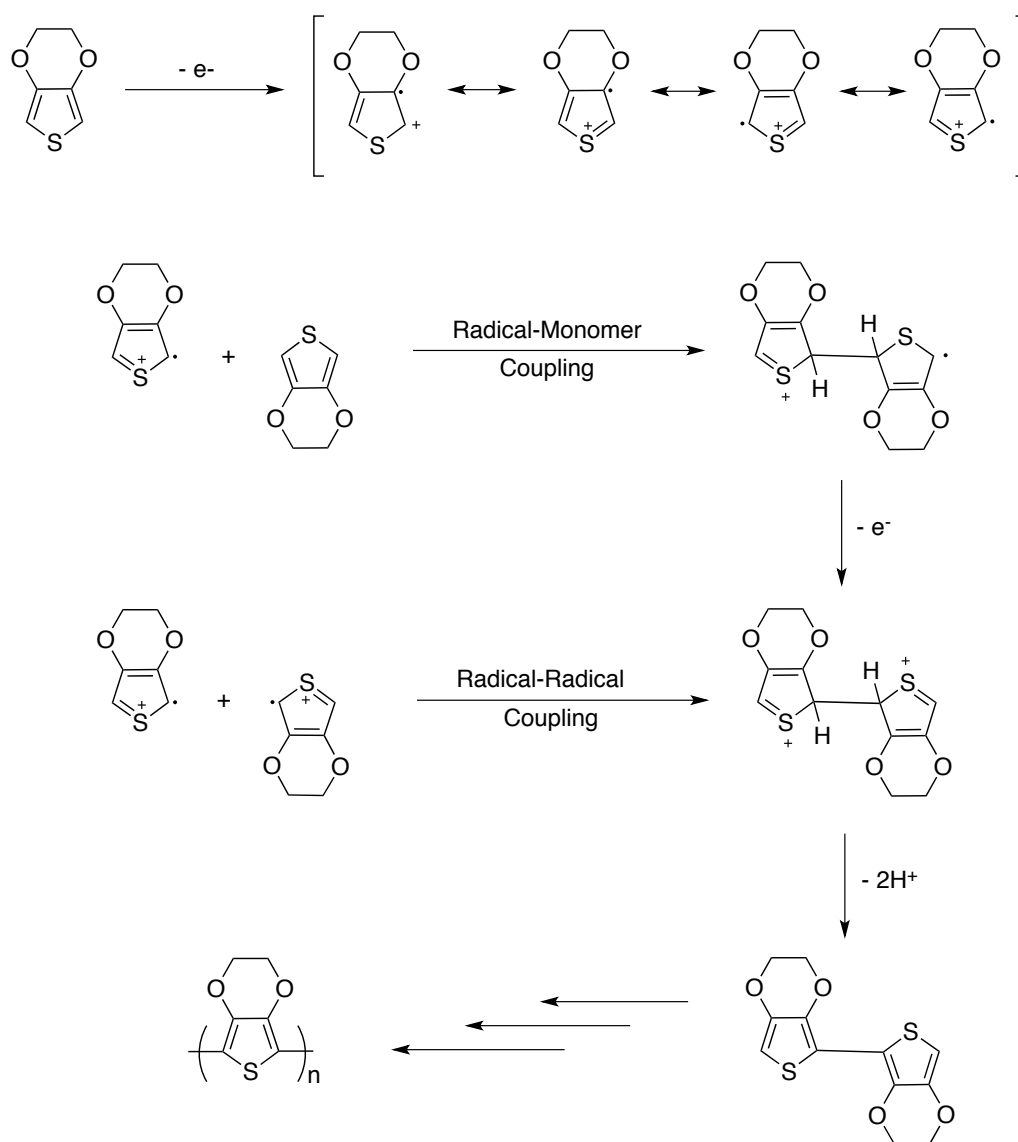
Figure 1.9. Electrochemical polymerization mechanism of EDOT.

Under applied electric field, an electron is removed from the monomer. Thus the monomer is oxidized and converted into its radical cation. After the formation of the radical cation, two reactions can occur. The radical cation can react with monomers present in the solution or it can couple with an another radical cation [62, 63]. Both of the options yield the same dimer unit upon a two-proton loss. However, they are different mechanisms and they can be identified using spectroelectrochemistry studies. For the reaction of a radical cation with a neutral monomer, upon applied potential, the absorption band depletes while polaron and bipolaron bands increases. The same case is valid for the coupling of two radical cations but the polaron band starts to

deplete as the potential keeps increasing. This phenomenon yields in higher transparency in the oxidized state of the polymer. As a result of the repeated coupling reactions, the polymer is synthesized, being doped at the same time. Due to the high conjugation in the newly synthesized system, the polymer oxidation potential is lower than the monomer oxidation potential. The mechanism of electropolymerization is shown in Figure 1.7.

1.7.2. Oxidative Chemical Polymerization

Oxidative chemical polymerization is the coupling of heterocyclic compounds using Lewis acid catalysts such as $MoCl_5$, $FeCl_3$ and $RuCl_3$. Chemically synthesized polymers shows similar properties with the electrochemically synthesized ones. This polymerization technique is an important method for obtaining polymers with high molecular weights. Additionally, if the polymer is solution processable, it can be spray coated on ITO surface for electrochromic applications. For the industrial applications, spray coating is preferred over electrochemical polymerization since it can be expensive and operationally difficult for large area applications [64].
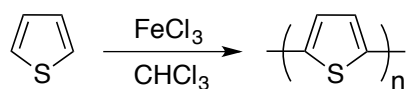
Figure 1.10. Oxidative chemical polymerization.

1.8. Characterization of Conducting Polymers

The characterization methods of conducting polymers includes cyclic voltammetry, spectroelectrochemistry, kinetic studies, NMR spectroscopy, FTIR spectroscopy, AFM and SEM measurements [60]. Cyclic voltammetry is an important tool for the investigation of the redox properties of polymers. Spectroelectochemistry studies combine electrochemical and spectroscopic techniques to maintain knowledge on band gap (E_g), λ_{max}, and polaron and bipolaron formation upon oxidation. Kinetic studies probe changes with transmittance with time. By stepping between neutral and oxidized states under repeated potential, the percent transmittance changes and the

17

switching times of the polymer are studied. ^{1}H-NMR spectra of the polymers give broad peaks and reveal many information on polymer formation, however if the polymer is not soluble, NMR is not an option for characterization. In this case, FTIR, AFM and SEM measurements supply valuable information. FTIR spectra of the polymer gives information about the success of polymerization and determine possible degradation reactions. AFM measurements reveals data on polymer film such as smoothness, roughness and film thickness. For the SEM measurements; cauliflower like forms, which are common type of structures for conjugated polymers, can be displayed.

1.9. Aim of the Study

In this study, our aim was the realization of novel, well-defined red to transmissive electrochromic polymers with high optical contrast, fast switching time and high switching stability. A monomer design principle was built in order to realize red to transmissive electrochromic polymer based on two significant observations from the literature results. Firstly, most of the conjugated polymers that utilize EDOT and ProDOT as donor units show remarkable electrochromic properties. Secondly, donor-acceptor type polymers, when there is a good match, tend to yield two absorption bands whereas a single absorption band is required for the red to transmissive materials. Hence, it was envisioned that if EDOT was combined with a highly conjugated donor material, the corresponding polymer should yield a single absorption band in the visible region that is red-shifted with respect to PEDOT. In order to see if our design principle is valid, two monomers were designed, synthesized and the electrochromic properties of their corresponding polymers were investigated in detail.

CHAPTER 2

RESULTS AND DISCUSSION

2.1. Monomer Syntheses

2.1.1. Synthesis of the Central Unit

Scheme 2.1 shows the synthetic pathway for the central phenanthrocarbazole unit.
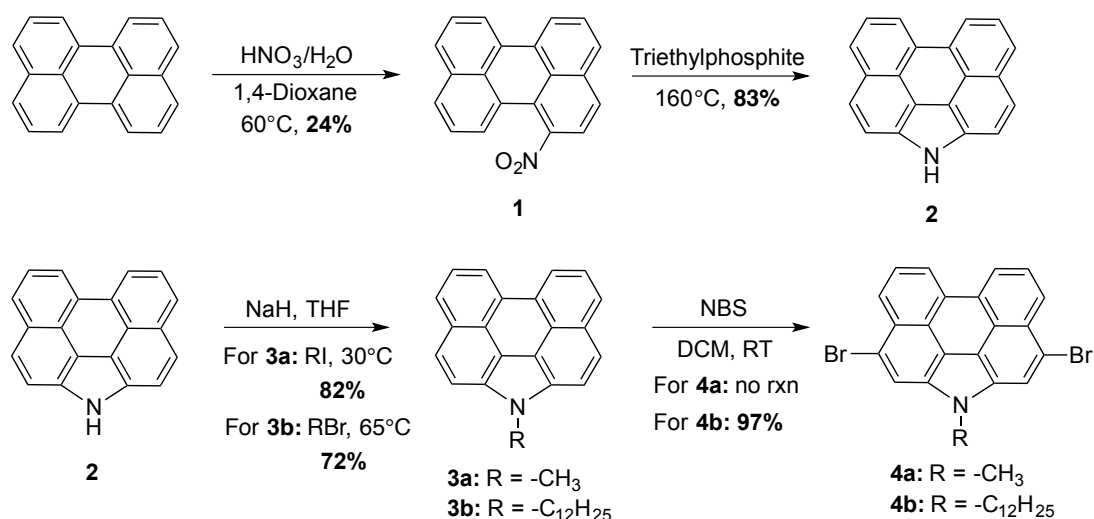
Scheme 2.1. Synthetic pathway of central unit.

The first step was the nitration of the perylene unit with fuming nitric acid. The major product of the reaction is the mononitration of the perylene at the 3 position, an undesired side product. Due to the close R_f values of the 1-nitroperylene (**1**) and 3-nitroperylene, purification was also another drawback for this reaction apart from its low yield. The filtration and column chromatography steps of this reaction have been optimized and synthesis of 1-nitroperylene was achieved in relatively large scale with

24% yield [65]. Then the treatment of 1-nitroperylene (**1**) with triethylphosphite yielded phenanthrocarbazole (**2**) with 78% yield [66]. In order to protect the nitrogen of the phenanthrocarbazole (**2**), firstly methylation was performed with 82% yield. Although many examples of the bromination of the alkylated phenanthrocarbazoles are present in the literature [67], bromination of the methylated phenanthrocarbazole (**3a**) was not successful. Protection of the nitrogen was achieved by the synthesis of the alkylated carbazole derivative with 12-carbon chain (**3b**) under the same conditions with 72% yield. Then the bromination of **3b** with NBS was successful with 97% yield. Hence the synthesis of the central donor group was completed.

2.1.2. Coupling of Central Unit with EDOT and ProDOT

2.1.2.1. Synthesis of 3,10-Bis(2,3-dihydrothieno[3,4-b][1,4]dioxin-5-yl)-1-dodecyl-1*H*-phenanthro[1,10,9,8-c,d,e,f,g]carbazole (DEP)

The synthetic pathway for the monomer is as shown in Scheme 2.2.
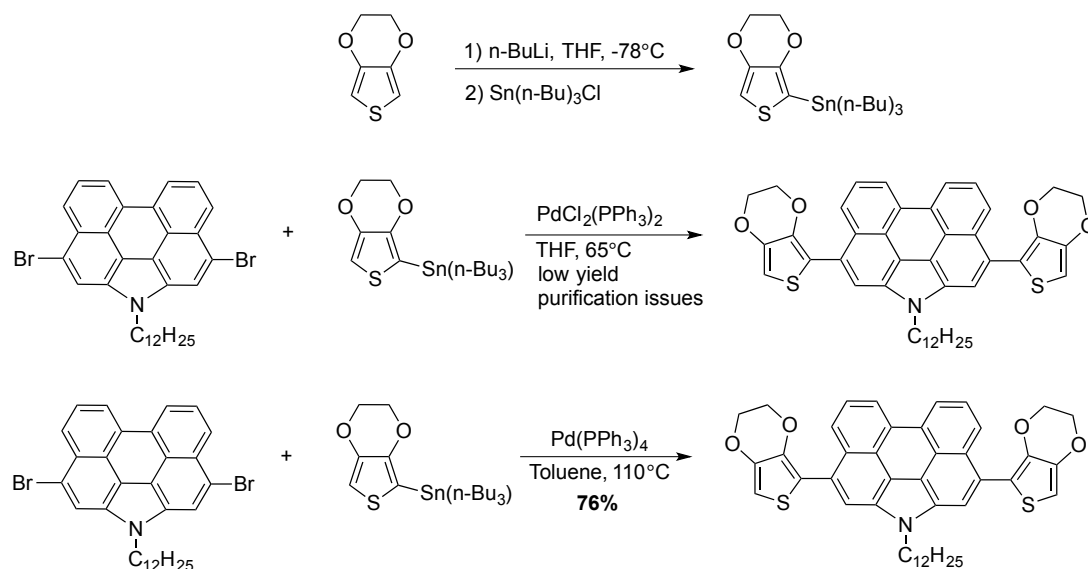
Scheme 2.2. Synthetic pathway of DEP.

EDOT unit was stannylated [68], and without any further purification coupled with the central group via Stille Coupling. Firstly, the catalyst and the solvent system was chosen as bis(triphenylphosphine)palladium(II) dichloride and THF. The monomer

20

was formed however, due to formation of various side products, purification problems were encountered. After performing the column chromatography right after the reaction and optimization of the reaction conditions (change of the catalyst, the solvent, and the temperature), monomer was successfully synthesized with a yield of 76%. The optimized conditions were tetrakis(triphenylphosphine)palladium(0) as the catalyst and Toluene as the solvent at 110 °C. The monomer was fully characterized by ^{1}H-NMR, ^{13}C-NMR and HRMS.

2.1.2.2. Synthesis of 3,10-Bis(3,3-bis(((2-ethylhexyl)oxy)methyl)-3,4-dihydro-2*H*-thieno[3,4-b][1,4]dioxepin-6-yl)-1-dodecyl-1*H*-phenanthro[1,10,9,8-c,d,e,f,g] carbazole (DPP)

The synthetic pathway for the monomer is as shown in Scheme 2.3.
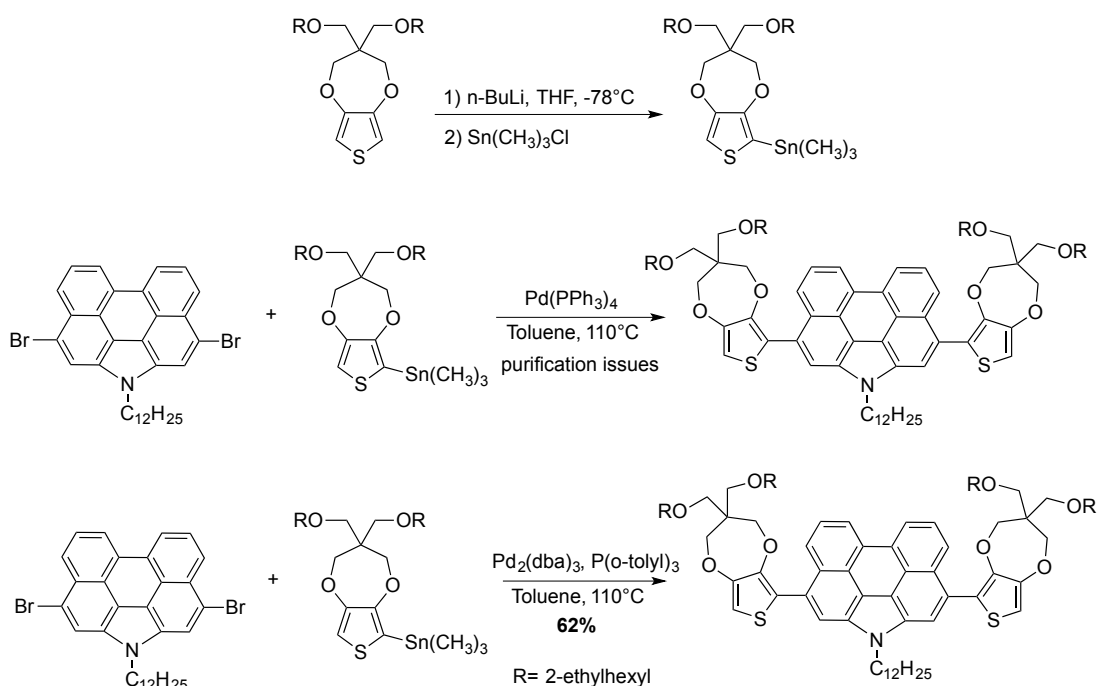
Scheme 2.3. Synthetic pathway of DPP.

ProDOT unit was stannylated [69] and coupled with the central unit without any further purification. The coupling was performed via Stille Coupling. Firstly, the coupling was performed with the optimized conditions used for DEP. However,

purification problems were encountered due to the high ratio of mono-coupled product and the relatively low yield. Then the catalyst was changed to %5 tris(dibenzylideneacetone) dipalladium(0) ($Pd_2(dba)_3$) and 15% tri(o-tolyl)phosphine ($P(o\text{-tolyl})_3$). This new conditions lowered yield of the mono coupled product, hence increasing the monomer yield. The purification was successful due to the decrease in the amount of side products and optimization of the column chromatography conditions. The monomer was fully characterized by ^{1}H-NMR and ^{13}C-NMR.

2.2. Polymer Synthesis

2.2.1. Synthesis of Poly-3,10-bis(3,3-bis(((2-ethylhexyl)oxy)methyl)-3,4-dihydro-2*H*-thieno[3,4-*b*][1,4]dioxepin-6-yl)-1-dodecyl-1*H*-phenanthro[1,10,9,8-c,d,e,f,g]carbazole (PDPP)

DPP was polymerized chemically using $FeCl_3$ as the catalyst in DCM as the solvent. After allowing polymerization for 11 hours at room temperature, the resulting polymer was treated with hydrazine monohydride to reduce the polymer to its neutral state. Following a common purification method, the polymer was obtained successfully and characterized by ^{1}H-NMR.

2.3. Electrochemical and Electrochromic Properties of Polymers Based on Phenanthrocarbazole

2.3.1. Electropolymerization of Monomers

All polymerizations were performed using a three electrode system by applying multiple scan voltammetry where a platinum wire was the counter electrode, a Ag wire was the reference electrode and an ITO coated glass was the working electrode.

2.3.1.1. Electropolymerization of DEP

The potentiodynamic polymerization of DEP on ITO coated glass slide was performed from a 10 mM solution of DEP in 0.1 M $TBAPF_6$/MeCN supporting electrolyte–solvent couple (Figure 2.1). An oxidation peak was observed at 0.69 V which was attributed to non-polymerizable radical cation formation most probably on the perylene unit.
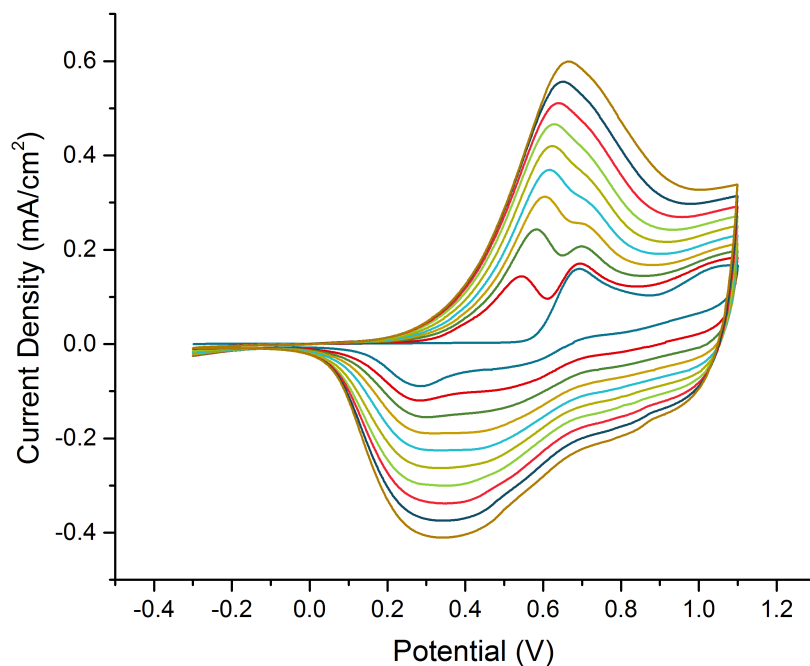
Figure 2.1. Repeated scan polymerization of DEP (WE: ITO, CE: Pt wire, RE: Ag wire, 0.1 M TBAPF$_6$/MeCN, 100 mV s^{-1}, 10 cycles).

The monomer oxidation centered on EDOT unit was observed at 1.07 V and formation of a highly electroactive polymer was observed in the following cycles. The polymer oxidation and reduction potentials (10th cycle) were observed as 0.68 V and 0.35 V respectively.

2.3.1.2. Electropolymerization of DPP

A solution of DPP (10 mM) was prepared in a mixture of DCM and acetonitrile (MeCN) (5/95, v/v) since the solution was becoming blurry in the absence of DCM. NaClO$_4$ and LiClO$_4$ was used as the supporting electrolytes. The potentiodynamic polymerization of DPP on ITO coated glass slide was shown in Figure 2.2. The monomer oxidation centered on ProDOT unit was observed at 0.69 V. Upon formation of a well-defined redox couple, formation of an electroactive polymer film was observed in the following cycles. The polymer oxidation and reduction potentials (10th cycle) were observed as 0.72 V and 0.35 V respectively.
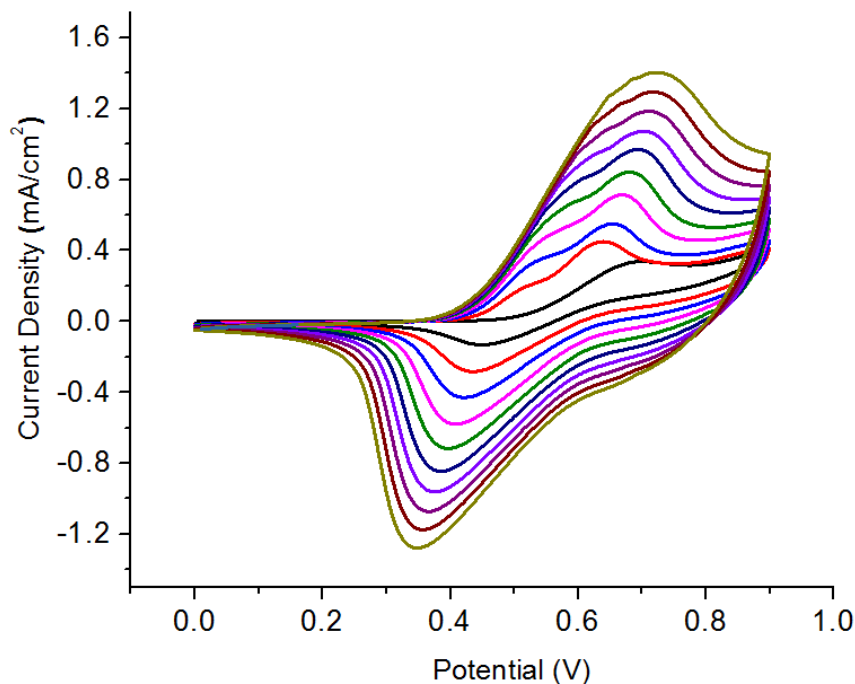
Figure 2.2. Repeated scan polymerization of DPP (WE: ITO, CE: Pt wire, RE: Ag wire, 0.1 M NaClO$_4$/LiClO$_4$/DCM/MeCN, 100 mV s^{-1}, 10 cycles).

2.3.1.3. Cyclic Voltammetry of Chemically Synthesized PDPP

DPP was chemically polymerized with FeCl$_3$ in DCM and the resulting polymer was spray-coated on ITO coated glass electrode from a solution of 5 mg/mL in chloroform in order to investigate its electrochemical and electrochromic properties. The measurement was performed in a monomer free 0.1 M NaClO$_4$/LiClO$_4$/DCM/MeCN solution. Cyclic voltammetry studies showed that the polymer was oxidized and reduced at very similar potentials compared to the electrochemically produced polymer (Figure 2.3). The oxidation and reduction potentials were calculated as 0.79 V and 0.49 V respectively.
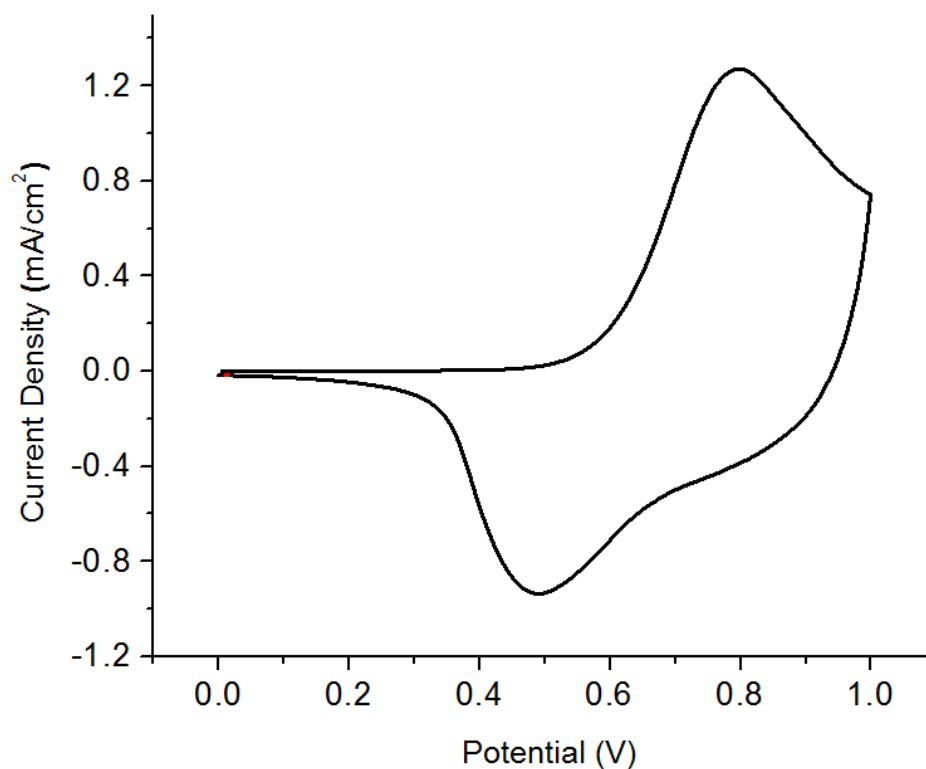
Figure 2.3. Single scan cyclic voltammetry of chemically synthesized PDPP (WE: ITO, CE: Pt wire, RE: Ag wire, 0.1 M NaClO$_4$/LiClO$_4$/DCM/MeCN, 100 mV s^{-1}, 1 cycle).

2.3.2. Characterization of Polymers

2.3.2.1. Characterization of PDEP

For the characterization of the polymer, ATR-FTIR, SEM and AFM measurements were performed since NMR was not an option due to the insolubility of the polymer.

2.3.2.1.1. ATR-FTIR

The monomer solution in CHCl$_3$ was drop casted on ITO glass and the ATR- FTIR was recorded (Figure 2.4). The polymer was electrochemically coated as described in the electropolymerization part and ATR-FTIR was recorded (Figure 2.5).
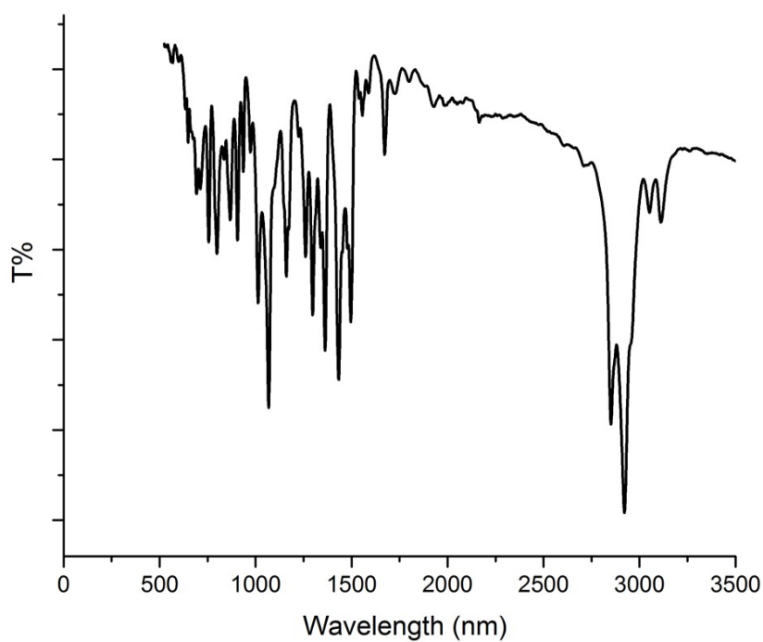
Figure 2.4. ATR-FTIR of DEP.
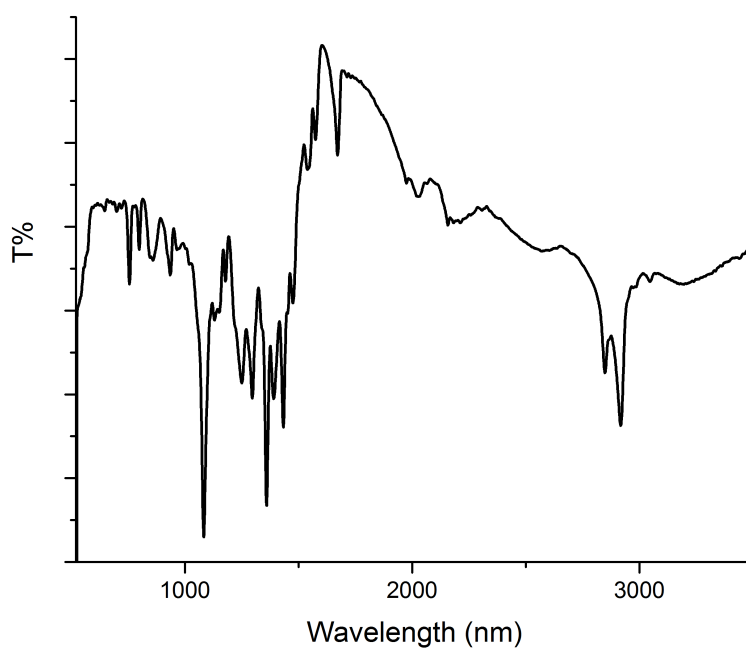
Figure 2.5. ATR-FTIR of PDEP.

As can be seen from the spectra (Figure 2.5), C-H stretching of the EDOT units in the monomer (3020-3170 cm^{-1}) almost completely disappeared as the polymer film formed on the surface. The expected peaks, C-N stretching (1080-1360 cm^{-1}), C-O stretching (1000- 1300 cm^{-1}), Aromatic C-H stretching ($\sim$2950 cm^{-1}), aliphatic C-H stretching ($\sim$2850 cm^{-1}) are clearly observed in the IR spectrum of the polymer.

26

2.3.2.1.2. SEM

Scanning electron microscopy analyses showed the polymer film formed on ITO surface uniformly (Figure 2.6). Closer images (Figure 2.7) clearly show cauliflower like forms, which are the common type of structures that are observed for conjugated polymer films.
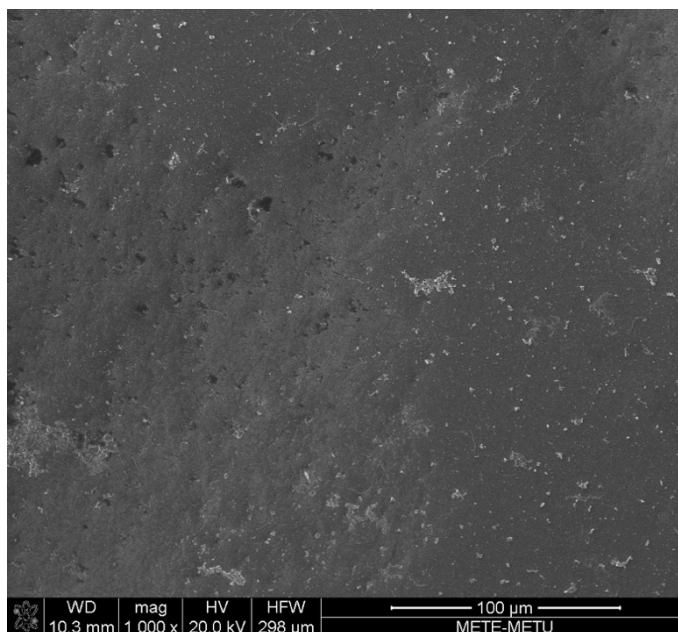
Figure 2.6. SEM images of PDEP at 1000x magnification.
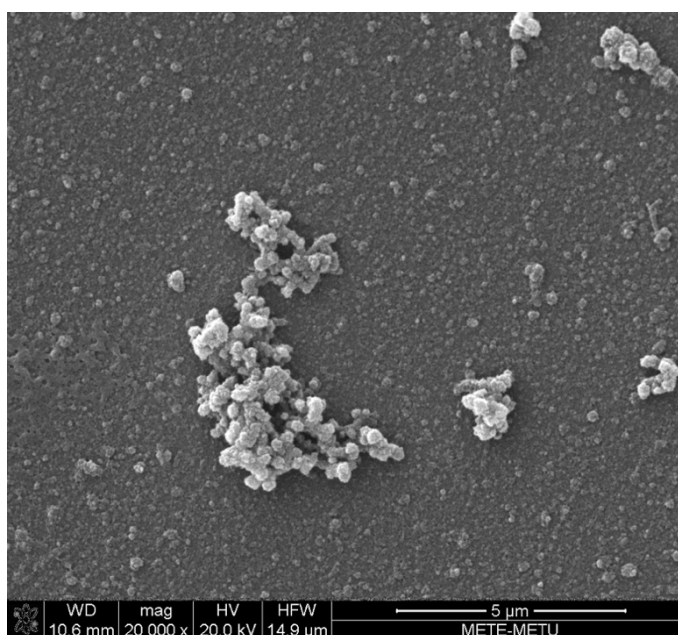
Figure 2.7. SEM images of PDEP at 20000x magnification.

2.3.2.1.3. AFM
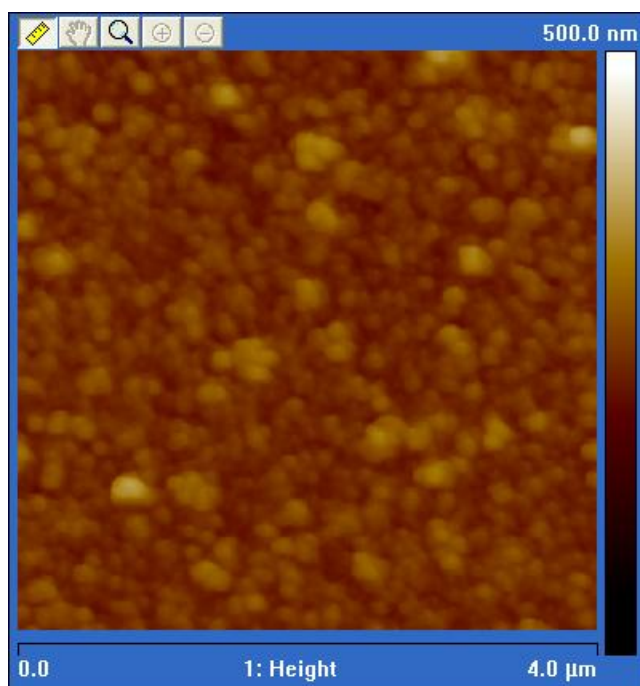
Figure 2.8. AFM image of PDEP (4 μm x 4 μm).

AFM images also show the formation of a smooth film on ITO surface (Figure 2.8).A roughness of 16 nm was determined over a large area (Figure 2.9).
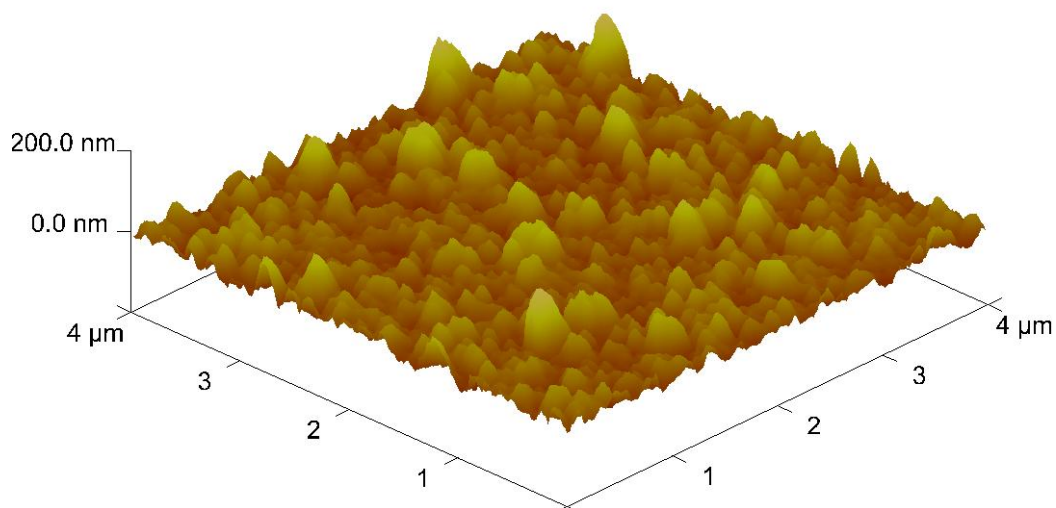
Figure 2.9. Roughness analysis of PDEP (4 μm x 4 μm x 200 nm).

The film thickness was determined form 3 different points that averaged to a thickness of 147 nm (Figure 2.10).
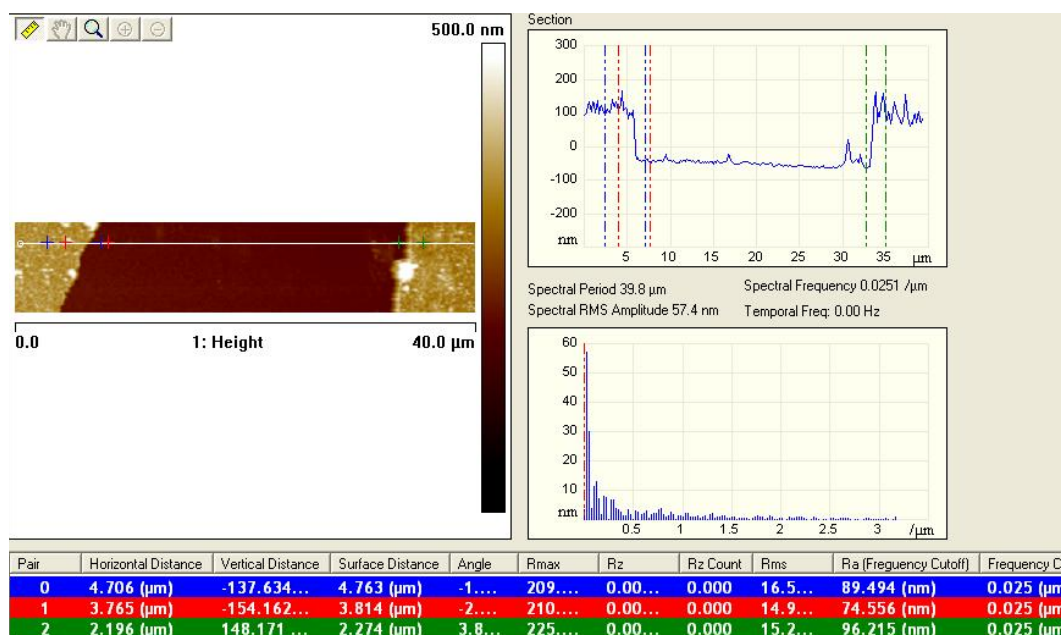
Figure 2.10. Film thickness analysis of PDEP.

2.3.2.2. Characterization of PDPP

Characterization of the PDPP was achieved by ^{1}H-NMR since the polymer was soluble in chloroform. AFM and SEM measurements will be performed in order to further investigate the polymer film.

2.3.2.2.1. ^{1}H-NMR of PDPP

The peak located at 6.66 ppm in the ^{1}H-NMR of the DPP is arising from the protons of the ProDOT moiety (Figure 2.11). As can be seen from Figure 2.12, ^{1}H-NMR of the PDPP revealed the complete disappearance of this peak which is the main proof of the successful polymerization process.
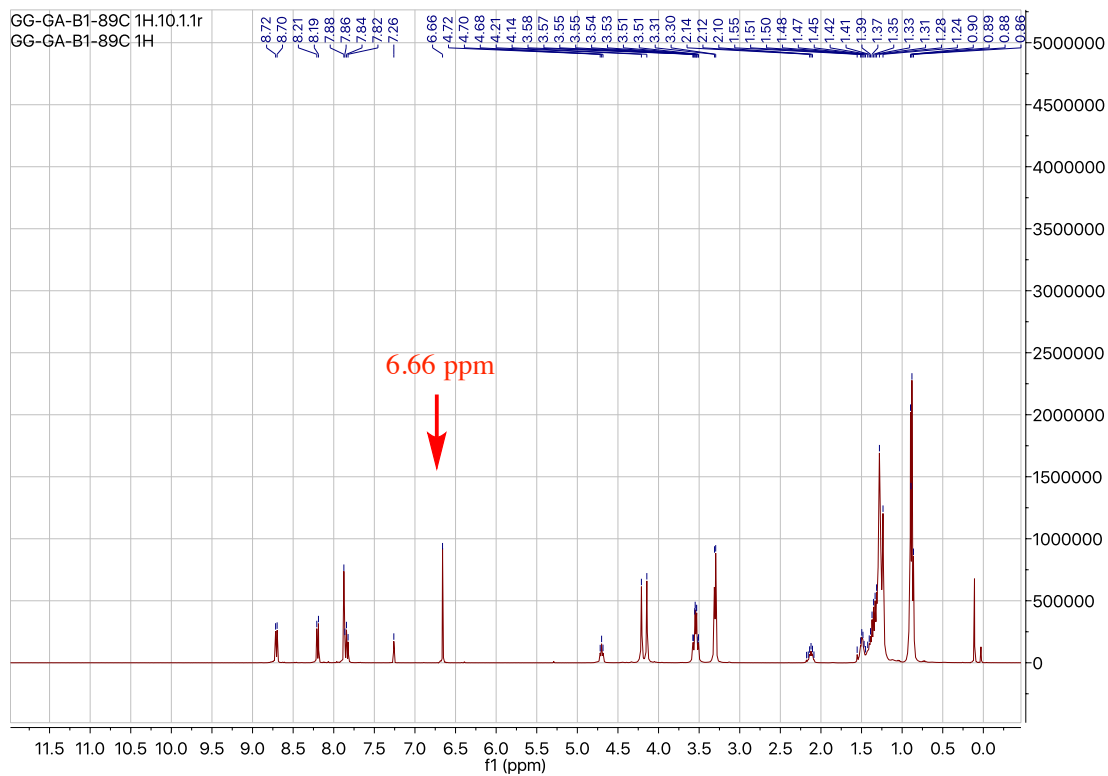
Figure 2.11. ^{1}H-NMR of DPP.
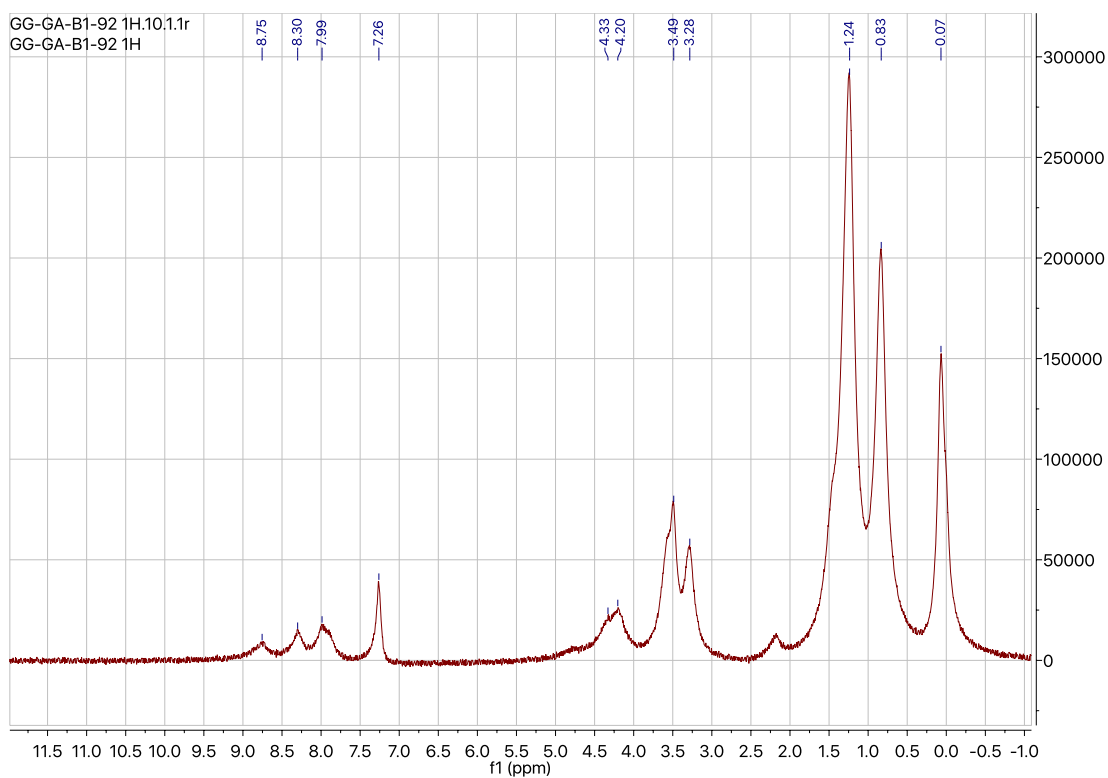
Figure 2.12. ^{1}H-NMR of PDPP.

2.3.3. Spectroelectrochemistry Studies of Polymers

In order to investigate the optical and structural responses of the polymers upon doping process, spectroelectrochemistry studies were performed. These studies prove the evolution of charge carriers upon doping process. Polymer films that were grown potentiodynamically on ITO or by spray coating was subjected to spectroelectro-chemistry studies. The UV-vis-NIR spectra were recorded as a function of applied potential in a monomer free 0.1 M TBAPF$_6$/ACN solution.

2.3.3.1. Spectroelectrochemistry Studies of PDEP

For the UV-vis-NIR spectra of PDEP, applied potential was -0.3 V to 1.1 V with 0.1 V increments. The results are shown below (Figure 2.13). In its neutral state the PDEP show a narrow absorption band centered at 480 nm. Upon applied potential the strong absorption gradually depletes and a transmissive state is achieved.
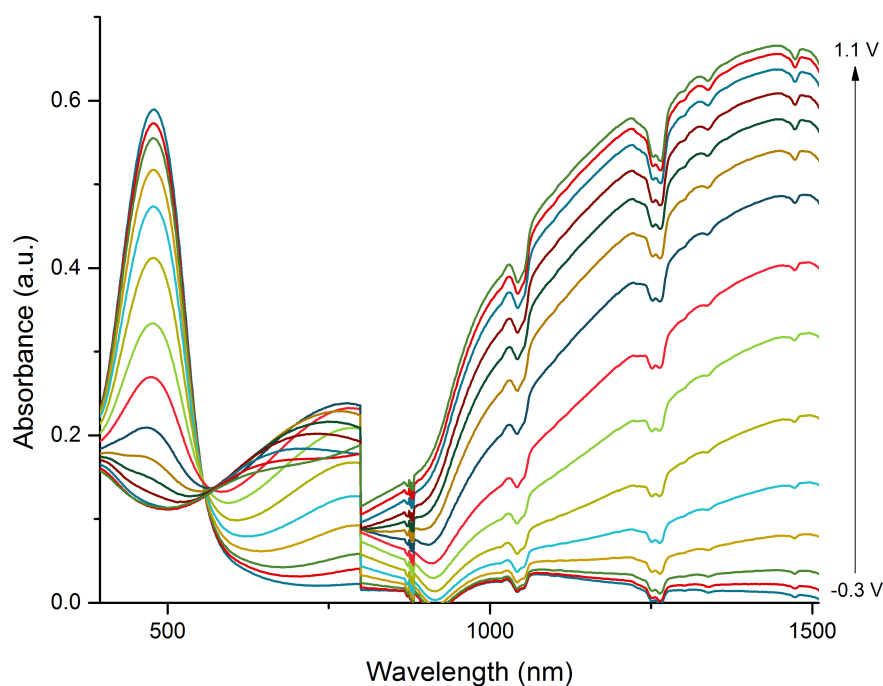
Figure 2.13. Spectroelectrochemistry studies of PDEP (-0.3 V to 1.1 V with 0.1 V increments).

31

The polaron band (centered at 770 nm) increases upon applied positive potential. As the potential keeps increasing however, depletion of this band was observed. This is a crucial phenomenon resulted in higher transparency in the oxidized state (Figure 2.13). The colors of the polymer at its neutral and oxidized states can be seen from Figure 2.14.

-0.3 V vs Ag wire
CIE-L*ab : 48, 44, 21

1.1 V vs Ag wire
CIE-L*ab : 60, -2, 10
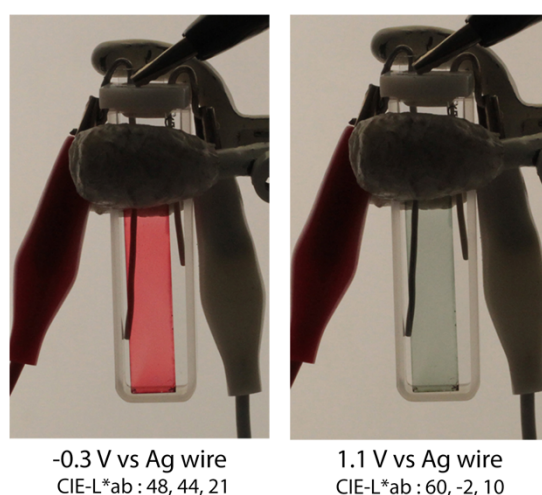
Figure 2.14. Photographs of the PDEP at its neutral and oxidized states.

2.3.3.2. Spectroelectrochemistry Studies of PDPP

2.3.3.2.1. Spectroelectrochemistry Studies of Electrochemically Synthesized PDPP

The UV-vis-NIR spectra was recorded by applying series of positive potentials (Figure 2.15). For the electrochemically synthesized PDPP, the absorbance changes were recorded between -0.2 V and 0.85 V.

In its neutral state the electrochemically synthesized PDPP showed a narrow absorption band centered at 480 nm. Upon applied potential the strong absorption gradually depletes and polaron and bipolaron bands increases.
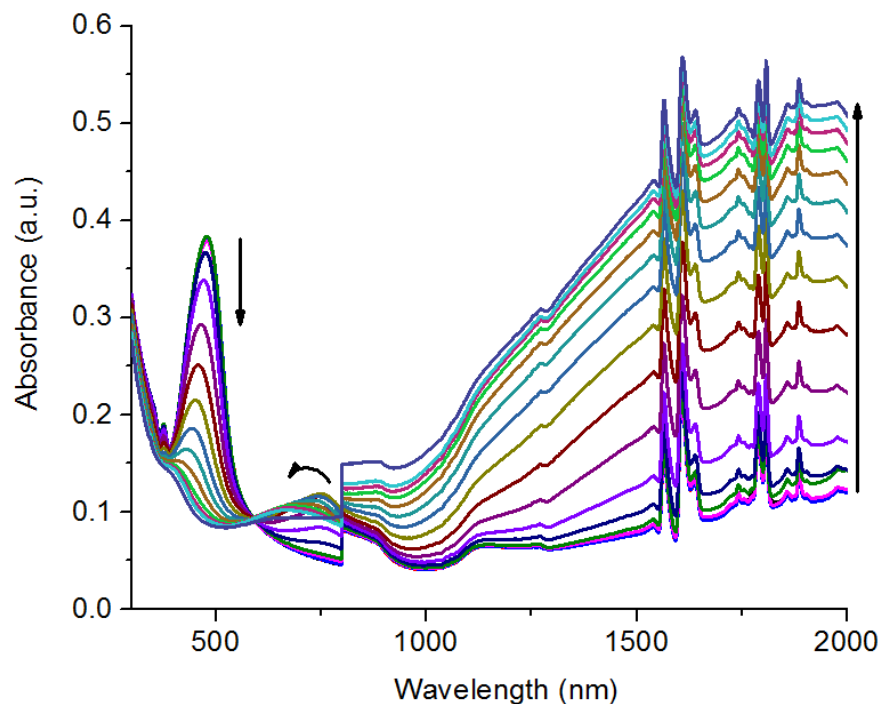
Figure 2.15. Spectroelectrochemistry studies of electrochemically synthesized PDPP (-0.2 V to 0.85 V).

Unlike PDEP, PDPP showed orange color in its neutral state, rather than the expected red color. Upon applied potential, green and transmissive gray colors were achieved respectively (Figure 2.16). PDPP showed luminescent properties in its neutral state and the luminescence was completely disappeared at the oxidized state (Figure 2.17). Photoluminescence spectroscopy studies will be performed in order to further investigate the luminescent properties and the dynamics of the luminescence lost (whether it is happening gradually or not).

-0.20   0.65   0.70   0.75   0.85   V
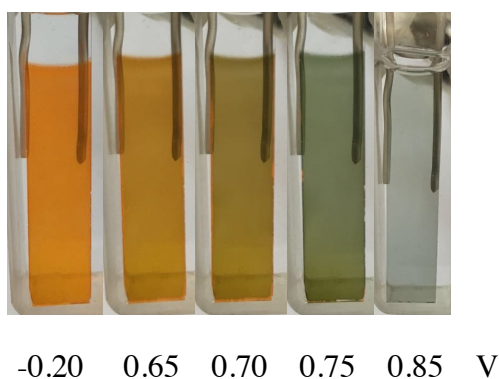
Figure 2.16. Photographs of electrochemically synthesized PDPP upon oxidative doping.

33

neutral state   oxidized state
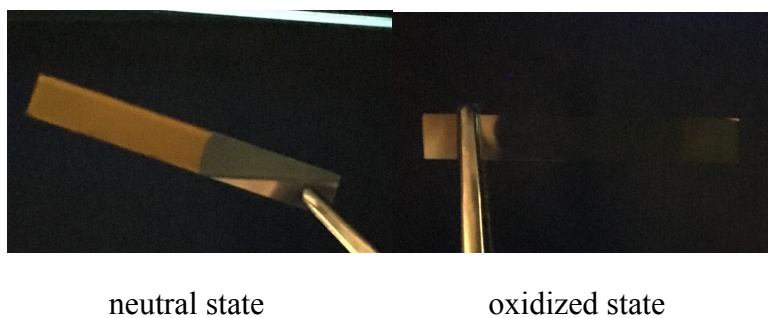
Figure 2.17. Photographs of electrochemically synthesized PDPP under the UV light (365 nm) at its neutral and oxidized states.

2.3.3.2.2. Spectroelectrochemistry Studies of Chemically Synthesized PDPP

The UV-vis-NIR spectra was recorded by applying series of positive potentials (Figure 2.18). For the chemically synthesized PDPP, the absorbance changes were recorded between -0.2 V and 0.85 V.
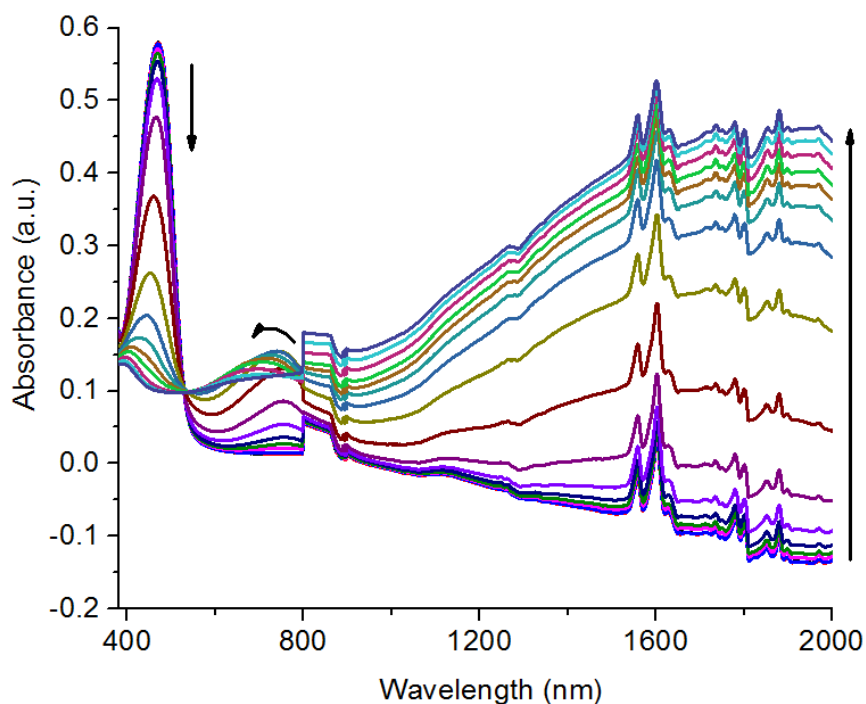
Figure 2.18. Spectroelectrochemistry studies of chemically synthesized PDPP (-0.2 V to 0.75 V).

In its neutral state the chemically synthesized PDPP showed a narrow absorption band centered at 470 nm. Upon applied potential the strong absorption gradually depletes and polaron and bipolaron bands increases. The polymer film showed the similar electrochromic (Figure 2.19) and luminescent properties (Figure 2.20) with the electrochemically synthesized PDPP.

-0.20   0.65   0.70   0.75   V
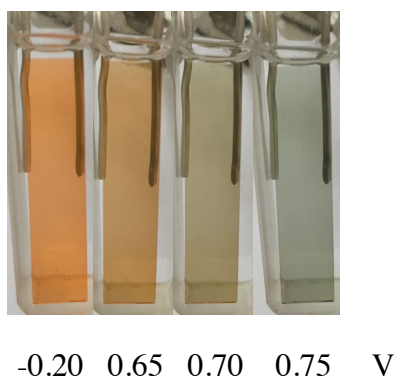
Figure 2.19. Photographs of chemically synthesized PDPP upon oxidative doping.

neutral state   oxidized state
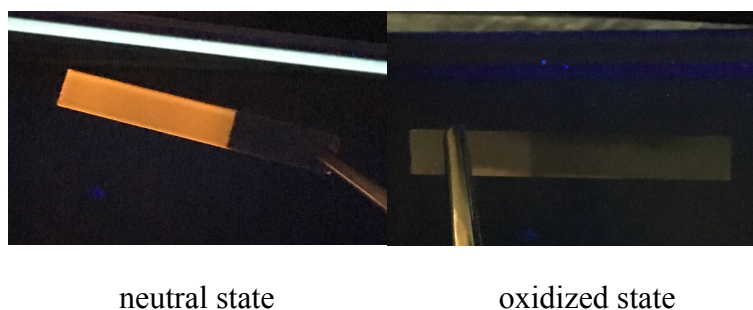
Figure 2.20. Photographs of chemically synthesized PDPP under the UV light (365 nm) at its neutral and oxidized states.

2.3.4. Kinetic Studies of Polymers

The kinetic studies for the polymers were performed in order to probe changes in transmittance with time, while the polymer was repeatedly stepped between the neutral and oxidized states. The studies were performed at the maximum absorption of the polymers at their neutral state in order to investigate their response times and switching

abilities. The polymer film was deposited on ITO glass slide by repeated scanning (15 cycles) in 0.1M TBAPF$_6$/MeCN (monomer free).

2.3.4.1. Kinetic Studies of PDEP

The optical contrast of the PDEP was found to be 51% at 480 nm (λ_{max}) (Figure 2.21) with a fast switching time of 0.65 seconds for oxidation and 0.52 seconds for reduction (Figure 2.22). The optical contrast is comparable with the other red to transmissive polymers (60%, 57%, 56%) in the literature, however the switching time was found to be considerably faster (0.65 s versus, 3.6 s, 2.3 s, 1.6 s) [37-39]. The coloration efficiency of the material was calculated to be 172 cm^2 C^{-1}, a comparable value to the high performance electrochromic material PEDOT (183 cm^2 C^{-1}) [70].

After 50 steps between neutral and oxidized states (Figure 2.21), the optical contrast value remained the same which is a good indicator of stability. In order to further investigate the stability, cyclic voltammetry stability test was performed.
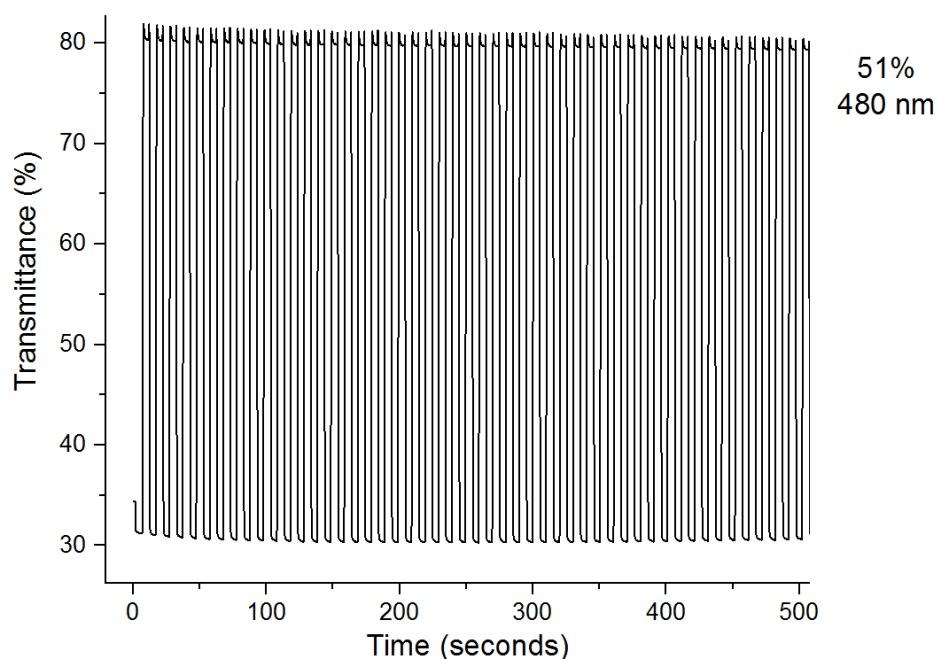
Figure 2.21. Electrochromic switching and optical absorbance change of PDEP monitored at 480 nm (50 cycles).

The polymer film was coated (TBAPF$_6$/MeCN) on Pt electrode (0.12 cm^2) was cycled 200 times (TBAPF$_6$/PC) with 100 mV s^{-1} scan rate (Figure 2.23). The polymer retained 92% of its activity after 200 cycles showing that PDEP has good stability.
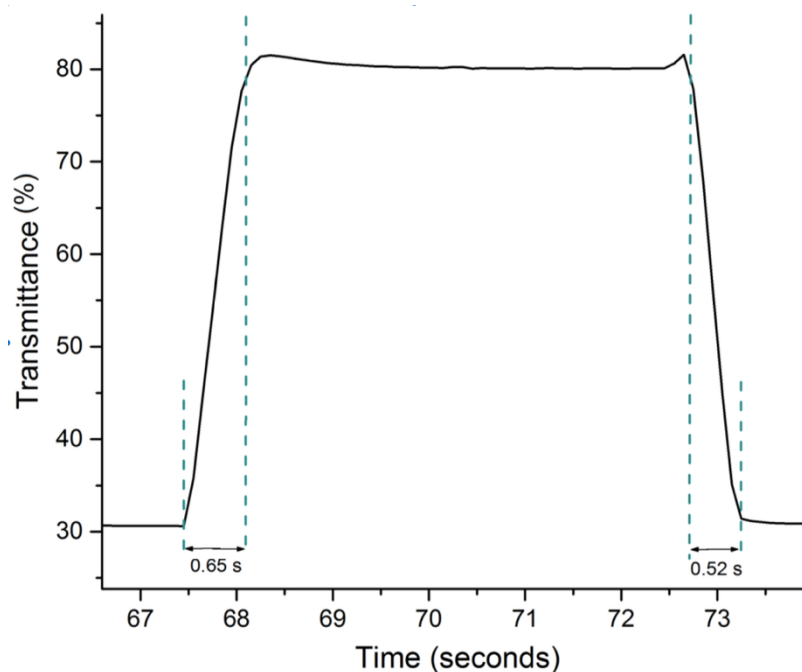
Figure 2.22. Electrochromic switching time and optical absorbance change of PDEP monitored at 480 nm (1 cycle).
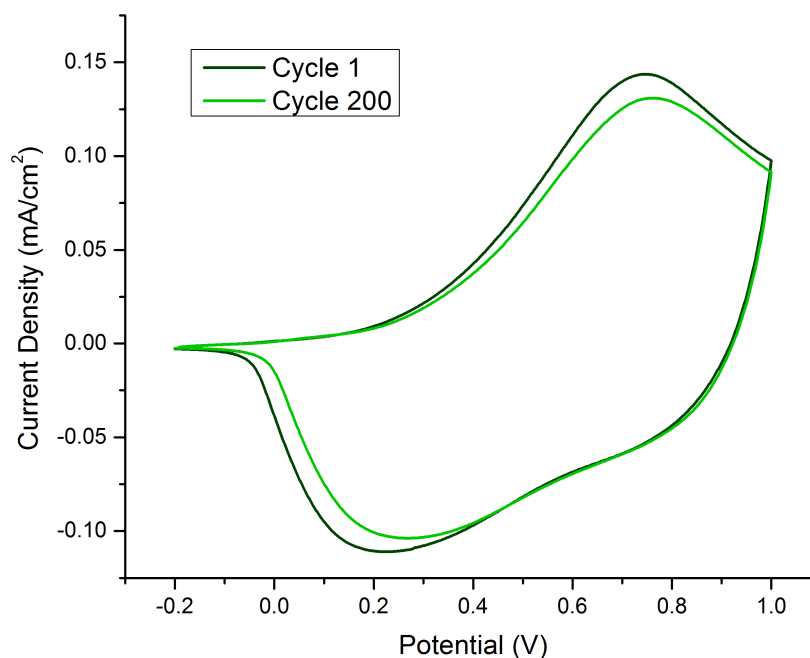
Figure 2.23. Cyclic voltammetry stability test of PDEP (WE: Pt, RE: Ag wire, 0.1 M TBAPF$_6$/PC, 100mV s^{-1}).

37

2.3.4.2. Kinetic Studies of PDPP

2.3.4.2.1. Kinetic Studies of Electrochemically Synthesized PDPP

The optical contrast and the switching time of the electrochemically synthesized PDPP were investigated in both visible and near-IR regions. The optical contrast values were found to be 58% at 480 nm (λ_{max}) (Figure 2.24) and 78% at 1940 nm with switching times of 1.3 s and 0.8 s respectively (Figure 2.25).

After 29 steps between neutral and oxidized states (Figure 2.24), the polymer retained 99% of its optical contrast value which is a good indicator of stability. For the future studies, stability will be further investigated by performing cyclic voltammetry stability test.
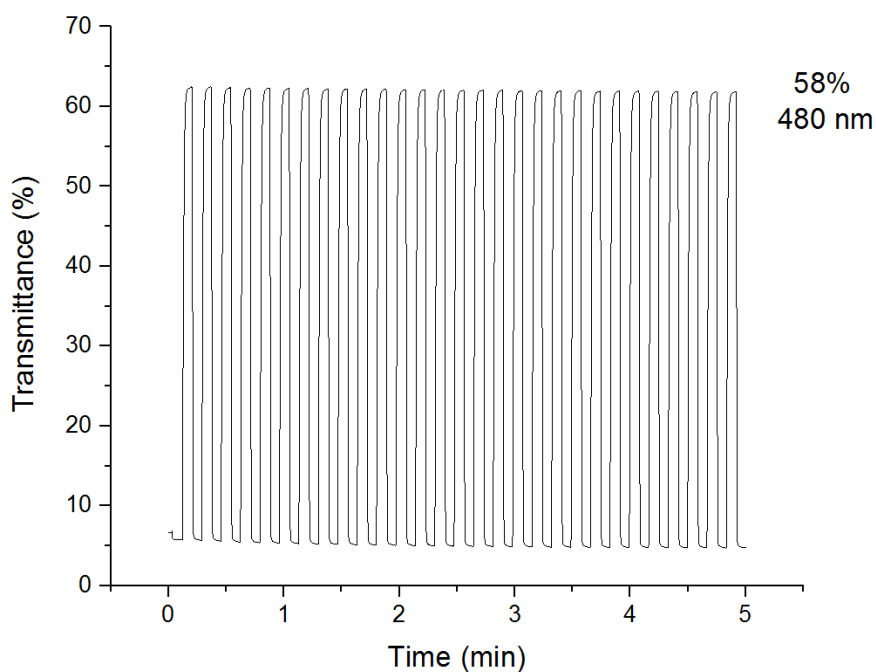
Figure 2.24. Electrochromic switching and optical absorbance changes of electrochemically synthesized PDPP monitored at 480 nm.
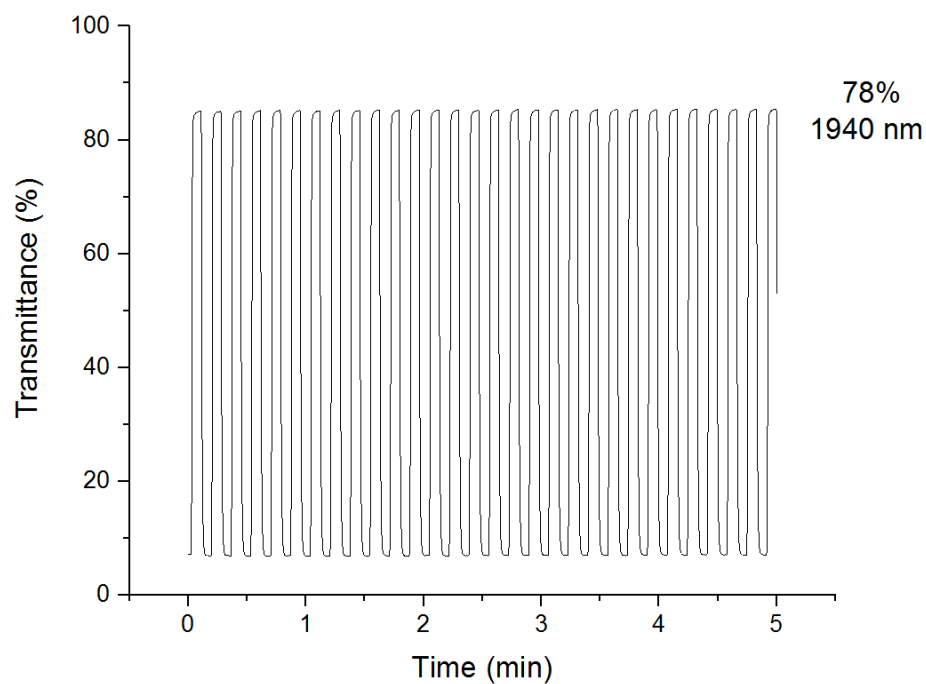
Figure 2.25. Electrochromic switching and optical absorbance changes of electrochemically synthesized PDPP monitored at 1940 nm.

2.3.4.2.2. Kinetic Studies of Chemically Synthesized PDPP
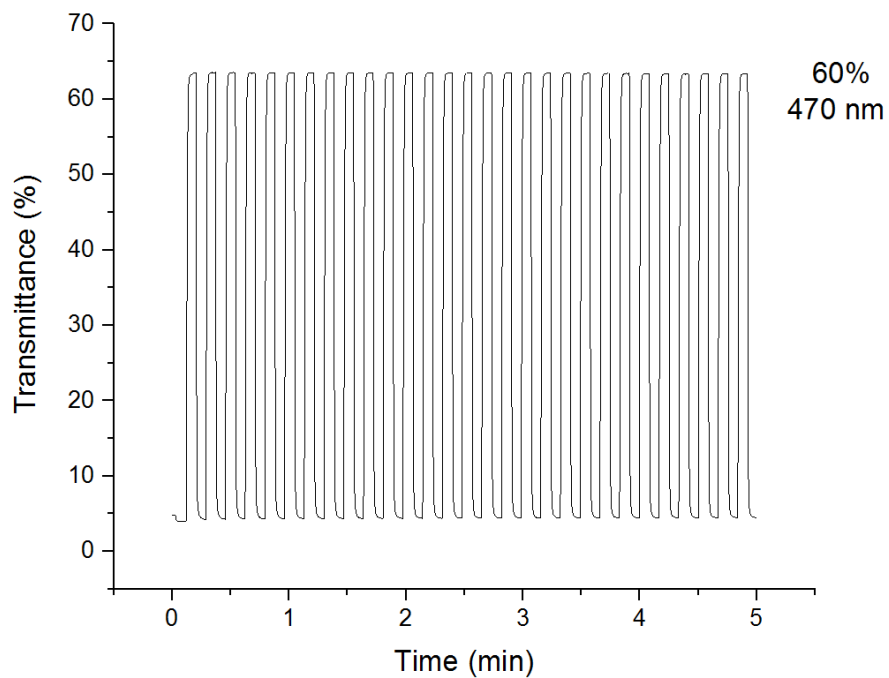
Figure 2.26. Electrochromic switching and optical absorbance changes of chemically synthesized PDPP monitored at 470 nm.
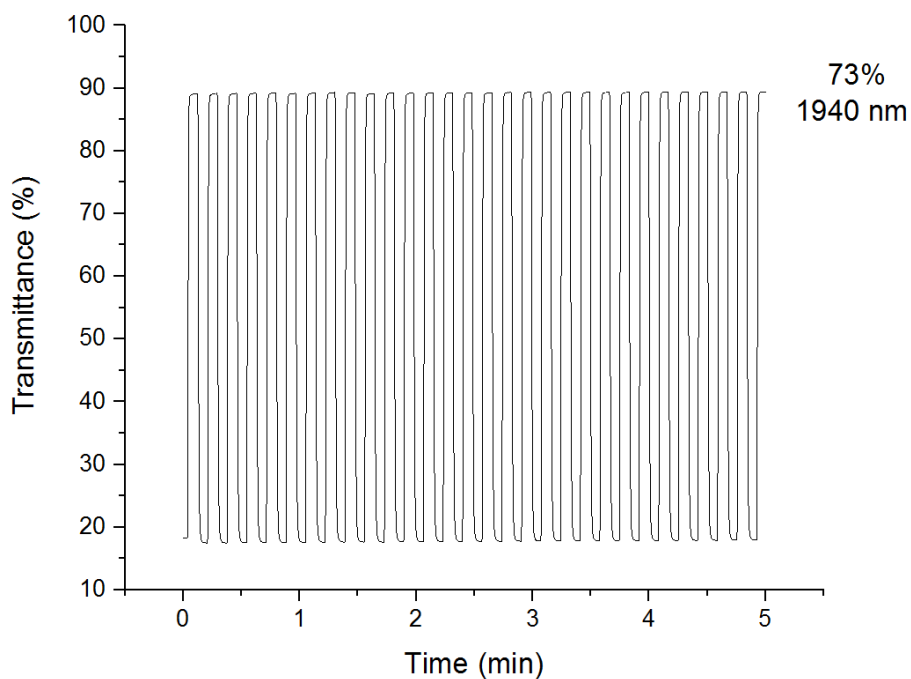
Figure 2.27. Electrochromic switching and optical absorbance changes of chemically synthesized PDPP monitored at 1940 nm.

The optical contrast and the switching time of the chemically synthesized PDPP were also investigated in both visible and near-IR regions. The optical contrast values were calculated as 60% at 480 nm (λ_{max}) (Figure 2.26) and 73% at 1940 nm with switching times of 0.9 s and 0.7 s respectively (Figure 2.27).

After 29 steps between neutral and oxidized states (Figure 2.26), the optical contrast values remained the same which a good indicator of stability. Cyclic voltammetry stability test will be performed for the future studies in order to further investigate the stability of the polymer.

CHAPTER 3

CONCLUSIONS

Novel D-D-D type monomers were synthesized via Stille coupling reaction and the monomers were fully characterized by NMR and Mass Analyses. The polymers of the corresponding monomers were synthesized by electrochemical methods. ProDOT containing polymer was also synthesized by chemical methods. For the polymers; cyclic voltammetry, spectroelectrochemistry, kinetic studies and stability experiments were performed in order to investigate electrochemical and electrochromic properties.

EDOT and phenanthrocarbazole containig polymer (PDEP) showed red color in its neutral state and becomed highly transmissive in the oxidized state. PDEP showed a high optical contrast ratio of 51% which comparable with the other red to transmissive electrochromic polymers in the literature [37-39]. The polymer revealed very fast switching times, the fastest among red-transmissive polymers, of 0.65 s for oxidation and 0.52 s reduction. ProDOT and phenanthrocarbazole containing polymer (PDPP) switched between orange and grey colors with a green intermediate color. The polymer showed high optical contrast values of 58% for electrochemically synthesized and 60% for chemically synthesized with fast switching times of 1.3 s and 0.9 s respectively. Different than PDEP, PDPP showed luminescent properties in its neutral state and the properties were completely vanished in its oxidized state, making PDPP an important candidate for electrochemical fluorescence and electrochromic applications. As a result, this study shows that PDEP and PDPP are important candidates for simple electrochromic display applications. In addition, results revealed that phenanthrocarbazole is a promising unit towards realization of novel, high performance electrochromic materials. Synthesis of other novel phenanthrocarbazole containing polymers are currently pursued for our future research.

The studies regarding PDEP were published in RSC Advances [71] and the manuscript concerning the results of PDPP is currently being prepared and will be submitted to Macromolecules.

CHAPTER 4

EXPERIMENTAL

4.1. Materials and Methods

All chemicals were purchased from Aldrich except fuming nitric acid and triethylphosphite which were purchased from Merck. All reactions were carried out under argon atmosphere. THF and toluene were dried over Na/benzophenone ketyl and freshly distilled or they were directly used from the Mbraun MBSPS5 solvent drying system. Column chromatography of all products was performed using Merck Silica Gel 60 (particle size: 0.040–0.063 mm, 230–400 mesh ASTM).

4.2. Equipment

For the electropolymerization of monomers, a three-electrode cell was used where the counter electrode was platinum wire, the reference electrode was the Ag wire and working electrode was the ITO doped coated glass. During the measurements, a potentiostat was used in order to keep the voltage constant between the working and the reference electrodes and to compensate the decrease in voltage. For spectroelectrochemistry studies, Varian Cary 5000 UV-Vis spectrometer was used. $CDCl_3$ and d_6-DMSO was used as the solvent for the ^1H and ^{13}C-NMR analyses on Bruker Spectrospin Avance DPX-400 Spectrometer and tetramethylsilane was used as the internal reference. High resolution mass spectroscopy was performed in order to determine the exact masses of the newly synthesized compounds using Waters Synapt MS System.

4.3. Monomer Syntheses

4.3.1. Synthesis of 1-Nitroperylene
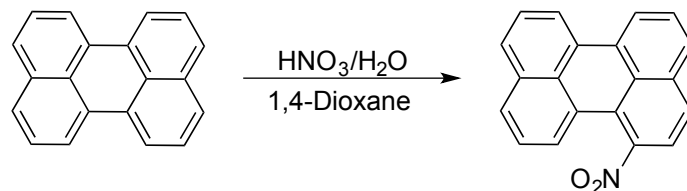
Scheme 4.1. Synthetic route of 1-Nitroperylene.

1-Nitroperylene was synthesized according to the literature with small modifications [65]. Perylene (1.03 g, 4.07 mmol) was dissolved in 1,4-dioxane (40 mL) at 30 °C under argon atmosphere. To the mixture was added 0.5 mL of nitric acid (fuming) in 0.8 mL of water dropwise and was heated to 60 °C for 30 min with vigorous stirring. Then the resulting mixture was cooled and poured into 170 mL of water. The solid was filtered, washed, dried, and further purified by column chromatography on silica gel (5:1 petroleum ether/DCM) to yield a brick-red solid (280 mg, 24%): ^{1}H-NMR (400 MHz, DMSO) δ 8.50 (dd, 2H), 8.01-7.93 (m, 4H), 7.80 (d, $J=8.7 Hz$, 1H), 7.73 (dd, 2H), 7.65 (t, $J=7.8 Hz$, 1H), 7.56 (t, $J=7.9 Hz$, 1H); ^{13}C-NMR(400 MHz, DMSO) δ 145.90, 134.31, 133.71, 131.22, 130.17, 128.90, 128.81, 128.79, 128.75, 127.98, 127.69, 127.57, 127.12, 126.67, 125.60, 124.76, 122.77, 122.59, 122.12, 122.07.

4.3.2. Synthesis of 1*H*-Phenanthro[1,10,9,8-*c,d,e,f,g*]carbazole
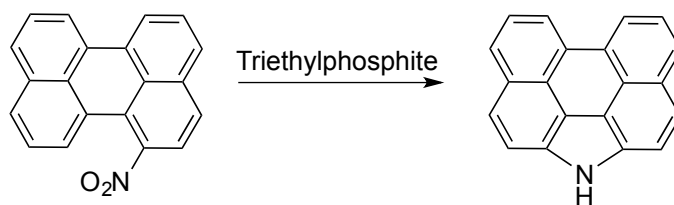
Scheme 4.2. Synthetic route of 1*H*-Phenanthro[1,10,9,8-c,d,e,f,g]carbazole.

1*H*-Phenanthro[1,10,9,8-c,d,e,f,g]carbazole was synthesized according to the literature with small modifications [66]. A mixture of 1-nitroperylene (151 mg, 0.51 mmol) and triethyl phosphite (1.5 mL) was refluxed at 160 °C under argon atmosphere

for 3 hours. Upon cooling to room temperature, the product was crystallized. The crystals were washed with petroleum ether, dried and yellow-brown crystals were collected (110 mg, 83%): ^{1}H-NMR (400 MHz, DMSO) δ 12.21 (s, NH, 1H), 8.71 (d, *J=8.0 Hz*, 2H), 8.17 (d, *J=7.5 Hz*, 2H), 7.96 (dd, 4H), 7.80 (t, *J= 7.8 Hz*, 2H); ^{13}C-NMR (400 MHz, DMSO) δ 130.65, 129.73, 128.33, 125.07, 124.58, 124.25, 123.58, 120.81, 116.99, 115.57.

4.3.3. Synthesis of 1-Methyl-1*H*-phenanthro[1,10,9,8-c,d,e,f,g]carbazole
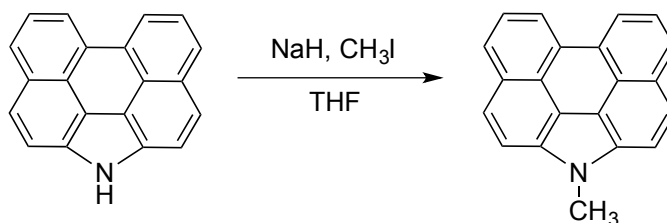
Scheme 4.3. Synthetic route of 1-Methyl-1*H*-phenanthro[1,10,9,8-c,d,e,f,g]carbazole.

To a mixture of compound 1*H*-phenanthro[1,10,9,8-c,d,e,f,g]carbazole (87.9 mg, 0.33 mmol) in dry THF (1 mL), was added NaH (18.0 mg, 0.75 mmol). Then methyl iodide (228 mg, 1.60 mmol) in 1 mL dry THF was added and the reaction was refluxed at 30 °C (kept below the boiling point of methyl iodide, 42 °C) for 18 hours. After cooling to room temperature, 0.1 mL water was added and the reaction was stirred for an addiditional 10 min at 0 °C. The reaction mixture was extracted with diethyl ether, dried over MgSO$_4$ and concentrated in vacuo. The crude product was purified by column chromatography on silica gel (3 : 1 petroleum ether/DCM) to yield a bright yellow solid (75.7 mg, 82%): ^{1}H-NMR (400 MHz, DMSO) δ 8.74 (d, *J=7.5 Hz*, 2H), 8.18 (d, *J=7.9 Hz*, 2H), 8.00 (dd, 4H), 7.81 (t, *J=7.7 Hz*, 2H), 4.37 (s, 3H); ^{13}C-NMR (400 MHz, DMSO) δ 132.08, 129.53, 128.28, 125.10, 124.60, 123.93, 123.53, 120.95, 116.20, 114.09, 31.56.

45

4.3.4. Synthesis of 3,10-Dibromo-1-methyl-1*H*-phenanthro[1,10,9,8-c,d,e,f,g]carbazole
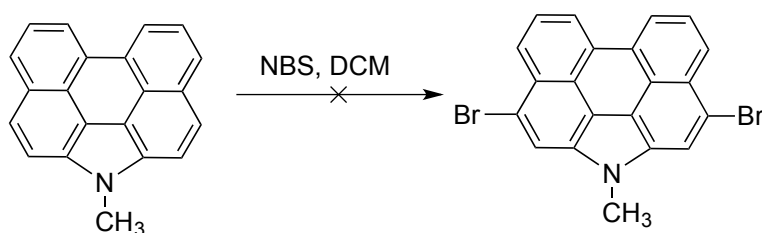
Scheme 4.4. Synthetic route of 3,10-Dibromo-1-methyl-1*H*-phenanthro[1,10,9,8-c,d,e,f,g] carbazole.

To a solution of 1-methyl-1*H*-phenanthro[1,10,9,8-c,d,e,f,g]carbazole (100 mg, 0.38 mmol) in dry DCM (20 mL) was added NBS (72.8 mg, 0.41 mmol) portion wise and the mixture was stirred at room temperature for 30 min under argon atmosphere. The solvent was evaporated under reduced pressure. The crude NMR of the reaction showed no product peaks.

4.3.5. Synthesis of 1-Dodecyl-1*H*-phenanthro[1,10,9,8-c,d,e,f,g]carbazole
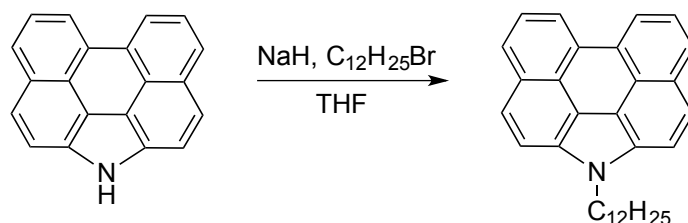

Scheme 4.5. Synthetic route of 1-Dodecyl-1*H*-phenanthro[1,10,9,8-c,d,e,f,g]carbazole

1-Dodecyl-1*H*-phenanthro[1,10,9,8-c,d,e,f,g]carbazole was synthesized according to the literature with small modifications [72]. To a mixture of compound 1*H*-phenanthro[1,10,9,8-c,d,e,f,g]carbazole (300 mg, 1.13 mmol) in dry THF (30 mL), was added NaH (40.8 mg, 1.70 mmol) and 1-bromo- dodecane (425 mg, 1.71 mmol) respectively. The mixture was refluxed at 65 °C for 23 hours under argon atmosphere. After gradually cooling to 0 °C, the mixture was stirred for 30 min. Water was carefully

(2 mL) added drop wise to quench any remaining NaH, and the mixture was then poured into water. The mixture was then extracted with diethyl ether (3x100 mL). The combined organic layers were washed with brine, dried (Na_2SO_4), and concentrated in vacuo. The crude product was purified by column chromatography on silica gel (6 : 1 petroleum ether/DCM) to yield a yellow wax (353 mg, 72%): ^{1}H-NMR (400 MHz, $CDCl_3$) δ 8.65 (d, $J = 7.5 Hz$, 2H), 8.12 (d, $J=8.0 Hz$, 2H), 7.91 (d, $J=8.8 Hz$, 2H), 7.84–7.76 (m, 4H), 4.67 (t, $J=6.9 Hz$, 2H), 2.08 (quin., $J=7.1 Hz$, 2H), 1.46–1.11 (m, 18H), 0.88 (t, $J=6.9 Hz$, 3H); ^{13}C-NMR (400 MHz, $CDCl_3$) δ 132.0, 130.48, 128.88, 125.08, 125.00, 124.58, 123.70, 120.79, 117.53, 113.46, 45.94, 32.04, 31.34, 29.71, 29.67, 29.59, 29.45, 29.42, 27.29, 22.82, 14.26 (one carbon peak was overlapped).

4.3.6. Synthesis of 3,10-Dibromo-1-dodecyl-1*H*-phenanthro[1,10,9,8-c,d,e,f,g] carbazole
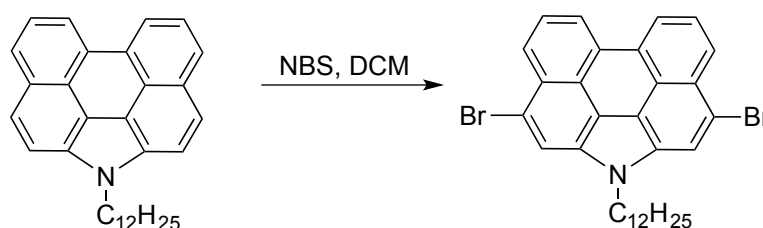
Scheme 4.6. Synthetic route of 3,10-Dibromo-1-dodecyl-1*H*-phenanthro[1,10,9,8-c,d,e,f,g]carbazole.

To a solution of 1-dodecyl-1*H*-phenanthro[1,10,9,8-c,d,e,f,g]carbazole (351 mg, 0.81 mmol) in dry DCM (21 mL) was added NBS (297 mg, 1.67 mmol) portion wise and the mixture was stirred at room temperature for 30 min under argon atmosphere. The solvent was evaporated under reduced pressure, and the resulting residue was purified by column chromatography on silica gel (3 : 1 petroleum ether/DCM) to yield a yellow solid (465 mg, 97%): ^{1}H-NMR (400 MHz, $CDCl_3$) δ 8.24 (d, $J=7.6 Hz$, 2H), 8.09 (d, $J=8.2 Hz$, 2H), 7.67 (t, $J=7.8 Hz$, 2H), 7.65 (s, 2H), 4.12 (t, $J=7.1 Hz$, 2H), 1.81 (quin., $J=7.1 Hz$, 2H), 1.42–1.05 (m, 18H), 0.86 (t, $J=6.9 Hz$, 3H); ^{13}C-NMR (400 MHz, $CDCl_3$) δ 130.93, 129.33, 127.41, 125.21, 124.75, 123.43, 121.44, 117.84, 116.58, 115.69, 45.77, 32.03, 31.10, 29.70, 29.65, 29.56, 29.44, 29.29, 27.15, 22.81, 14.26 (one carbon peak was overlapped). HRMS calculated for $C_{32}H_{33}Br_2N$: 591.0959. Found: 591.0961.

4.3.7. Synthesis of Tributyl(3,4-ethylenedioxythienyl-2)stannane
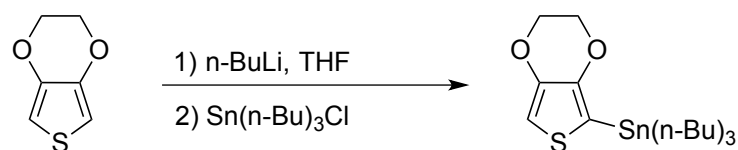
Scheme 4.7. Synthetic route of Tributyl(3,4-ethylenedioxythienyl-2)stannane.

Tributyl(3,4-ethylenedioxythienyl-2)stannane was synthesized according to the literature with small modifications [68]. To a solution of 3,4-ethylenedioxythiophene (EDOT, 1.02 g, 7,17 mmol) in dry THF (21 mL) at −78 °C, 2.5 M n-butyllithium (3.1 mL, 7.75 mmol, in hexanes) was added dropwise. The solution was stirred for 1.5 hours while maintaining the temperature at -78 °C. Then, (n-Bu)$_3$SnCl (2.3 mL, 8.48 mmol) was added dropwise. The reaction mixture was slowly warmed up to room temperature and stirred overnight. After evaporation of the solvent, water was added and the mixture was extracted with diethyl ether three times. The combined organic phases were washed with brine, dried over anhydrous MgSO$_4$, filtered and concentrated in vacuo yielding a golden yellow liquid (3.19 g, 91%). The stannic derivative was used without any further purification in the Stille coupling reaction.

4.3.8. Synthesis of 3,3-Bis(2-ethylhexyloxy)methyl)-3,4-dihydro-2H-thieno[3,4-b][1,4]dioxepine-6-yl)trimethyl-stannane
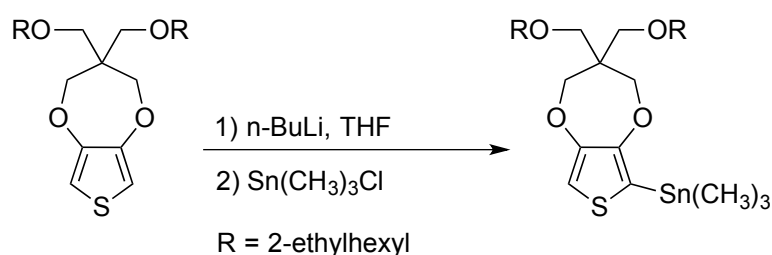
Scheme 4.8. Synthetic route of 3,3-Bis(2-ethylhexyloxy)methyl)-3,4-dihydro-2H-thieno[3,4-b][1,4]dioxepine-6-yl)trimethyl-stannane.

3,3-Bis(2-ethylhexyloxy)methyl)-3,4-dihydro-2H-thieno[3,4-b][1,4]dioxepine-6-yl)trimethyl-stannane was synthesized according to the literature with small modifications [69]. 3,3-Bis-(2-ethylhexyloxy)methyl)-3,4-dihydro-2H-thieno[3,4-b][1,4]dioxepine (ProDOT(CH$_2$OEtHx)$_2$), 456 mg, 1.03 mmol) was dissolved in dry

48

THF (6 mL) and cooled down to -78 °C. 2.5 M n-butyllithium (0.51 mL, 1.28 mmol, in hexanes) was added dropwise and the solution was stirred for 1.5 hours while maintaining the temperature at -78 °C. Trimethyltinchloride (216 mg, 1.08 mmol) was dissolved in 1 mL THF and subsequently added to the solution. After the addition, the mixture was allowed to slowly warm to room temperature and stirred overnight. The solvent was evaporated in vacuo affording a brown oil (721 mg, 96%) which was used in Stille coupling reaction without any further purification.

4.3.9. Synthesis of 3,10-Bis(2,3-dihydrothieno[3,4-b][1,4]dioxin-5-yl)-1-dodecyl-1*H*-phenanthro[1,10,9,8-c,d,e,f,g]carbazole (DEP)
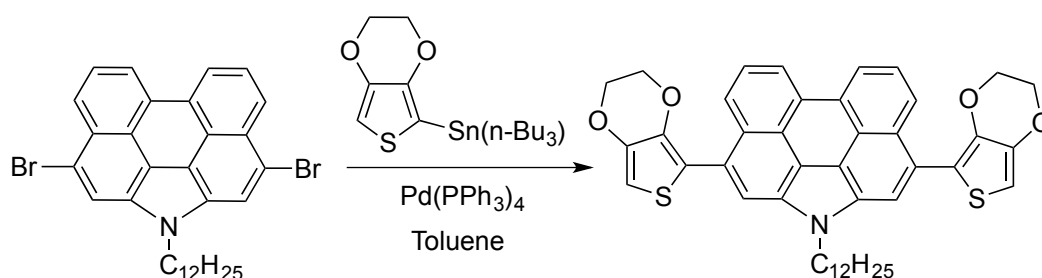
Scheme 4.9. Synthetic route of DEP.

3,10-Dibromo-1-dodecyl-1*H*-phenanthro[1,10,9,8-c,d,e,f,g]carbazole (100 mg, 0.170 mmol), and tributyl(2,3-dihydrothieno[3,4-b][1,4]dioxin-7-yl)stannane (313 mg, 0.730 mmol) were dissolved in dry toluene (30 mL) and the mixture was purged with argon for 30 min. Then, tetrakis(triphenylphosphine)palladium(0) (35 mg, 0.030 mmol) was added at room temperature under argon atmosphere. The mixture was heated to 115 °C and stirred in the dark for 24 hours. The solvent was evaporated under reduced pressure, and the crude oily residue was purified by column chromatography on silica gel (1 : 1 petroleum ether/DCM) to yield a yellow-orange solid (91 mg, 76%): ^{1}H-NMR (400 MHz, CDCl$_3$) δ 8.71 (d, *J=7.5 Hz*, 2H), 8.24 (d, *J=8.2 Hz*, 2H), 7.91 (s, 2H), 7.85 (t, *J=7.9 Hz*, 2H), 6.54 (s, 2H), 4.71 (t, *J=7.0 Hz*, 2H), 4.46–4.19 (m, 8H), 2.11 (quin., *J=7.1 Hz*, 2H), 1.49–1.13 (m, 18H), 0.85 (t, *J=6.9 Hz*, 3H); ^{13}C-NMR (400 MHz, CDCl$_3$) δ 141.78, 138.19, 132.04, 130.65, 127.77, 126.75, 124.79, 124.76, 124.69, 121.22, 117.61, 117.19, 116.07, 98.80, 64.95, 64.85, 45.94, 32.03, 31.33, 29.73, 29.70, 29.64, 29.45, 29.42, 27.30, 22.81, 14.27 (one carbon peak was overlapped). HRMS calculated for C$_{44}$H$_{43}$NO$_4$S$_2$: 713.2643. Found: 713.2634.

4.3.10. Synthesis of 3,10-Bis(3,3-bis(((2-ethylhexyl)oxy)methyl)-3,4-dihydro-2*H*-thieno[3,4-b][1,4]dioxepin-6-yl)-1-dodecyl-1*H*-phenanthro[1,10,9,8-c,d,e,f,g]carbazole (DPP)
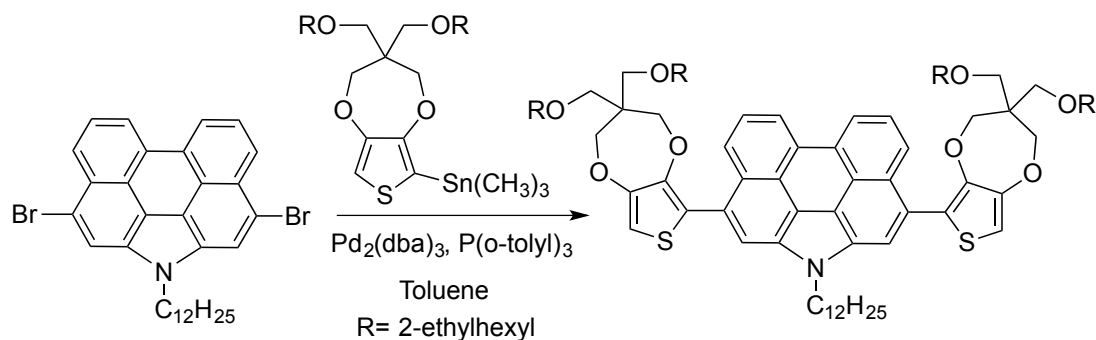
Scheme 4.10. Synthetic route of DPP.

3,10-Dibromo-1-dodecyl-1*H*-phenanthro[1,10,9,8-c,d,e,f,g]carbazole (182 mg, 0.307 mmol), and 3,3-bis(2-ethylhexyloxy)methyl)-3,4-dihydro-2H-thieno[3,4-b][1,4] dioxepine-6-yl)trimethyl-stannane (516 mg, 0.854 mmol) were dissolved in dry toluene (23 mL) and the mixture was purged with argon for 30 min at room temperature. Then, tris(dibenzylideneacetone)dipalladium(0) (Pd$_2$(dba)$_3$, 17.5 mg, 0.015 mmol) and tri(o-tolyl)phosphine (P(o-tolyl)$_3$, 15.7 mg, 0.046 mmol) was added under argon atmosphere. The mixture was heated to 115 °C and stirred in the dark for 17.5 hours. The solvent was evaporated under reduced pressure, and the crude oily residue was purified by column chromatography on silica gel (4 : 1 hexane/DCM) to yield an orange oil (249 mg, 62%): ^{1}H-NMR (400 MHz, CDCl$_3$) δ 8.71 (d, *J=7.6 Hz*, 2H), 8.20 (d, *J=8.3 Hz*, 2H), 7.88-7.82 (m, 4H), 6.66 (s, 2H), 4.70 (t, *J=6.9 Hz*, 2H), 4.21 (s, 2H), 4.14 (s, 2H), 3.54 (qd, *J=8.9, 2.5 Hz*, 8H), 3.30 (d, *J=5.7 Hz*, 8H), 2.12 (quin., 2H), 1.55-1.24 (m, 58H), 0.90-0.86 (m, 27H); ^{13}C-NMR (400 MHz, CDCl$_3$) δ 147.85, 144.18, 130.09, 128.75, 126.15, 125.44, 122.75, 122.73, 122.71, 119.69, 119.15, 115.73, 114.18, 101.56, 72.54, 72.09, 72.03, 68.28, 46.29, 44.01, 37.82, 30.05, 29.38, 28.87, 28.85, 27.76, 27.73, 27.69, 27.47, 27.30, 22.20, 21.23, 20.81, 12.22, 9.31, 9.30.

4.4. Polymer Synthesis

4.4.1. Synthesis of Poly-3,10-bis(3,3-bis(((2-ethylhexyl)oxy)methyl)-3,4-dihydro-2*H*-thieno[3,4-b][1,4]dioxepin-6-yl)-1-dodecyl-1*H*-phenanthro[1,10,9,8-c,d,e,f,g]carbazole (PDPP)
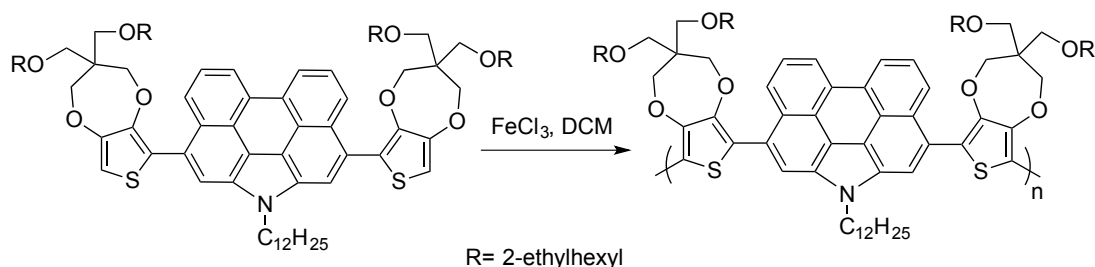

Scheme 4.11. Synthetic route of PDPP.

To a solution of anhydrous iron (III) chloride (18.1 mg, 0.112 mmol) in 2 mL chloroform 3,10-bis(3,3-bis(((2-ethylhexyl)oxy)methyl)-3,4-dihydro-2*H*-thieno[3,4-b][1,4]dioxepin-6-yl)-1-dodecyl-1*H*-phenanthro[1,10,9,8-c,d,e,f,g]carbazole (41.9 mg, 0.032 mmol) in 2 mL chloroform was added drop wise under argon atmosphere. The mixture was stirred for 10 hours 45 min under argon atmosphere at room temperature. Then cold methanol was added to the reaction mixture and the precipitated polymer was filtered and washed with cold methanol until the filtrate becomes colorless. To a 100 mL 4% hydrazine monohydride in methanol solution, the polymer was added and stirred for 3 hours until its color turns bright orange-red. Then the polymer is filtered and washed with cold methanol. After drying, a bright orange-red polymer was obtained (38.0 mg).

REFERENCES

[1] P. R. Somani and S. Radhakrishnan, *Mater. Chem. Phys.*, **2003**, *77*, 117.

[2] A. Durmus, G. E. Gunbas, P. Camurlu and L. Toppare, *Chem. Commun.*, **2007**, *31*, 3246.

[3] S. H. Hsiao and Y. T. Chiu, *RSC Adv.*, **2015**, *5*, 90941.

[4] R. J. Mortimer, *Electrochromic materials and devices*, Wiley-VCH, Weinheim, 2015.

[5] G. Gunbas and L. Toppare, *Chem. Commun.*, **2012**, *48*, 1083.

[6] Z. G. Shi, W. T. Neo, T. T. Lin, H. Zhouand and J. W. Xu, *RSC Adv.*, **2015**, *5*, 96328.

[7] T. Soganci, M. Ak, E. Giziroglu and H. C. Soyleyici, *RSC Adv.*, **2016**, *6*, 2810.

[8] S. L. Ming, S. J. Zhen, K. W. Lin, L. Zhao, J. K. Xu and B. Y. Lu, *ACS Appl. Mater. Interfaces*, **2015**, *7*, 11089.

[9] C. M. Cho, Q. Ye, W. T. Neo, T. T. Lin, X. H. Lu and J. W. Xu, *Polym. Chem.*, **2015**, *6*, 7570.

[10] C. M. Cho, Q. Ye, W. T. Neo, T. T. Lin, J. Song, X. H. Lu and J. W. Xu, *J. Mater. Sci.*, **2015**, *50*, 5856.

[11] R.J. Mortimer, *Electrochim. Acta*, **1999**, *44*, 2971.

[12] D. Milstein, J. K. Stille, *J. Am. Chem. Soc.*, **1978**, *10*0, 3636.

[13] T. T. Steckler, P. Henriksson, S. Mollinger, A. Lundin, A. Salleo and Mats R. Andersson, *J. Am. Chem. Soc.*, **2014**, *136*, 1190−1193.

[14] J.-H. Wu and G.-S. Liou, *Adv. Funct. Mater.*, **2014**, *24*, 6422–6429.

[15] C. Reus, M. Stolar, J. Vanderkley, J. Nebauer and T. Baumgartner, *J. Am. Chem. Soc.*, **2015**, *137*, 11710−11717.

[16] J. Sun, Y. Wu, Y. Wang, Z. Liu, C. Cheng, K. J. Hartlieb, M. R. Wasielewski and J. F. Stoddart, *J. Am. Chem. Soc.*, **2015**, *137*, 13484−13487.

[17] T. Xu, E. C. Walter, A. Agrawal, C. Bohn, J. Velmurugan, W. Zhu, H. J. Lezec and A. A. Talin, *Nat. Commun.*, **2016**, *7*, 10479.

[18] A. Cannavale, P. Cossari, G. E. Eperon, S. Colella, F. Fiorito, G. Gigli, H. J. Snaith and A. Listorti, *Energy Environ. Sci.*, **2016**, Advance Article.

[19] T. A. Skotheim, J. R. Reynolds, eds. 2007, *Handbook of Conducting Polymers,* Boca Raton, FL: CRC 3rd ed.

[20] A. A. Argun, P. H. Aubert, B. C. Thompson, I. Schwendeman, C. L. Gaupp, J. Hwang, N. J. Pinto, D. B. Tanner, A. G. MacDiarmid, J. R. Reynolds; *Chem. Mater.* **2004**, *16*, 4401.

[21] K. Fesser, A. R. Bishop and D. K. Campbell, *Phys. Rev. B*, **1983**, *27*, 4804.

[22] C. M. Amb, J. A. Kerszulis, E. J. Thompson, A. L. Dyer and J. R. Reynolds, *Polym. Chem.*, **2011**, *2*, 812.

[23] R. C. Gonzalez and R. E. Woods, *Digital Image Processing*. Addison-Wesley, 1993.

[24] W. K. Pratt, *Digital Image Processing, 2nd Edition*. John Wiley & Sons, New York, 1991.

[25] C. Ponyton, *Digital Video and HD: Algorithms and Interfaces*, Elsevier, San Fransisco, 2003.

[26] N. Boughen, *Lightwave 3D 7.5 Lighting*, Wordware Publishing, Texas, 2003.

[27] T. Deutschmann, S. Roth and E. Oesterschulze, *J. Micromech. Microeng.*, **2013**, *23*, 065032.

[28] A. Balan, G. Gunbas, A. Durmus, L. Toppare, *Chem. Mater*., **2008**, *20*, 7510.

[29] B. Karabay, L. C. Pekel and Atilla Cihaner, *Macromolecules,* **2015**, *48*, 1352.

[30] M. I. Ozkut, S. Atak, A. M. Onal and A. Cihaner, *J. Mater. Chem*., **2011**, *21*, 5268.

[31] C. M. Amb, P. M. Beaujuge and J. R. Reynolds, *Adv. Mater.,* **2010**, *22*, 724.

[32] G. Sonmez, C. K. F. Shen, Y. Rubin, and F. Wudl, *Angew. Chem. Int. Ed*., **2004**, *43*, 1498.

[33] A. Durmus, G. Gunbas, P. Camurlu, L. Toppare, *Chem. Commun*., **2007**, 3246-3248.

[34] G. Gunbas, A. Durmus, and L. Toppare, *Adv. Mater*., **2008**, *20*, 691.

[35] G. Gunbas, A. Durmus, and L. Toppare, *Adv. Funct. Mater.,* **2008**, *18*, 2026.

[36] P. M. Beaujuge, S. Ellinger, and J. R. Reynolds, *Adv. Mater.,* **2008**, *20*, 2772.

[37] A. L. Dyer, M. R. Craig, J. E. Babiarz, K. Kiyak and J. R. Reynolds, *Macromolecules,* **2010**, *43*, 4460.

[38] X. Chen, Z. Xu, S. Mi, J. Zhenga and C. Xu, *New J. Chem*., **2015**, *39*, 5389.

[39] Z. Xu, X. Chen, S. Mi, J. Zheng, C. Xu, *Org. Electron.,* **2015**, *26*, 129.

[40] CMYK color model. Retrieved August 06, 2016, from
https://en.wikipedia.org/wiki/CMYK_color_model.

[41] O. Celikbilek, M. I. Ozkut, F. Algi, A. M. Onal and Atilla Cihaner, *Org. Electron.,* **2012**, *13*, 206.

[42] R. H. Bulloch, J. A. Kerszulis, A. L. Dyer and J. R. Reynolds, *ACS Appl. Mater. Interfaces,* **2015**, *7*, 1406.

[43] S.-H. Hsiao, L.-C. Wu, *Dyes and Pigments*, **2016**, *134*, 51-63.

[44] A. Cihaner and F. Algı, *Electrochim. Acta*, **2008**, *54*, 665-670.

[45] S. Mai, J. Wu, J. Liu, Z. Xu, X. Wu, G. Luo, J. Zheng and C. Xu, *ACS Appl. Mater. Interfaces*, **2015**, *7*, 27511-27517.

[46] H. A. M. Mullekom, J. A. J. M. Vekemans, E. E. Havinga and E. W. Meijer, *Mater. Sci. Eng.,* **2001**, *R32*, 1.

[47] J. W. Jo, J. H. Kim and J. W. Jung, *Dyes and Pigments*, **2016**, *13*, 333-338.

[48] J. Roncali, Macromol. *Rapid Commun*., 2007, **28**, 1761–1775.

[49] a) C. A. Thomas, K. Zong, K. A. Abboud, P. J. Steel and J. R. Reynolds, *J. Am.*

Chem. Soc., **2004**, *126*, 16440-16450. b) U. Salzner and M. E. Köse, *J. Phys. Chem. B,* **2002**, *106*, 9221-9226.

[50] G. Heywang, F. Jonas, *Adv. Mater.*, **1992**, *4*, 116.

[51] L. Groenendaal, F. Jonas, D. Freitag, H. Pielartzik, R. Reynolds, *Adv. Mater.*, **2000,** *12*, 481.

[52] C. A. Thomas, K. Zong, K. A. Abboud, P. J. Steel, J. R. Reynolds,, *J. Am. Chem. Soc.,* **2004**, *126*, 16440.

[53] M. Dietrich, J. Heinze, G. Heywang, F. Jonas, *J. Electroanal. Chem.,* **1994***, 369*, 87–92.

[54] J. Padilla, V. Seshadri, J. Filloramo , W. K. Mino, S. P. Mishra, B. Radmard, A. Kumar, G. A. Sotzing and T. F. Otero, **2001**, *Synth. Met.*, *157*(6), 261-268.

[55] Z. Q. Deng, L. Chen and Y. W. Chen, *J. Polym. Sci., Part A: Polym. Chem.,* **2013**, *51*, 4885.

[56] H. J. Chen, Y. L. Guo, X. N. Sun, D. Gao, Y. Q. Liuand and G. Yu, *J. Polym. Sci., Part A: Polym. Chem.*, **2013**, *51*, 2208.

[57] C. Winder and N. S. Sariciftci, *J. Mater. Chem.*, **2004**, *14*, 1077-1086.

[58] P. Espinet and A. M. Echavarren, *Angew. Chem. Int. Ed.*, **2004**, *43*, 4704-4734.

[59] The Nobel Prize in Chemistry 2010. Retrieved August 14, 2016, from http://www.nobelprize.org/nobel_prizes/chemistry/laureates/2010.

[60] S. Göker, *Synthesis and Investigation of Optoelectronic Properties of 5,6-Bis(octyloxy)benzo[c][1,2,5]oxadiazole Derivatives* (Master's Thesis), 2014. Retrieved from METU Library E-Theses Index.

[61] J. L. Reddinger and J. R. Reynolds, *Adv. Polym. Sci.*, **1999**, *145*, 57-122.

[62] G. Zotti, G. Schiavon, A. Berlin and G. Pagani, *Chem. Mater.*, **1993**, *5*, 430.

[63] P. Audebert and P. Hapiot, *Synth. Met.*, **1995**, *75*, 95-102.

[64] K. Yoshino, S. Hayashi and R. Sugimoto, *Jpn. J. Appl. Phys. Part 2*, **1984**, *23*(12), L899-L900.

[65] W. Jiang, H. Qian, Y. Li and Z. Wang, *J. Org. Chem.*, **2008**, *73*, 7369–7372.

[66] J. J. Looker, *J. Org. Chem.*, **1972**, *37*, 3379-3381.

[67] Y. Li and Z. Wang, *Org. Lett.*, **2009**, *11*, 1385-1387.

[68] L. Chen, B. Zhang, Y. Cheng, Z. Xie, L. Wang, X. Jing and F. Wang, *Adv. Funct. Mater.*, **2010**, *20*, 31413-3153.

[69] P. M. Beaujuge, S. V. Vasilyeva, D. Y. Liu, S. Ellinger, T. D. McCarley and J. R. Reynolds, *Chem. Mater.*, **2012**, *24*, 255-268.

[70] C. L. Gaupp, D. M. Welsh, R. D. Rauh and J. R. Reynolds, *Chem. Mater.*, **2002**, *14*, 3964.

[71] G. Atakan and G. Gunbas, *RSC Adv.*, **2016**, *6*, 25620–25623.

[72] Y. Li, L. Hao, H. B. Fu, W. Pisula, X. Feng and Z. Wang, *Chem. Commun.*, **2011**, *47*, 10088-10090.

APPENDIX A

NMR SPECTRA

NMR measurements were performed with Bruker Avance III Ultrashield 400 Hz using $CDCl_3$, or d_6-DMSO as the solvents.
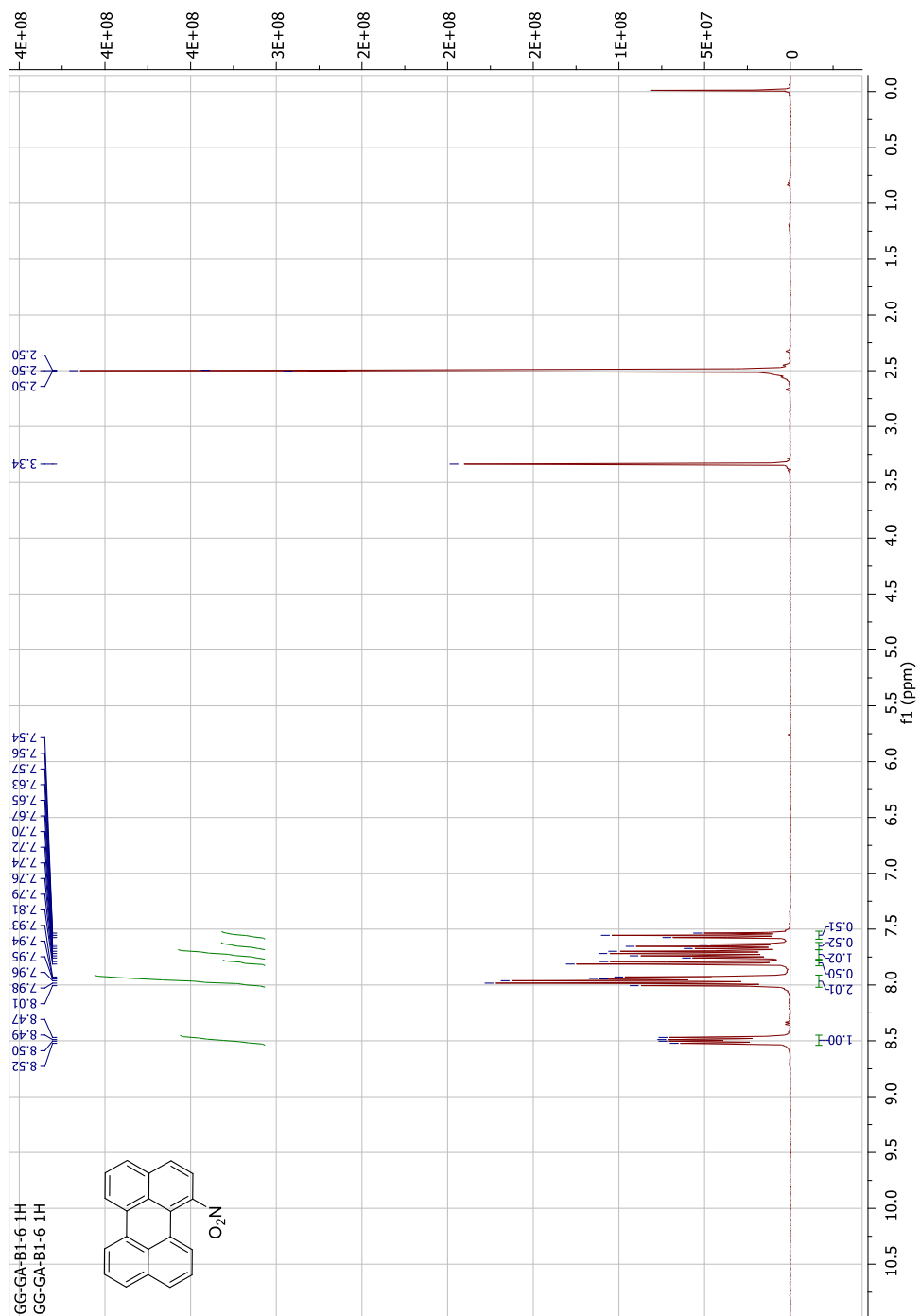
**Figure A.1.** ^{1}H-NMR spectrum of 1-Nitroperylene.

GG-GA-B1-6 1H
GG-GA-B1-6 1H

7.54
7.56
7.57
7.63
7.65
7.67
7.70
7.72
7.74
7.76
7.79
7.81
7.93
7.94
7.95
7.96
7.98
8.01
8.47
8.49
8.50
8.52

2.50
2.50
2.50

3.34

0.51
0.52
0.52
1.02
1.02
0.50
2.01
2.01
1.00
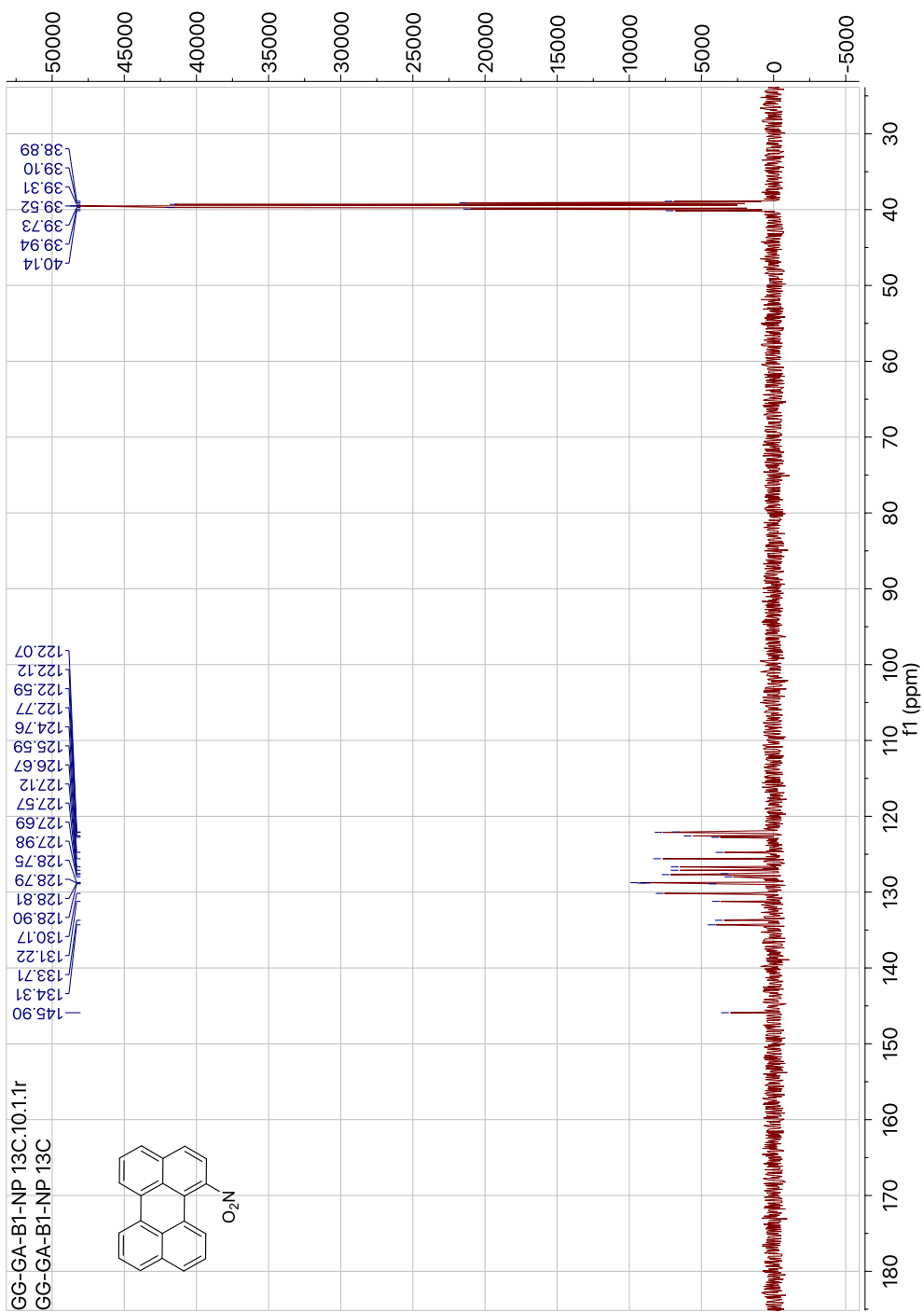
Figure A.2. ^{13}C-NMR spectrum of 1-Nitroperylene.
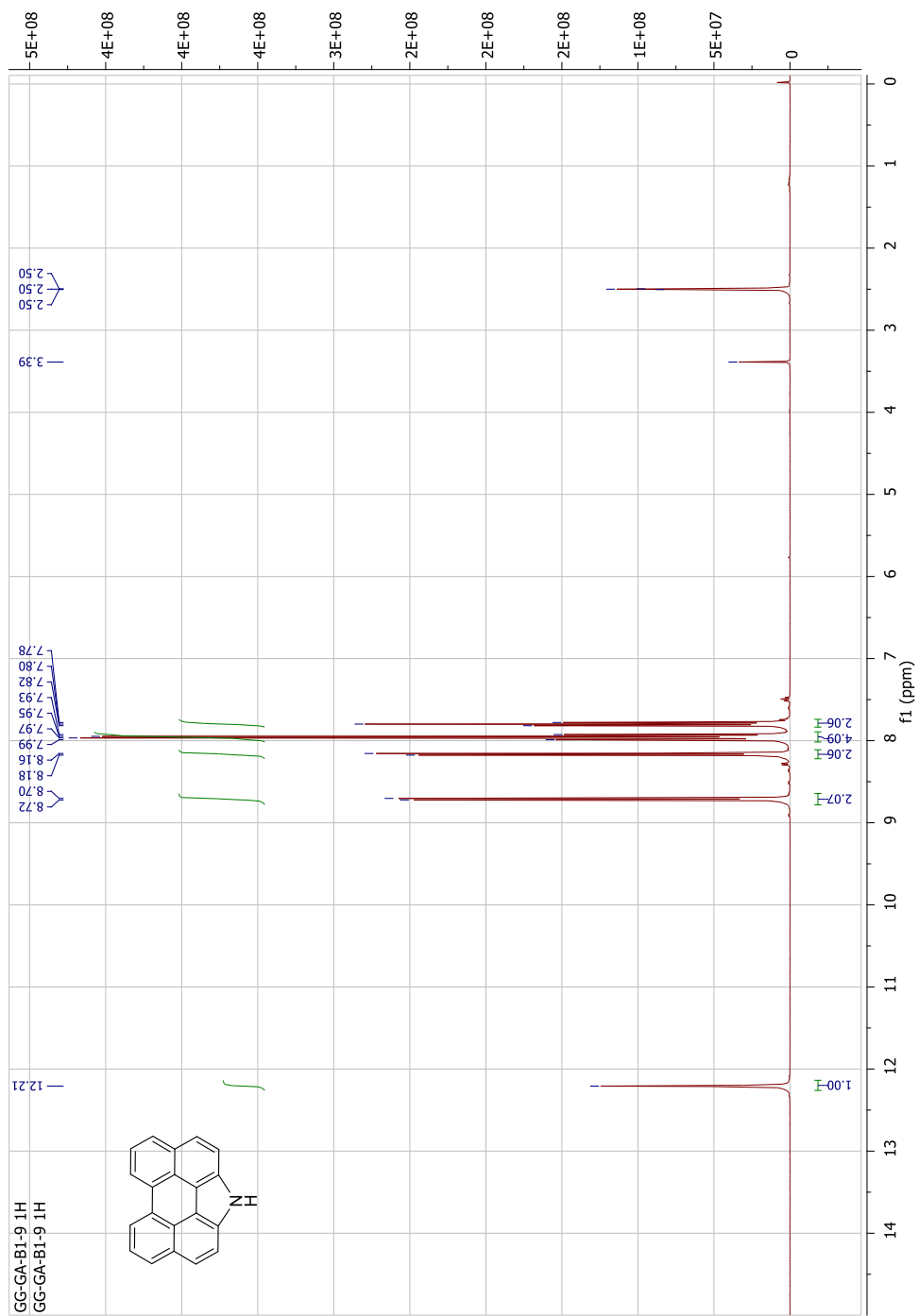
Figure A.3. ^{1}H-NMR spectrum of 1*H*-Phenanthro[1,10,9,8-c,d,e,f,g]carbazole.
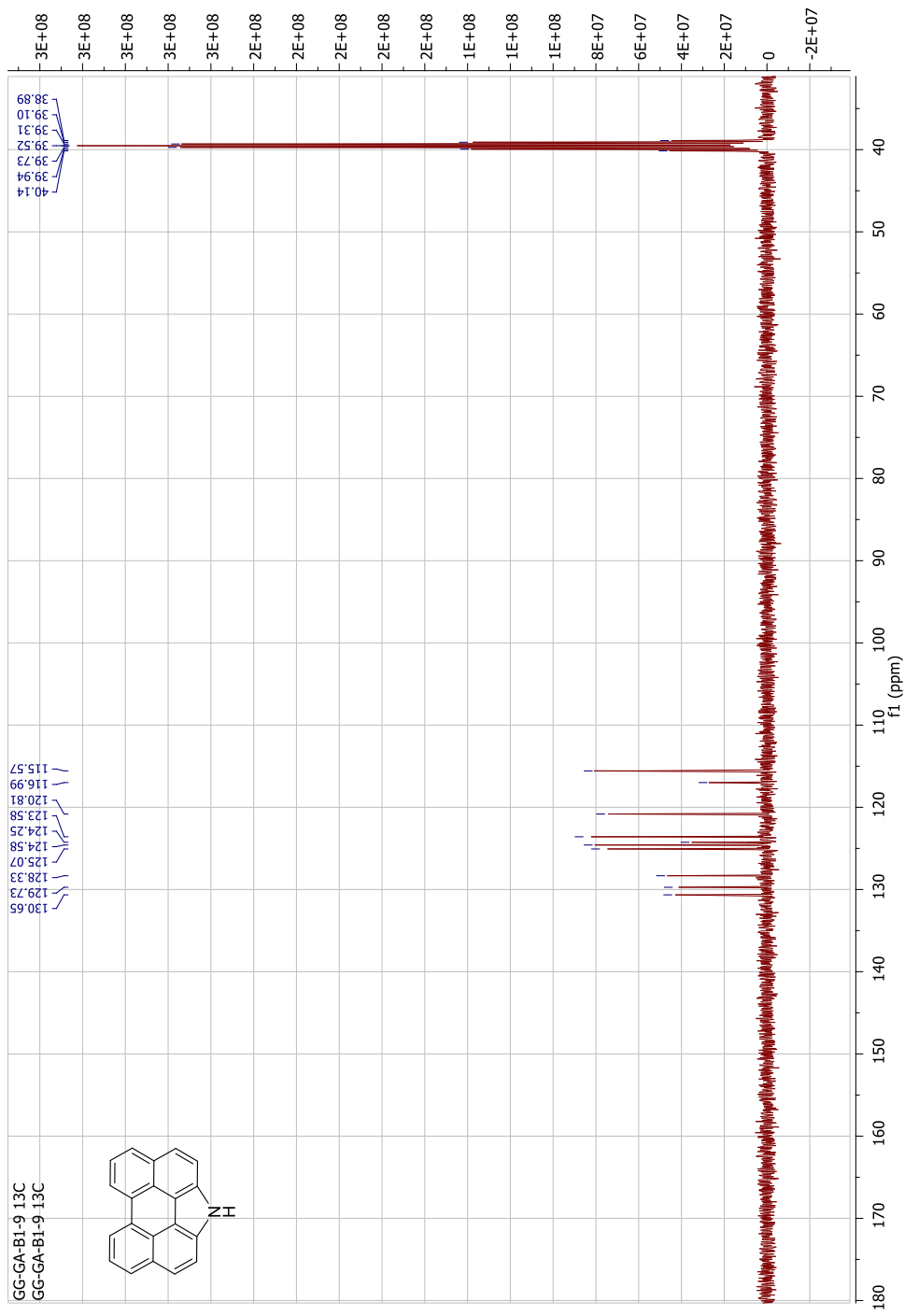
**Figure A.4.** ^{13}C-NMR spectrum of 1*H*-Phenanthro[1,10,9,8-c,d,e,f,g]carbazole.

63
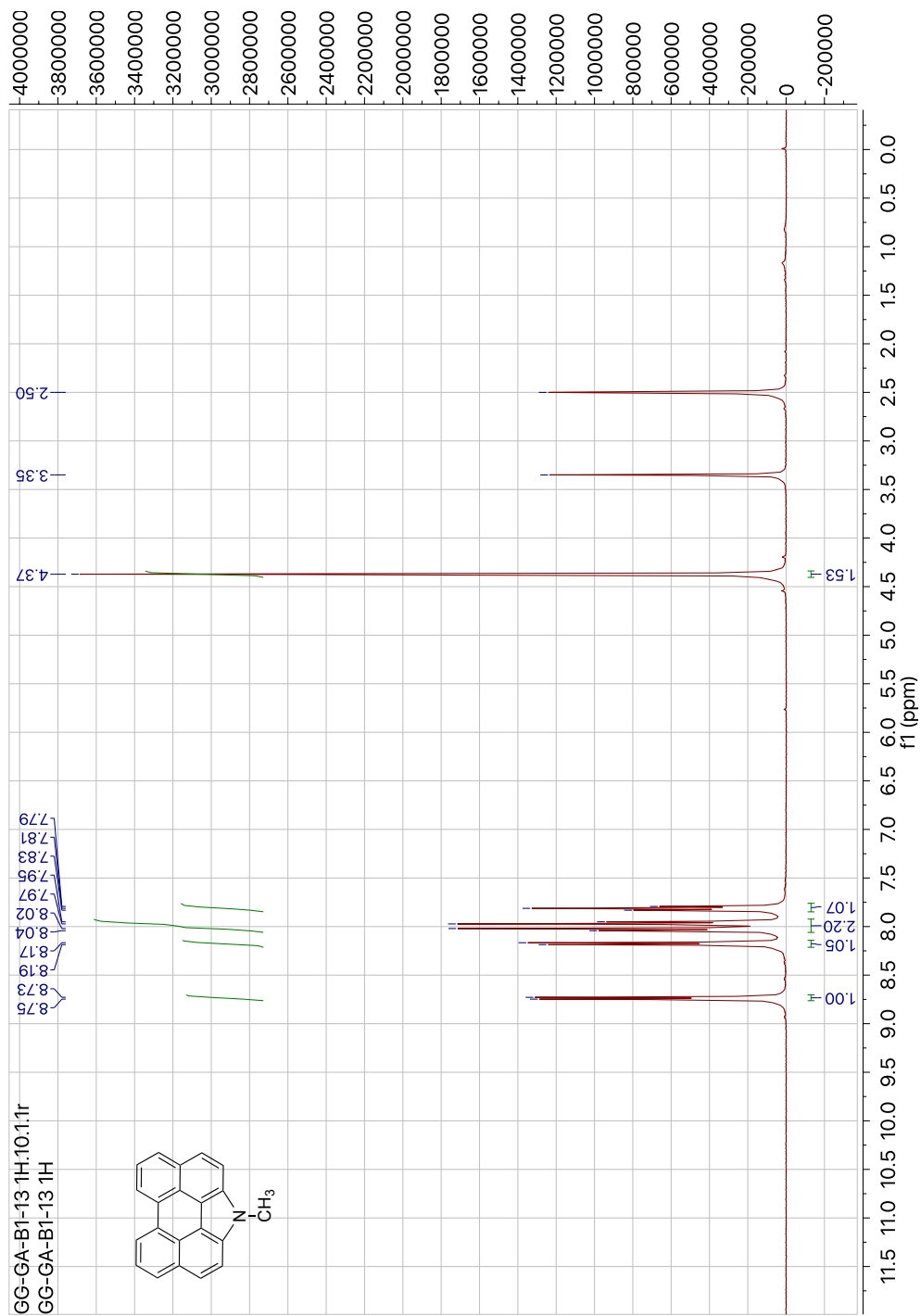
Figure A.5. ^{1}H-NMR spectrum of 1-Methyl-1H-phenanthro[1,10,9,8-c,d,e,f,g] carbazole.

64
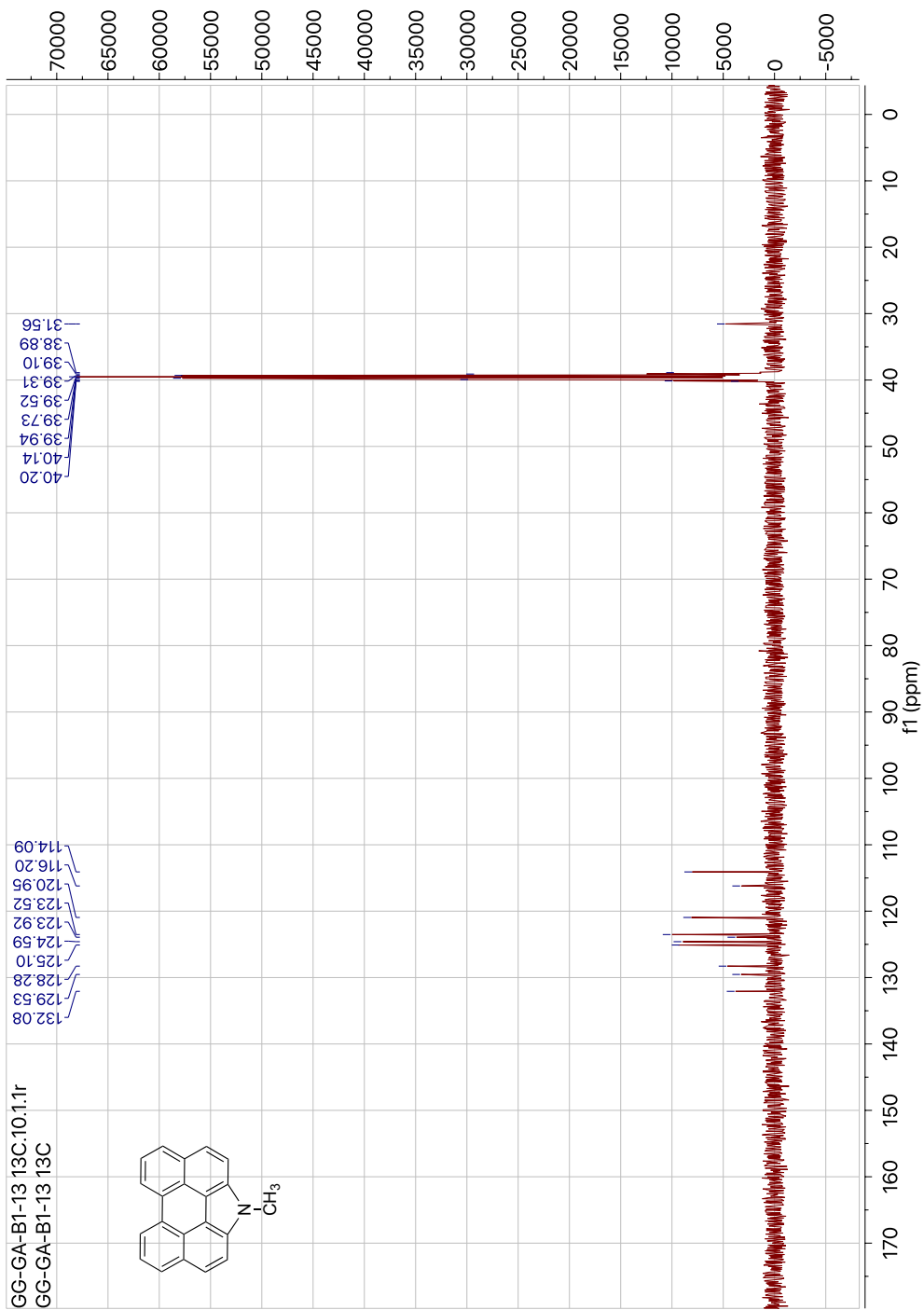
Figure A.6. ^{13}C-NMR spectrum of 1-Methyl-1*H*-phenanthro[1,10,9,8-c,d,e,f,g] carbazole.
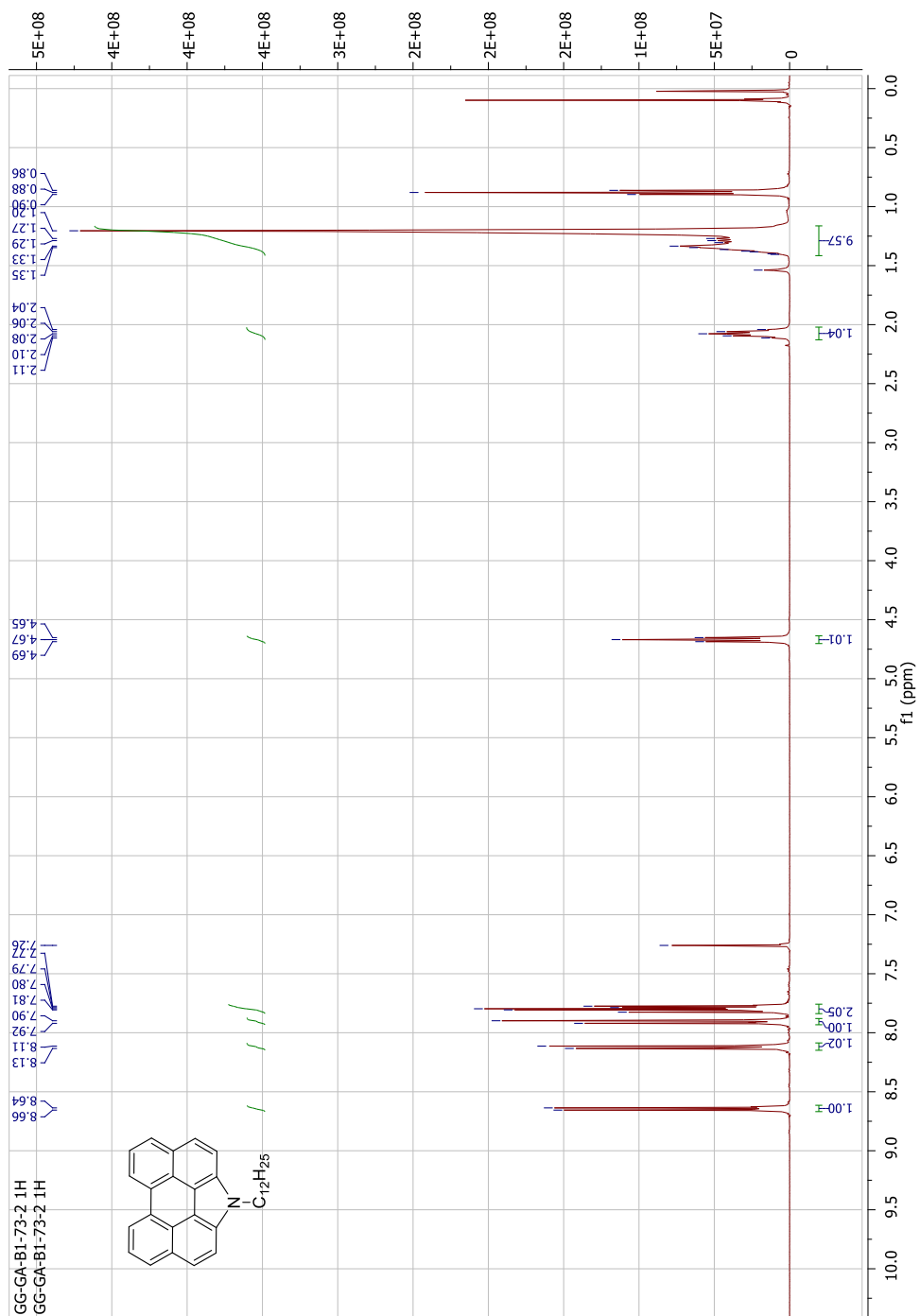
Figure A.7. ^{1}H-NMR spectrum of 1-Dodecyl-1*H*-phenanthro[1,10,9,8-c,d,e,f,g]carbazole.
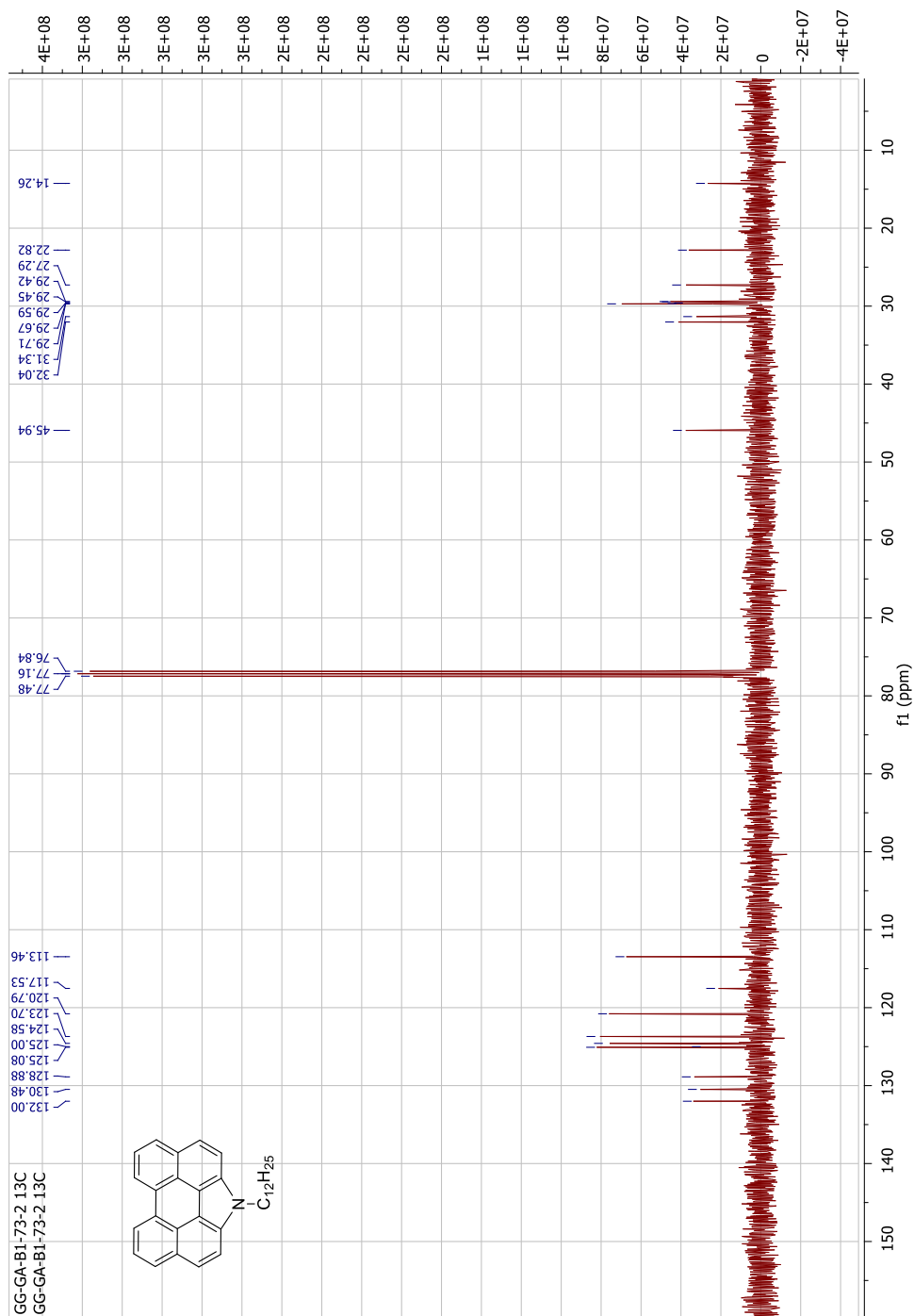
**Figure A.8.** ^{13}C-NMR spectrum of 1-Dodecyl-1H-phenanthro[1,10,9,8-c,d,e,f,g]carbazole.
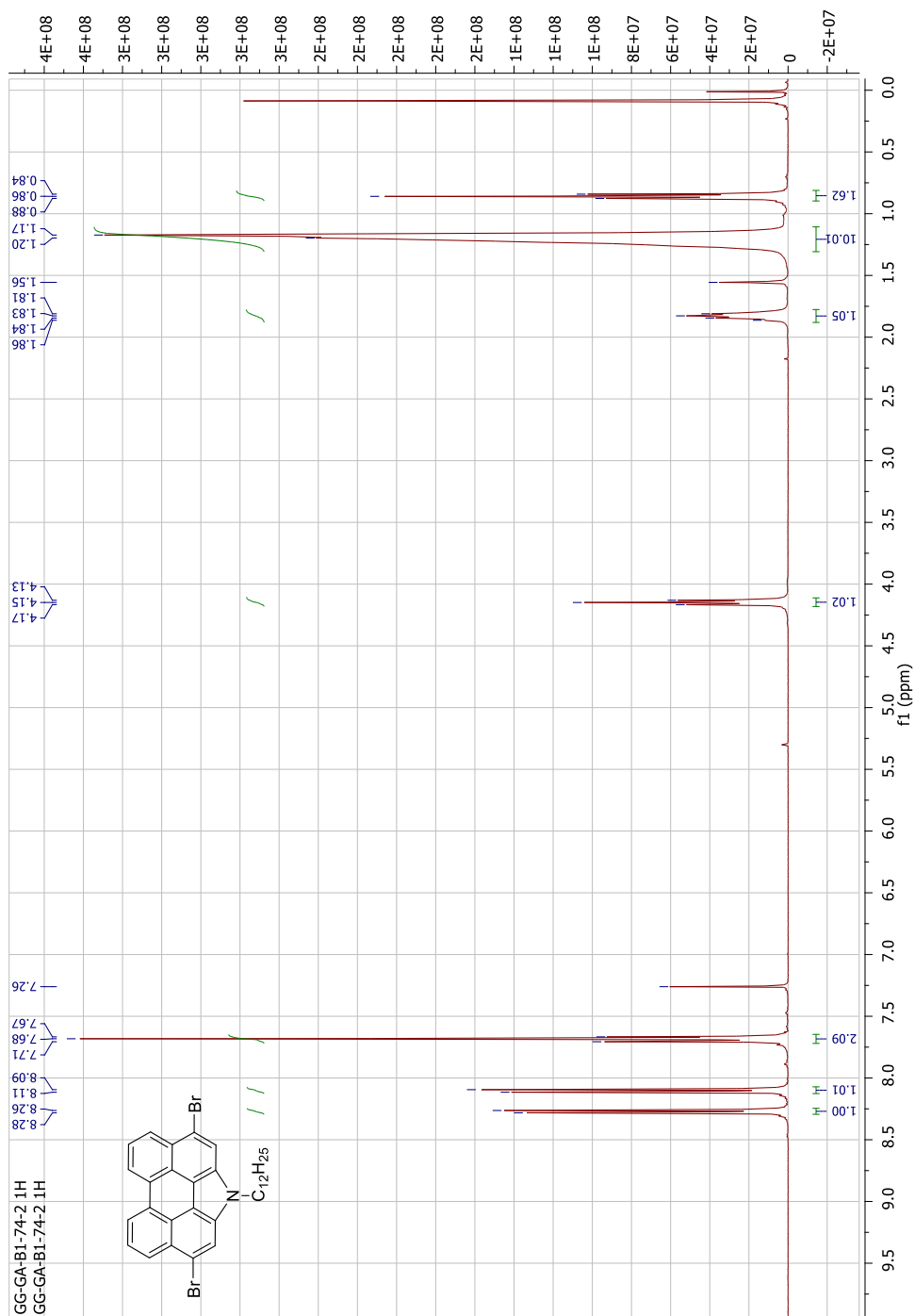
Figure A.9. ^{1}H-NMR spectrum of 3,10-Dibromo-1-dodecyl-1*H*-phenanthro[1,10,9,8-c,d,e,f,g]carbazole.
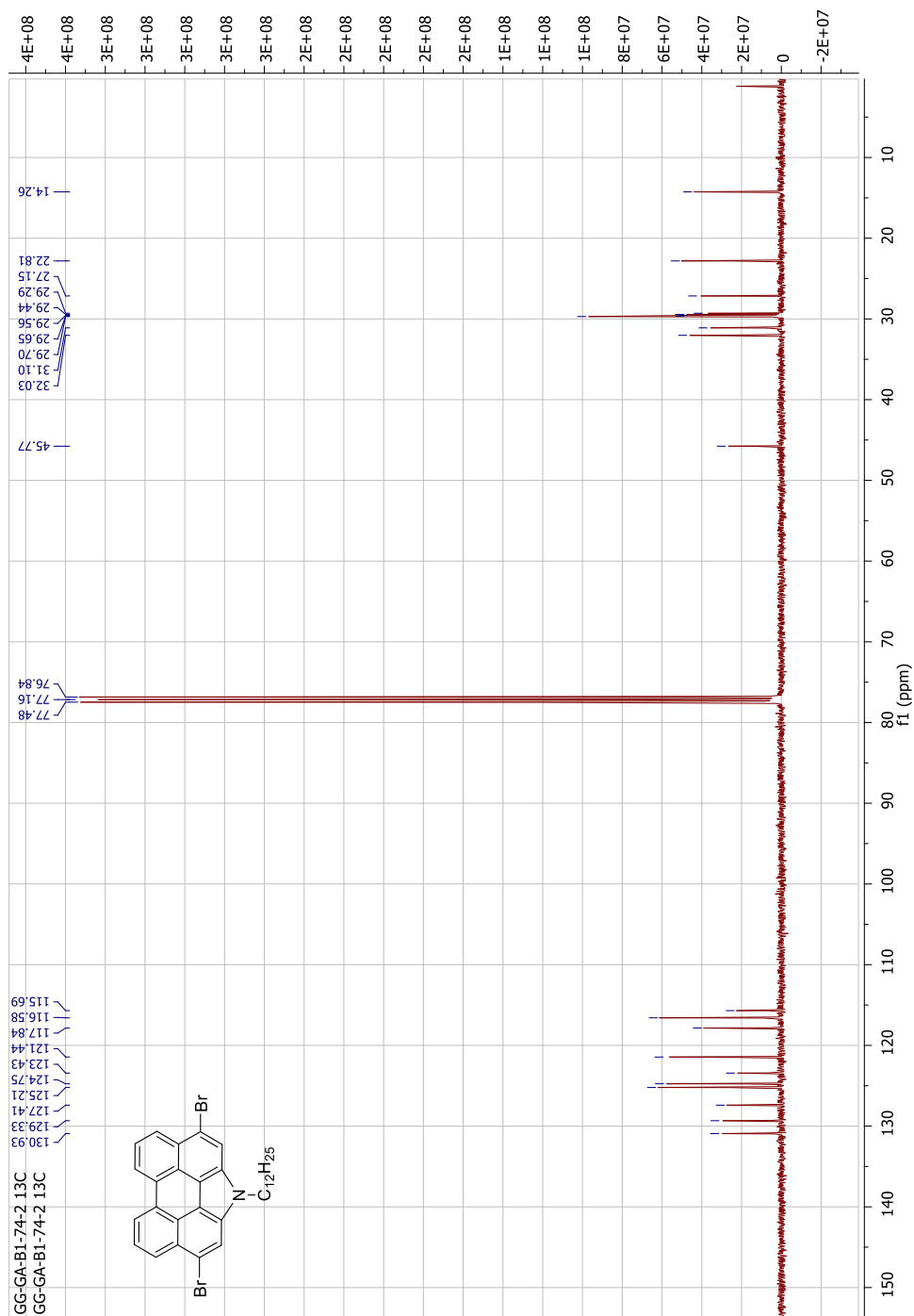
Figure A.10. ^{13}C-NMR spectrum of 3,10-Dibromo-1-dodecyl-1H-phenanthro[1,10,9,8-c,d,e,f,g]carbazole.

69
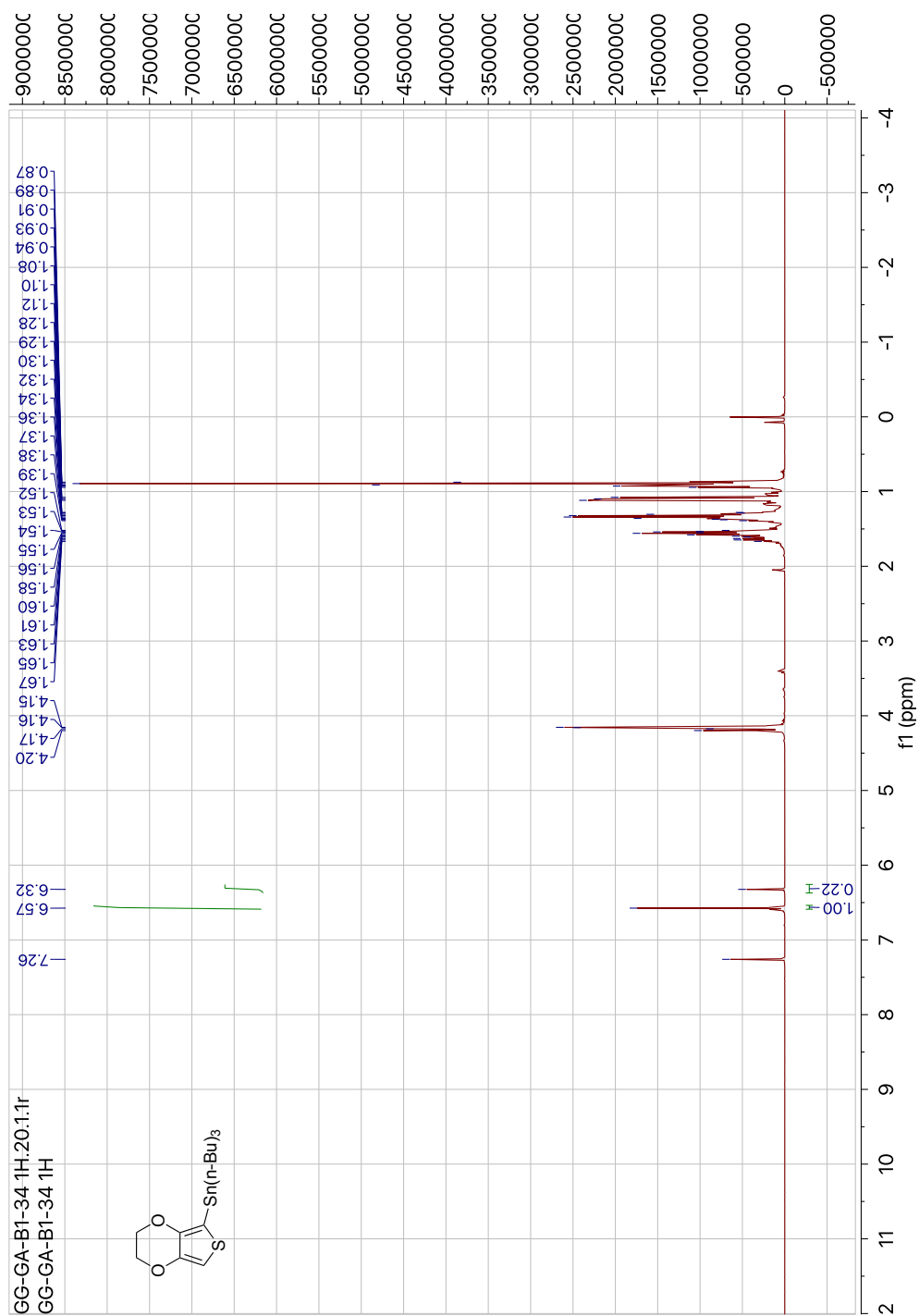
Figure A.11. ^{1}H-NMR spectrum of Tributyl(3,4-ethylenedioxythienyl-2)stannane.
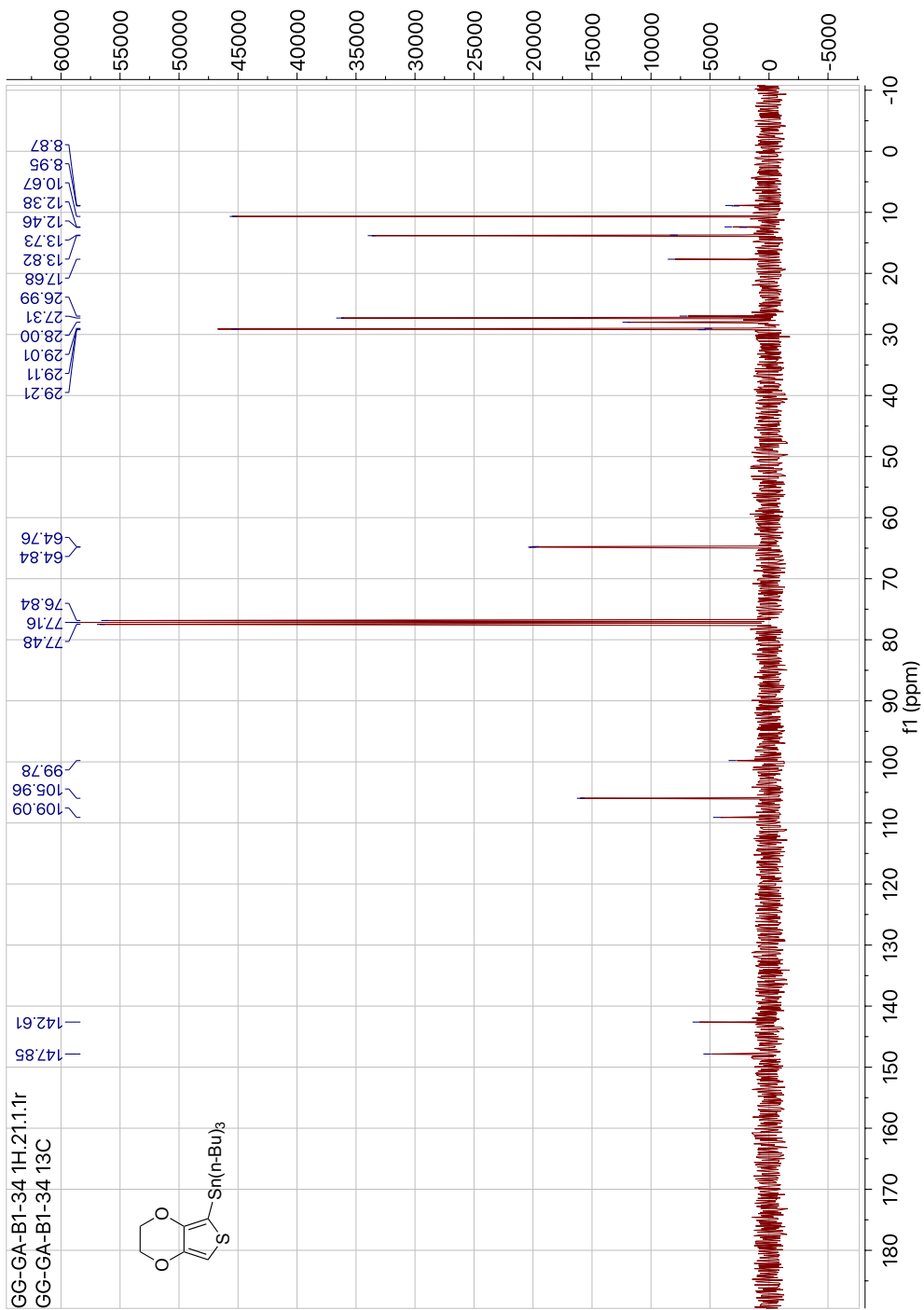
**Figure A.12.** ^{13}C-NMR spectrum of Tributyl(3,4-ethylenedioxythienyl-2)stannane.

71
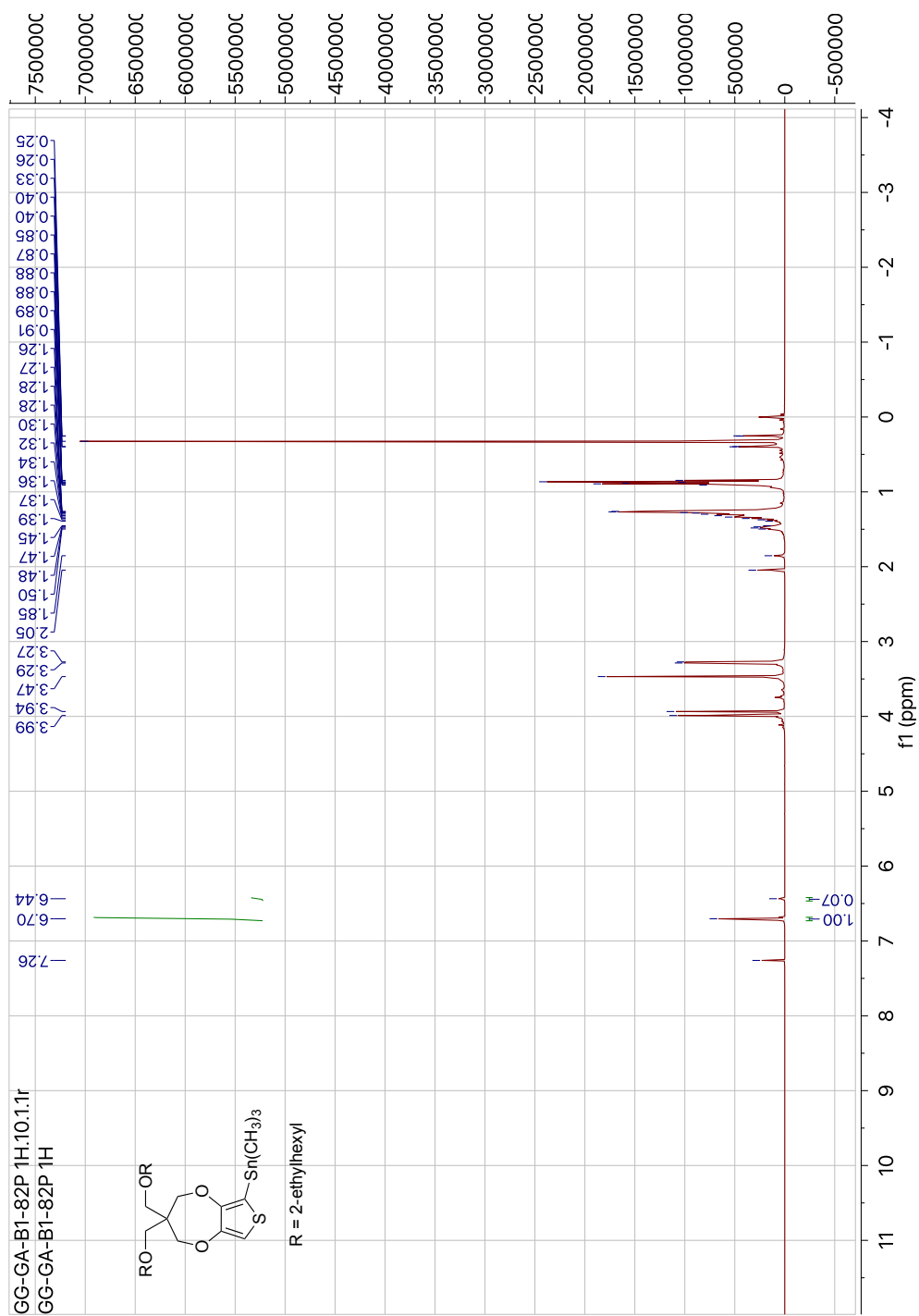
Figure A.13. ^{1}H-NMR spectrum of 3,3-Bis(2-ethylhexyloxy)methyl)-3,4-dihydro-2H-thieno[3,4-b][1,4]dioxepine-6-yl)trimethyl-stannane.
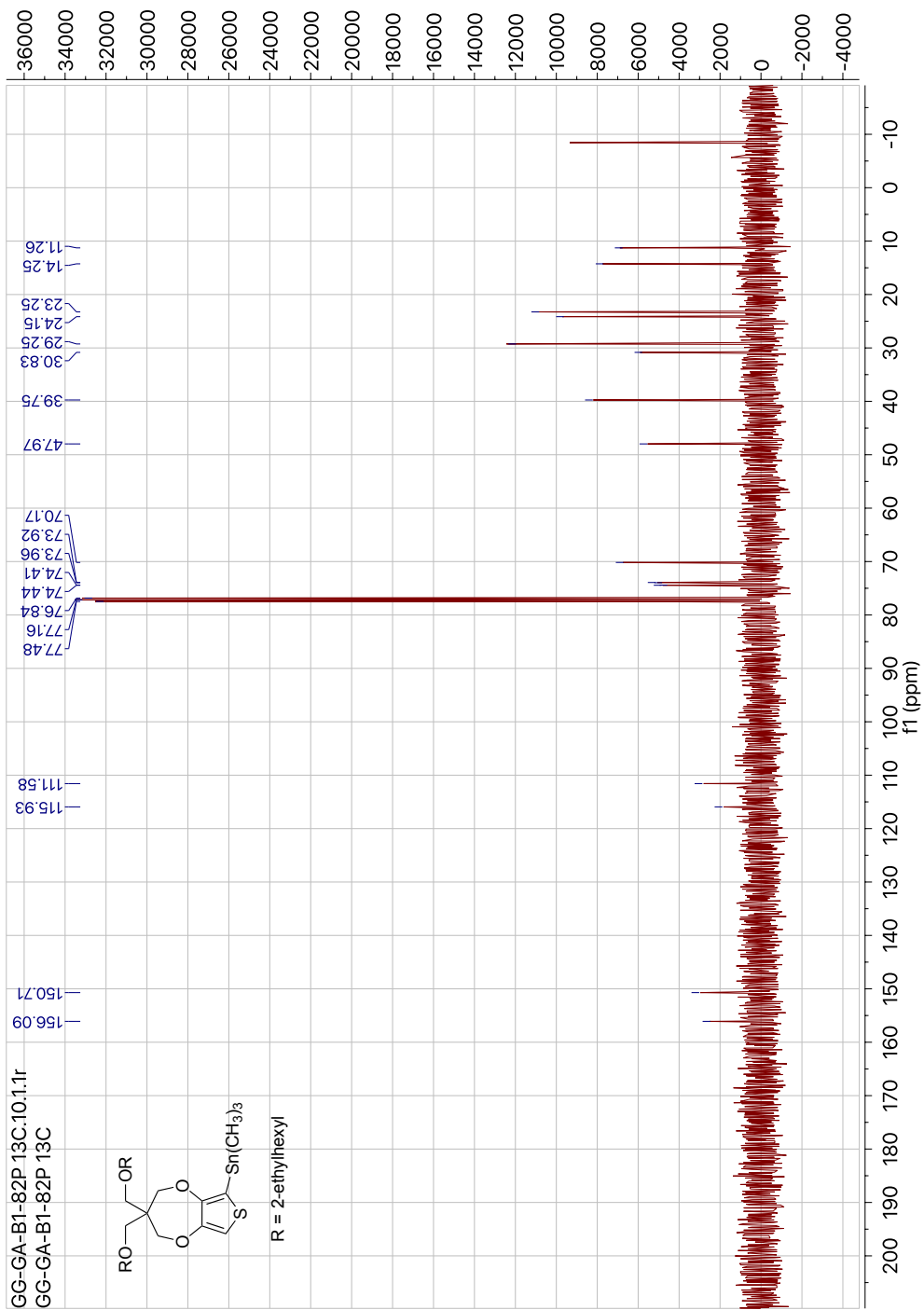
Figure A.14. ^{13}C-NMR spectrum of 3,3-Bis(2-ethylhexyloxy)methyl)-3,4-dihydro-2H-thieno[3,4-b][1,4]dioxepine-6-yl)trimethyl-stannane.
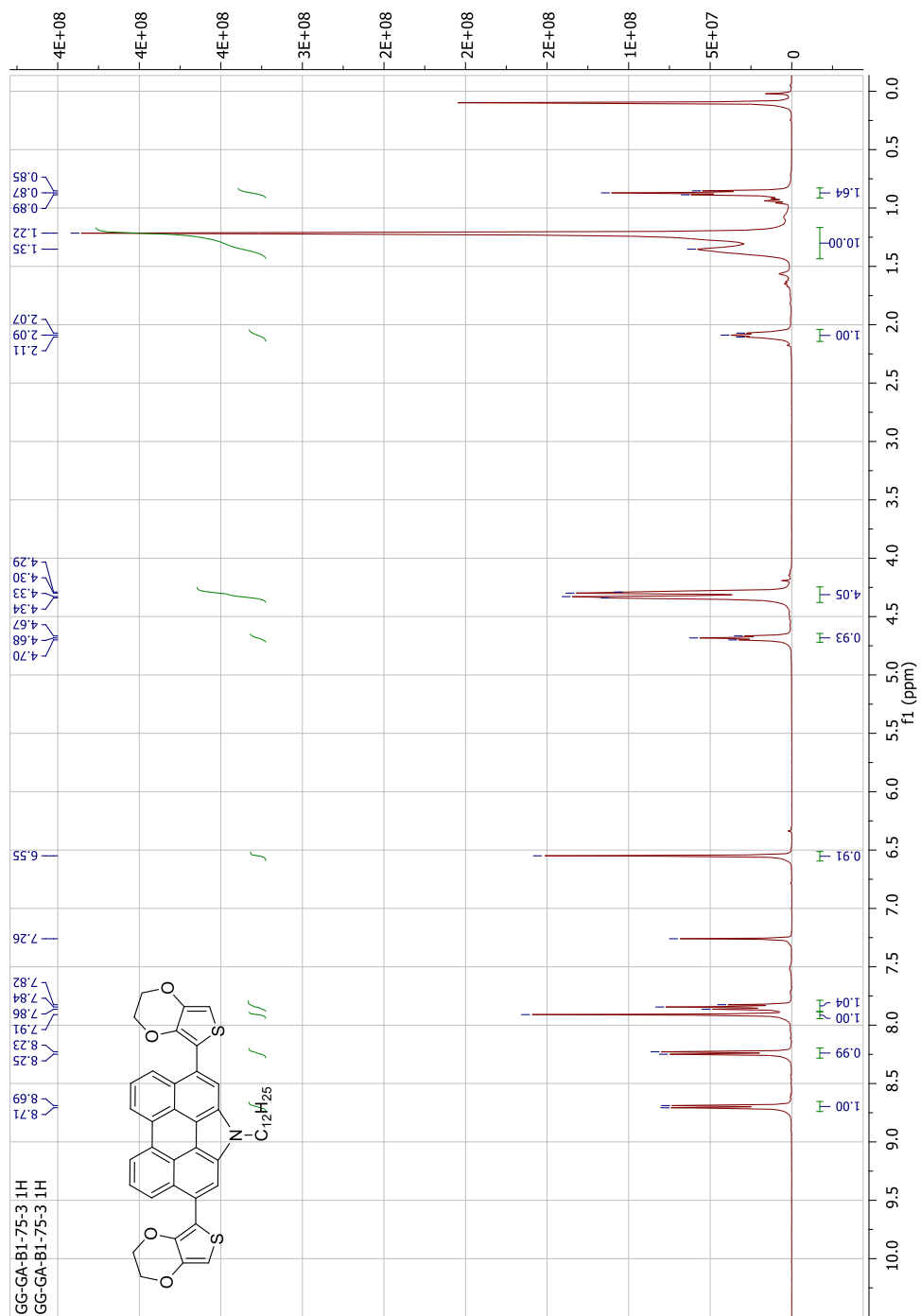
Figure A.15. ^{1}H-NMR spectrum of 3,10-Bis(2,3-dihydrothieno[3,4-b][1,4]dioxin-5-yl)-1-dodecyl-1*H*-phenanthro[1,10,9,8-c,d,e,f,g]carbazole (DEP).
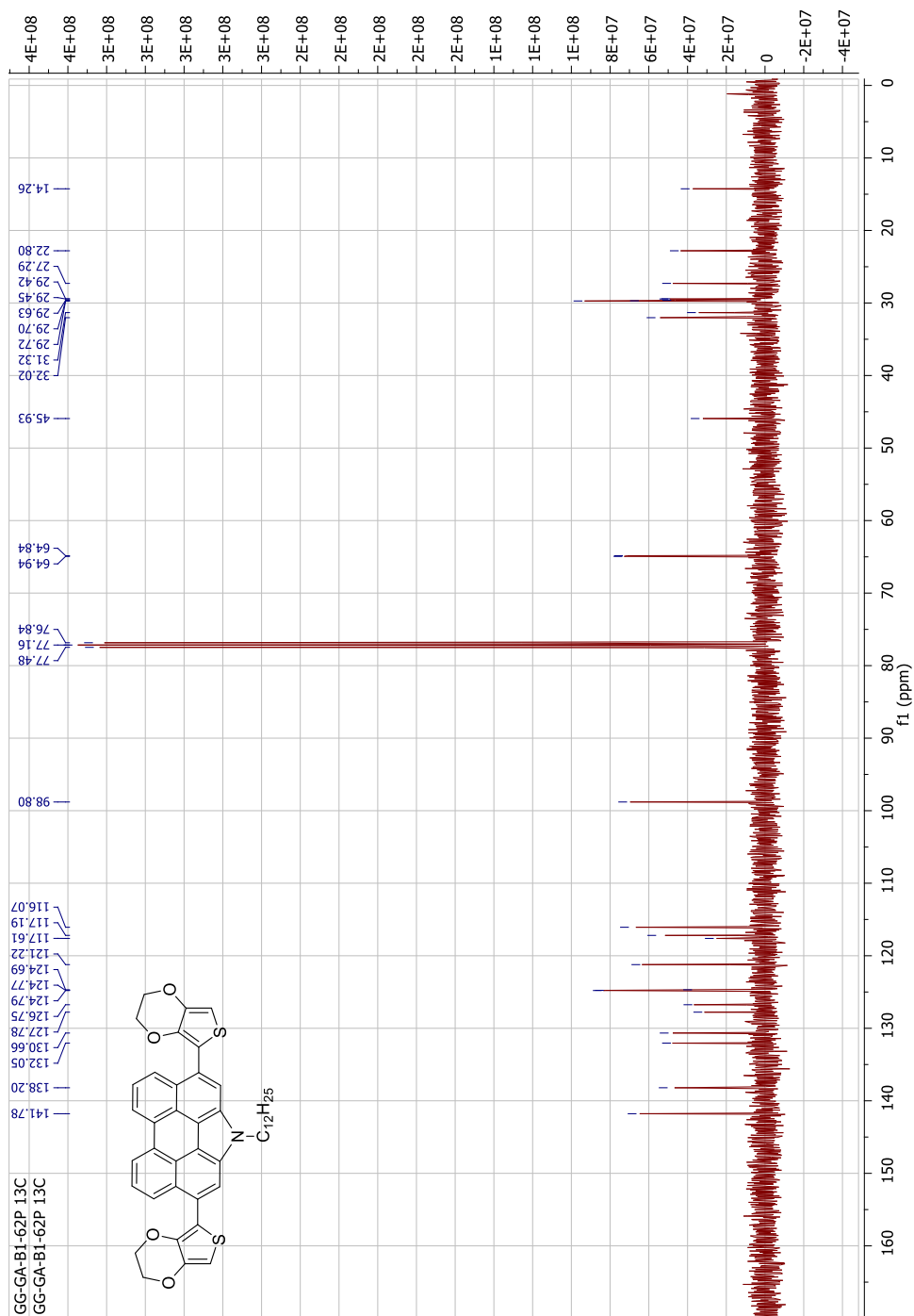
Figure A.16. ^{13}C-NMR spectrum of 3,10-Bis(2,3-dihydrothieno[3,4-b][1,4]dioxin-5-yl)-1-dodecyl-1*H*-phenanthro[1,10,9,8-c,d,e,f,g]carbazole (DEP).
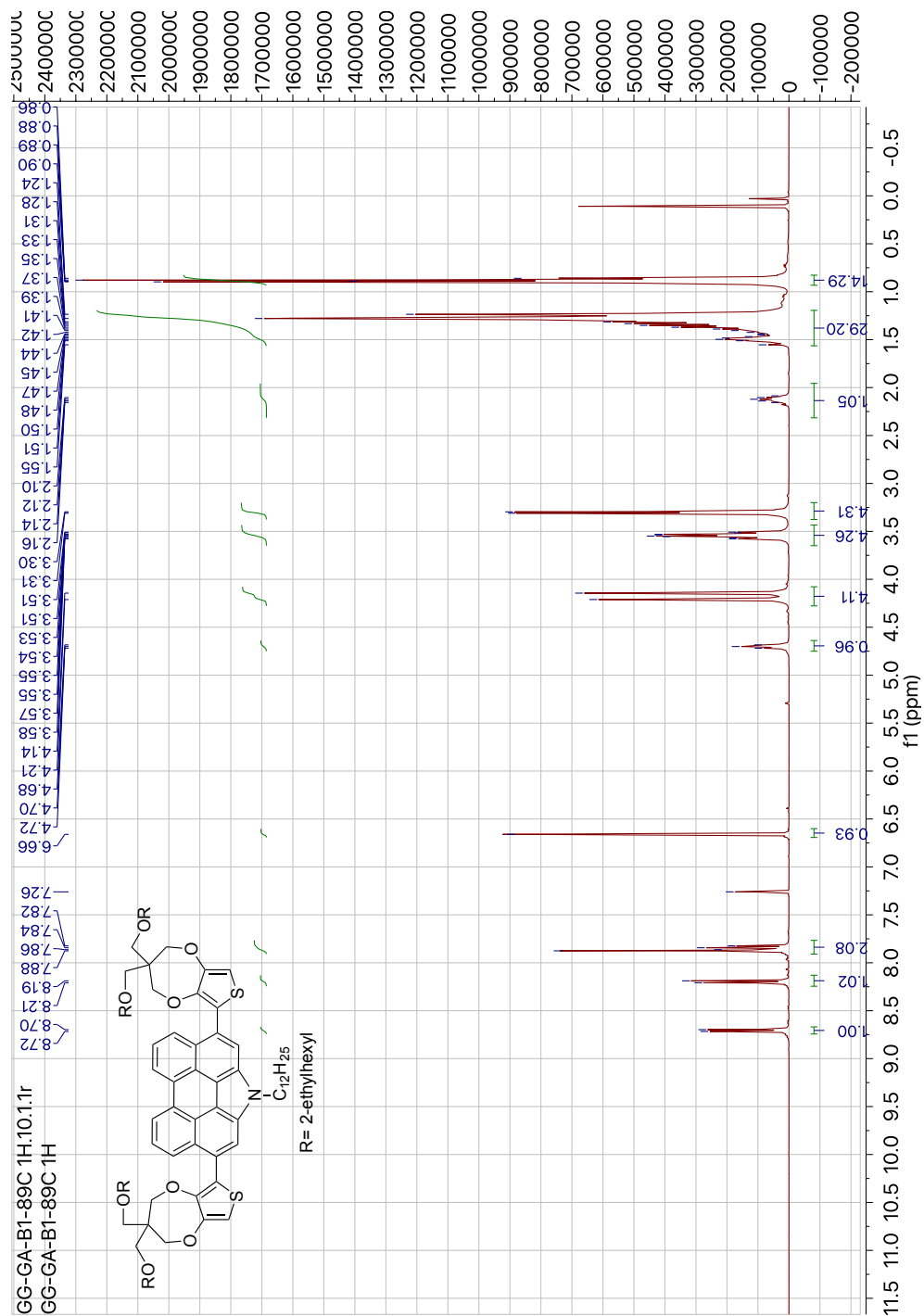
Figure A.17. ^{1}H-NMR spectrum of 3,10-Bis(3,3-bis(((2-ethylhexyl)oxy)methyl)-3,4-dihydro-2*H*-thieno[3,4-b][1,4]dioxepin-6-yl)-1-dodecyl-1*H*-phenanthro[1,10,9,8-c,d,e,f,g]carbazole (DPP).
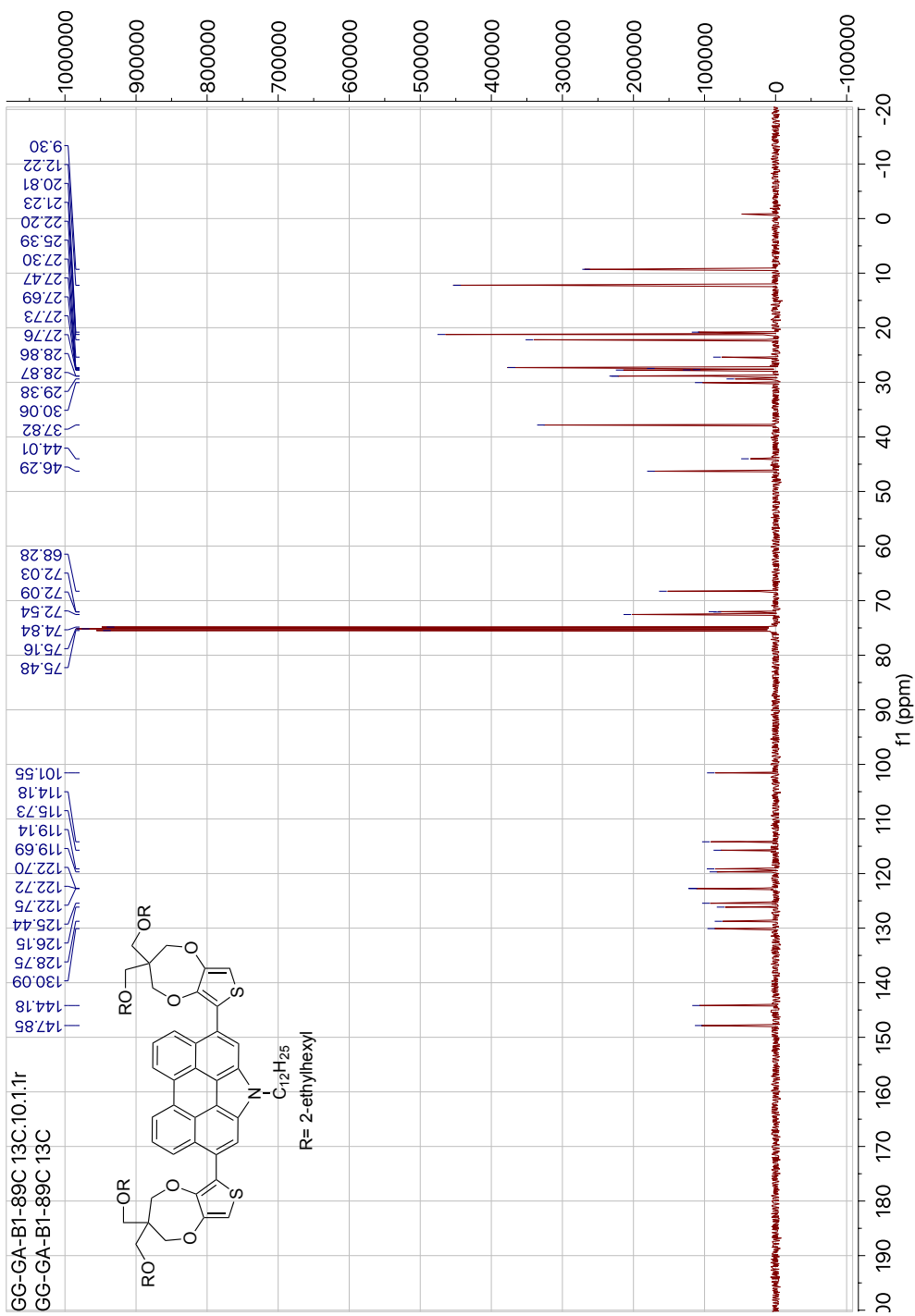
Figure A.18. ^{13}C-NMR spectrum of 3,10-Bis(3,3-bis(((2-ethylhexyl)oxy)methyl)-3,4-dihydro-2*H*-thieno[3,4-b][1,4]dioxepin-6-yl)-1-dodecyl-1*H*-phenanthro[1,10,9,8-c,d,e,f,g]carbazole (DPP).

77

Figure A.19. ^{1}H-NMR spectrum of Poly-3,10-bis(3,3-bis(((2-ethylhexyl)oxy)methyl)-3,4-dihydro-2*H*-thieno[3,4-b][1,4]dioxepin-6-yl)-1-dodecyl-1*H*-phenanthro[1,10,9,8-c,d,e,f,g]carbazole (PDPP).

HRMS DATA
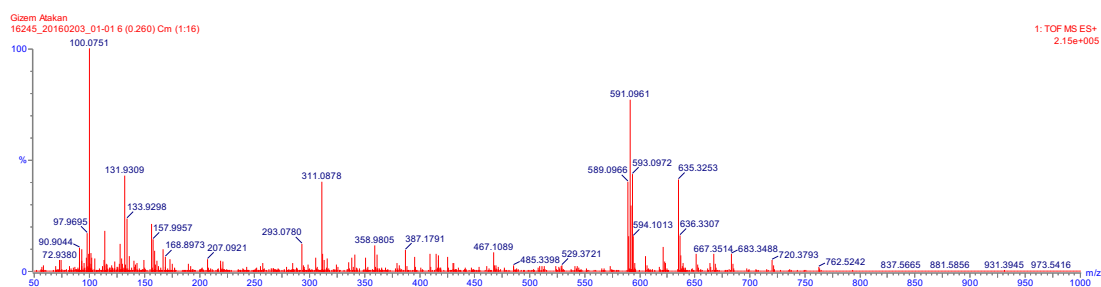
Calculated for $C_{32}H_{33}Br_2N$: 591.0959. Found: 591.0961.

Figure B.1. HRMS spectrum of 3,10-Dibromo-1-dodecyl-1*H*-phenanthro[1,10,9,8-c,d,e,f,g]carbazole.
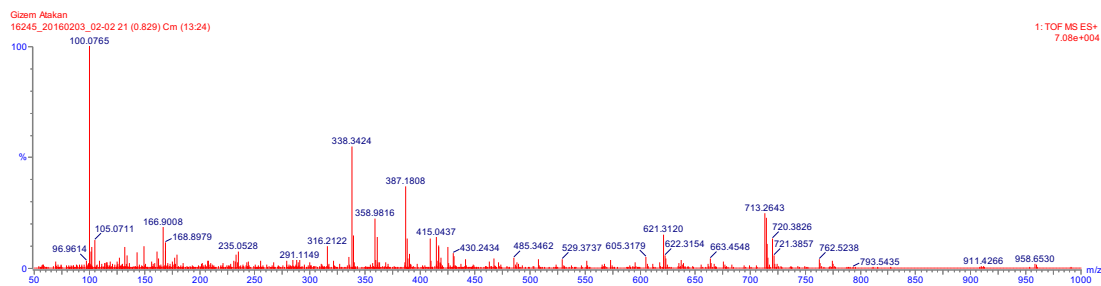
Calculated for $C_{44}H_{43}NO_4S_2$: 713.2643. Found: 713.2634.

Figure B.2. HRMS spectrum of 3,10-Bis(2,3-dihydrothieno[3,4-b][1,4]dioxin-5-yl)-1-dodecyl-1*H*-phenanthro[1,10,9,8-c,d,e,f,g]carbazole (DEP).